AD-A080 319 AERONAUTICAL RESEARCH ASSOCIATES OF PRINCETON INC NJ F/G 17/2
THE DEVELOPMENT AND TESTING OF AN ULTRAVIOLET VOICE COMMUNICATI--ETC(U)
JUL 79 M E NEER, J M SCHLUPF N66001-78-C-0180
UNCLASSIFIED ARAP-394 NL

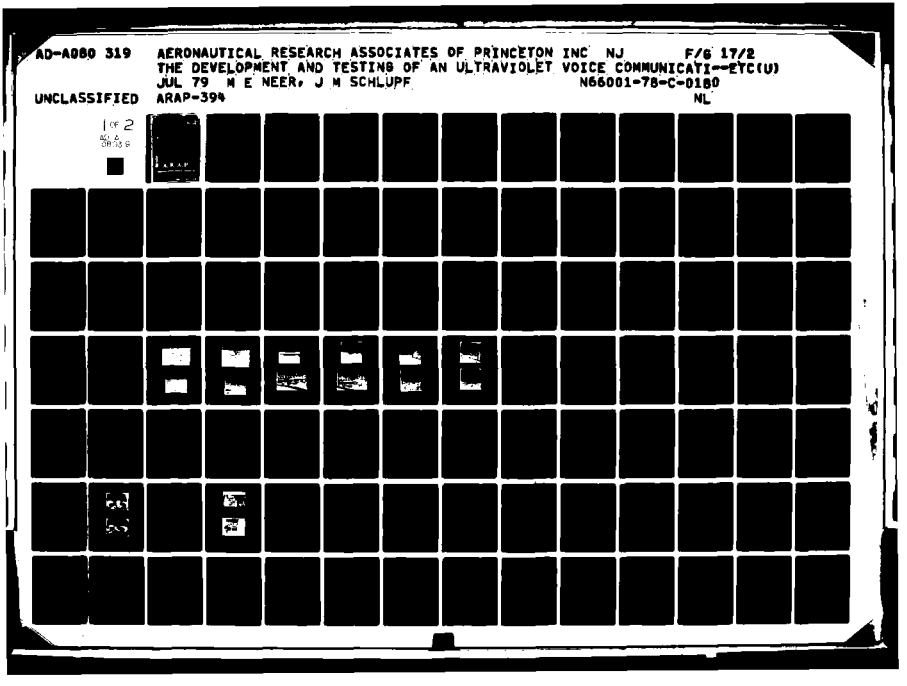

A.R.A.P. Report No. 394

THE DEVELOPMENT AND TESTING OF AN ULTRAVIOLET VOICE COMMUNICATION SYSTEM

Final Report
N66001-78-C-0180
June 1978 to July 1979

by

Michael E. Neer
and
Joseph M. Schlupf

Sponsored by

Department of the Navy
Naval Electronic Systems Command
Washington, D.C. 20360

Aeronautical Research Associates of Princeton, Inc.
P.O. Box 2229, 50 Washington Road
Princeton, New Jersey 08540

July 1979

Unclassified

SECURITY CLASSIFICATION OF THIS PAGE (When Data Entered)

REPORT DOCUMENTATION PAGE	READ INSTRUCTIONS BEFORE COMPLETING FORM
1. REPORT NUMBER	2. GOVT ACCESSION NO. / 3. RECIPIENT'S CATALOG NUMBER
4. TITLE (and Subtitle) (6) The Development and Testing of an Ultraviolet Voice Communication System.	5. TYPE OF REPORT & PERIOD COVERED (9) Final Report, June 1978 to July 1979 (4) TABAP
	6. PERFORMING ORG. REPORT NUMBER A.R.A.P. Report No. 394
7. AUTHOR(s) (10) Michael E. Neer, Joseph M. Schlupf	8. CONTRACT OR GRANT NUMBER(s) (15) N66001-78-C-0180
9. PERFORMING ORGANIZATION NAME AND ADDRESS Aeronautical Research Associates of Princeton, Inc. P.O. Box 2229, 50 Washington Road Princeton, New Jersey 08540	10. PROGRAM ELEMENT, PROJECT, TASK AREA & WORK UNIT NUMBERS
11. CONTROLLING OFFICE NAME AND ADDRESS Department of the Navy Naval Electronic Systems Command Washington, DC 20360 (11)	12. REPORT DATE July 1979 / 13. NUMBER OF PAGES 172 pages
14. MONITORING AGENCY NAME & ADDRESS (if different from Controlling Office) (12) 173	15. SECURITY CLASS. (of this report) Unclassified / 15a. DECLASSIFICATION/DOWNGRADING SCHEDULE

16. DISTRIBUTION STATEMENT (of this Report)

Approved for public release; distribution unlimited

17. DISTRIBUTION STATEMENT (of the abstract entered in Block 20, if different from Report)

18. SUPPLEMENTARY NOTES

19. KEY WORDS (Continue on reverse side if necessary and identify by block number)

Ultraviolet Communication
Background Rejection
Ultraviolet Scattering
Atmospheric Scattering
Pulse Frequency Modulation
Scatter Communications
Solar Blind

20. ABSTRACT (Continue on reverse side if necessary and identify by block number)

Measurements of the atmospheric propagation and scattering of ultraviolet radiation within the solar blind through the lower atmosphere have been made through the summer and fall months of 1978 in rural, industrial and maritime atmospheres. An ultraviolet propagation and scattering model has been improved as the result of these measurements and has been used successfully in an ultraviolet communications model. A research oriented, ultraviolet voice communications system has been designed and fabricated using the best available

DD FORM 1 JAN 73 1473 EDITION OF 1 NOV 65 IS OBSOLETE

components. The communications system has been field tested and found to perform quite well with a maximum line of sight range of 4.7 km and maximum nonline of sight range of 1.6 km when the ozone level is moderately high. Several advances have been made in component design including triggering circuitry for the high repetition rate flashlamps, voice modulation electronics, pulse amplitude discriminator design, and the collimation of transmitted radiation. Investigations of multi-channel concepts and safety have also been completed.

PREFACE

A portion of the work carried out under this contract was the completion of a year round series of atmospheric propagation and scattering measurements in the solar blind portion of the ultraviolet. These propagation and scattering measurements were sponsored by the Naval Electronic Systems Command and the Air Force Avionics Laboratory (AFAL/WRP-2) under Navelex Contract N00039-77-C-0278 and also by the Office of Naval Research under contract N00014-76-C-1094. For the sake of completeness, the results of the entire atmospheric propagation and scattering measurement program has been included in a single four volume report entitled "Atmospheric Propagation of Ultraviolet Radiation Through the Lower Atmosphere" by M. E. Neer, J. M. Schlupf, P. C. Petersen, and C. R. Dickson, A.R.A.P. Report No. 374b, November 1978. All of the reported ground to ground propagation and scattering measurements completed after May of 1978 were sponsored by the Naval Ocean Systems Center under the subject contract (N66001-78-C-0180). While the results of those measurements sponsored under the subject contract will be discussed in this report, the reader is referred to the report listed above for the complete description of all measurements made during the year long measurement program.

ACKNOWLEDGEMENTS

The authors would like to express their appreciation to Mr. Jack Kellock of the Princeton University for providing the use of the roof of the Jadwin Physics Building for conducting some of our experiments. Mr. C. Eugene Newsom of the U.S. Army Electronic Warfare Laboratory ERADCOM is acknowledged for providing the use of the Wayside Laser Test Range, Ft. Monmouth, New Jersey for some of the scattering and propagation measurements. Mr. Chuck Elliott, Ms. Mary Johnson, and Dr. Gary Matthews of the Pacific Missile Test Center are acknowledged for their cooperation in carrying out the scattering and propagation measurements on San Nicolas Island. The authors would like to thank Mr. Paul Zucchino of Princeton University for his help in designing and constructing the electronic circuitry used for the breadboard ultraviolet voice communication system. The help of Dr. David Burde, Ms. Priscilla Petersen, Dr. C. Robert Dickson, Dr. Robert McCullough, and Ms. Jeanne Kuhlman, all of Aeronautical Research Associates of Princeton, Inc., is also acknowledged. The help of Ms. Deborah Doolittle and Ms. Patricia Tobin in preparing the final report is also appreciated. Finally, the authors would like to thank Mr. Daniel Leonard and Mr. Myer Geller of the Naval Ocean Systems Center for supporting the research presented in this report.

TABLE OF CONTENTS

LIST OF FIGURES

LIST OF TABLES

ABSTRACT

Measurements of the atmospheric propagation and scattering of ultraviolet radiation within the solar blind through the lower atmosphere have been made through the summer and fall months of 1978 in rural, industrial and maritime atmospheres. An ultraviolet propagation and scattering model has been improved as the result of these measurements and has been used successfully in an ultraviolet communications model. A research oriented, ultraviolet voice communications system has been designed and fabricated using the best available components. The communications system has been field tested and found to perform quite well with a maximum line of sight range of 4.7 km and maximum nonline of sight range of 1.6 km when the ozone level is moderately high. Several advances have been made in component design including triggering circuitry for the high repetition rate flashlamps, voice modulation electronics, pulse amplitude discriminator design, and the collimation of transmitted radiation. Investigations of multi channel concepts and safety have also been completed.

INTRODUCTION

Ultraviolet voice communication systems transmit and receive ultraviolet radiation as the primary carrier frequency. In the existing systems, short bursts of ultraviolet radiation are transmitted into the atmosphere from a hydrogen xenon flashlamp. At the receiver end of the communications link, the ultraviolet radiation is collected by front surface mirrors or quartz lenses, passed through a solar blind filter and detected with a rubidium telluride or cesium telluride photomultiplier tube. The voice wave form is used to modulate the pulsing frequency of the lamp so that the pulse frequency becomes a secondary carrier.

Due to scattering by atmospheric aerosols and molecular species, ultraviolet radiation propagates over and around natural or manmade obstacles. Thus, nonline of sight communication can be accomplished and directional tracking requirements are relaxed. Because of absorption by atmospheric ozone, the ultraviolet radiation undergoes an exponential decay with distance. Thus, the communications signal becomes increasingly difficult to jam, intercept or even detect as the distance between the jammer or unintended receiver and the intended receiver increases beyond the intended range. Because the operating wavelength lies in the solar blind portion of the spectrum (2500 to 2850 Å) the ultraviolet system is not

affected by radiation from the sun or most other natural or manmade radiation sources. While the range of the ultraviolet voice communications system is decreased in very low visibility weather conditions, signal losses are not nearly so severe as for line of sight communications systems in which very narrow detector fields of view are used.

While the ultraviolet voice communications system can be used with isotropic transmission and omnidirectional detection, the potential directionality of both the transmitter and receiver can be used to obtain longer ranges as well as more covert, secure and jam resistant communications. Because of the short duration of the transmitted lamp flashes, time gating systems can be used to differentiate between UV communications signals and extraneous random ultraviolet radiation sources such as fires, flares and various types of munitions.

In establishing the feasibility of developing a practical ultraviolet voice communications system, it was necessary to establish through computations and field measurements the maximum upper limit of ultraviolet system performance. With increased research and development, the various components which make up the ultraviolet communications system can be expected to increase continually in efficiency. The one limiting factor which cannot be improved, however, barring some catastrophic geophysical change, is the ultraviolet scattering and transmission characteristics of the atmosphere.

Therefore, one of the primary tasks in the present and previous research efforts[1,2,3] has been to establish the ultimate limitations imposed on the ultraviolet communications channel by the atmosphere itself for a wide variety of weather conditions.

Historically, very little experimental or theoretical scattering work has been carried out in the ultraviolet portion of the spectrum. Line of sight attenuation measurements in the ultraviolet were made as early as the mid 1950's by Baum and Dunkelman[4] and Biberman and Johanboeke.[5] More recently, ultraviolet propagation work has been carried out by Knestrick and Curcio[6] of NRL. However, in the measurement of attenuation coefficients, great care must be taken to prevent scattered radiation from entering the detection device. Over long distances or for nonline of sight applications, the scattered light is also of interest. Therefore, A.R.A.P. conducted a preliminary experimental and theoretical study[1] of the ultraviolet scattering transmission characteristics of the lower atmosphere under a previous ARPA contract. A much more extensive ultraviolet scattering and propagation program[3] including both measurements and theoretical modeling was initiated under the joint sponsorship of the Air Force Avionics Laboratory, the Naval Electronic Systems Command, and the Office of Naval Research. Under these programs, an extensive series of measurements was made from the fall of 1977 through the spring of 1978.

The atmospheric measurements which were carried out can be divided into two general categories. The first category involves ground to ground and ground to air propagation and scattering measurements, while the second category involves the documentation of prevailing atmospheric conditions. Attenuation (extinction) coefficients and the nonaxisymmetric radiant intensity fields were measured along ground to ground paths for wavelength regions corresponding to the 225-245, 245-265, 265-285 nm regions. Similar measurements were carried out along ground to air slant paths for the 245-265, 265-285, and 245-285 nm regions. The single scattering phase functions at various wavelengths within the solar blind portion of the ultraviolet spectrum were measured using a scanning polar nephelometer.

Atmospheric documentation measurements included the barometric pressure, temperature, humidity, ozone concentration and aerosol particle size distribution. Color photographs were taken at ground level and at the airborne locations to show prevailing weather conditions and to indicate visibility. These basic atmospheric documentation measurements were used to obtain the basic atmospheric optical properties in the ultraviolet portion of the spectrum. Measured concentrations of molecular absorbers and scatterers were used to determine the exponential scattering and absorption coefficient due to molecular species. Likewise, measured concentrations and size distributions of aerosols were used to predict the

exponential scattering and absorption coefficients due to aerosols. The sum of these various exponential coefficients is equal to the overall attenuation or extinction coefficient which was also measured. The single scattering phase functions due to aerosol and molecular species were predicted from Mie and Rayleigh scattering theory and compared to measured values.

The various exponential coefficients and the single scattering phase functions are required input to all atmospheric propagation models. These propagation models include single scatter, forward scatter, solutions of the radiative transport equation, multiple recursion and the Monte Carlo techniques. These models generally predict the total energy,angular distribution, temporal distribution and statistical fluctuation of received energy at the aperture of the detector, all of which were measured directly.

From a less fundamental point of view, empirical correlations between the atmospheric documentation measurements and measured atmospheric propagation can be made. Direct empirical correlations have the advantage of not being limited by the assumptions made in atmospheric propagation models but have the disadvantage of being limited to a relatively small number of specific geometries and atmospheric conditions. Thus, while the validity of direct empirical correlations between atmospheric conditions and ultraviolet propagation cannot be questioned, the more fundamental approach is required

if the results are to be extrapolated to other weather conditions and other geometries.

One of the major tasks in the subject research effort has been to complete the atmospheric propagation and scattering measurements through the summer and early fall months of 1978. All reported ground to ground propagation measurements in Reference 3 made after May of 1978 were completed under the subject Naval Ocean Systems Center contract and therefore by reference constitute a portion of this final report. While a summary of the various measurements and a discussion of the results of those measurements will be presented in this report, an exhaustive description of all the measured data and its interpretation are presented in Reference 3 and will not be repeated here.

Another major objective of the subject research effort has been to design, fabricate and test a research oriented, two-way UV communications system. This two-way system utilizes one transmitter and one receiver originally constructed under the previous ARPA contract (Reference 1) and one new transmitter and receiver developed under the subject contract. The new transmitter and receiver are modular in construction so that various lamps, power supplies, optical systems, photomultiplier tubes and electronic components can be tested individually as they are developed. The new transmitter and receiver have a voice bandpass of 2400 Hz and a secondary carrier frequency of 5700 pulses per second.

An electronic gating system has been installed for rejecting extraneous background radiation from fires and flares and other random ultraviolet sources. Preemphasis-deemphasis techniques have been used in the voice modulation to enhance the transmission of the high frequency components of the voice. Two new high repetition rate flashlamps have been fabricated and tested during this effort, one of which employs a 150 watt lamp from the EG&G Company, while the other employs a 50 watt lamp from the USSI Company. Several major modifications have been made in the flashlamp triggering circuitry which prevent holdover from one pulse to the next and makes the ultraviolet energy per pulse much more uniform than in the past.

Lightweight mirrors with various types of coatings, including gold, aluminum and silver, have been tested to determine their relative reflectivity in the ultraviolet.

Two different types of photomultiplier tubes have been tested in this investigation, including a high quality cesium telluride photomultiplier tube, potted together with a pulse amplitude discriminator (PAD) and high voltage power supply manufactured by the EMR Corporation. The second photomultiplier tube, which is considerably less expensive was provided by the Hamamatsu Corporation with a pulse amplitude discriminator and high voltage power supply developed by Zucor Limited.

A test plan involving both laboratory and field measurements

has been carried out to thoroughly test both the individual components and the overall performance of the new transmitter and receiver. The field tests were conducted to verify the ultraviolet voice communications model presented in Reference 3 and to determine the range and nonline of sight capability of the new transmitter and receiver.

Various concepts for obtaining multi-channel operation have also been investigated and have led to the development of a multi-channel scheme involving the use of two flashlamps per transmitter for obtaining simultaneous communications on approximately ten channels.

Finally, recommendations have been made concerning future research in the development of ultraviolet voice communications. Paramount among these recommendations is additional research to improve the conversion efficiency of electrical energy to ultraviolet radiation by the high repetition rate flashlamps.

2. ATMOSPHERIC MEASUREMENTS AND MODELING

In order to determine the relative importance of various systems design parameters in accomplishing ultraviolet voice communications, an ultraviolet voice communications model was developed under the previous Navelex contract.[2] The most complex portion of the communications model dealt with the propagation and scattering of ultraviolet radiation from the transmitter to the receiver. That portion of the communications model is referred to as the atmospheric transfer function. The remainder of the communications model involves the size and efficiencies of the individual components which make up the transmitter and receiver.

One purpose of this section is to briefly review the UV communications model which will be verified in Section 3 using the research oriented communications system. Atmospheric propagation and scattering measurements carried out under this contract will also be presented.

2.1 Description of Ultraviolet Communications Model

The communications model has been described mathematically by a single equation shown in Figure 1. The basic premise upon which the mathematical formulation of Figure 1 has been derived is that the UV voice communications system will be operated in a pulsed mode with a photon counting detector. The detection of a pulse will be defined as the reception of

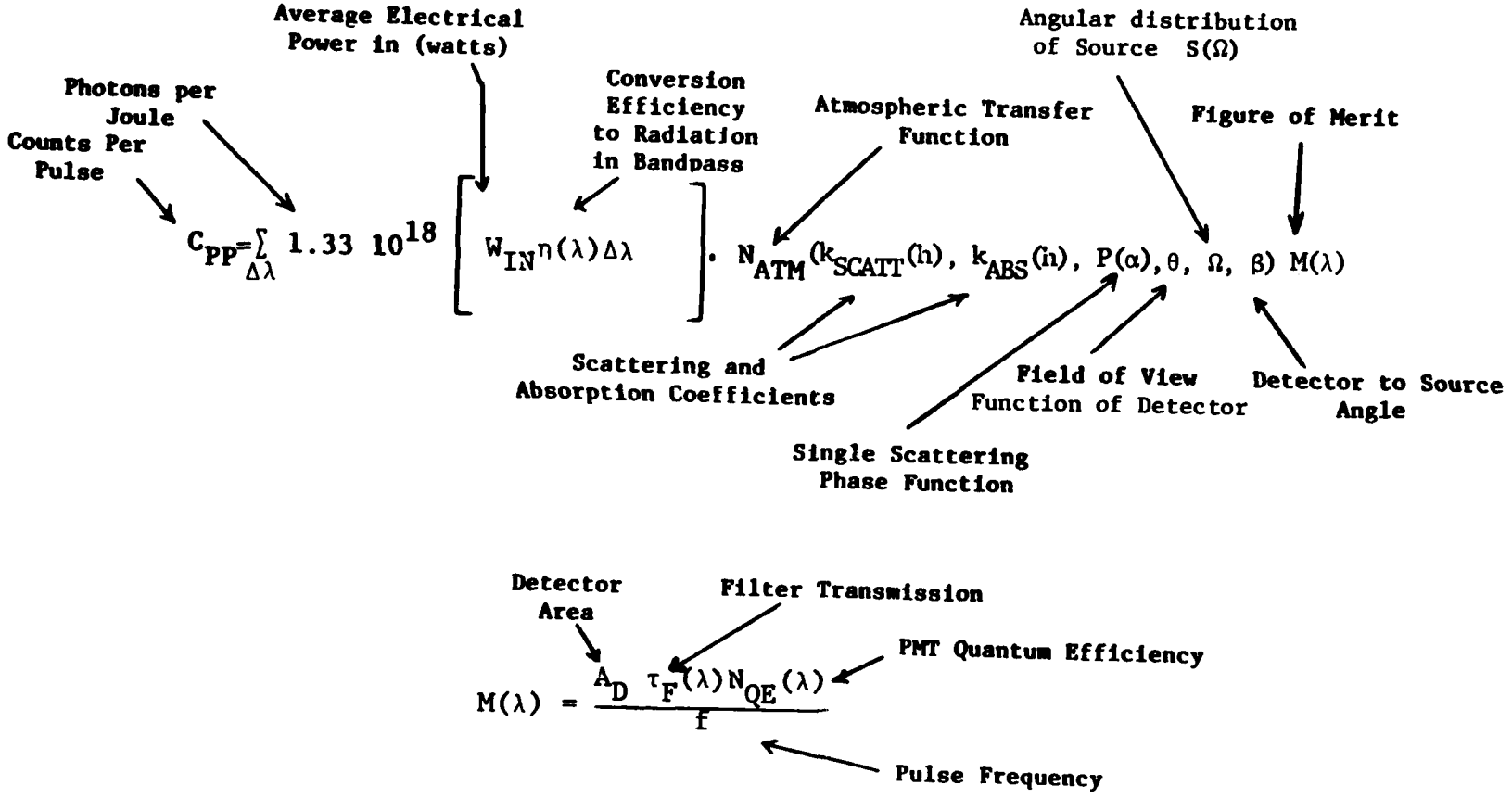

$C_{PP} \geq 2.0$ (Due to Poisson Statistics)

Figure 1. UV Communications Model.

one, or perhaps two, individual photon counts. The need for this minimum energy type of detection is dictated by the large energy per photon at ultraviolet wavelengths, by the small conversion efficiencies of the transmitter lamps and the low transmittances of solar blind filters. The peak conversion efficiency of electrical energy to ultraviolet radiation is currently at the 0.2% mark and the peak transmittance of solar blind filters are on the order of 4 or 5%. It is the purpose of the model shown in Figure 1 to describe the manner in which the number of counts received at the detector per pulse of the transmitter lamp depends on the various component efficiencies.

While one or two counts per pulse will suffice for transferring the communications information from the transmitter to the receiver, the natural statistical fluctuations such as those described by Poisson statistics, will result in a loss of signal. Therefore, it is necessary to obtain some minimum average number of counts per pulse in order to guarantee that a sufficient percentage of the transmitted pulses will be received. For the case of a two photon gating system, such as is employed in the present research oriented communications system, the probability of finding two or more photons during the time interval t is given by

$$P(k \geq 2, \lambda t) = 1 - P(0,\lambda t) - P(1,\lambda t) = 1 - e^{-\lambda t}(1 + \lambda t) \qquad \text{(Eq. 1)}$$

where P is the fraction of the time that two or more photon counts will occur during a time interval of length t when the average number of counts per time interval t is equal to λt. A complete treatment of the Poisson statistics involved in accomplishing UV voice communications in the pulse mode are given in Volume II of Reference 1.

For a pulsed system operating with a carrier frequency of approximately 5700 Hz, the Poisson statistics indicate that an average of 3.5 counts per pulse are required to guarantee that 97% of the pulses are represented by at least one photon count. For the case that two photon counts are required (such as for the electronic gating system described below) an average of 5.3 photon counts per pulse are required to guarantee good communications. The communications model has thus been formulated in terms of received counts per pulse assuming that the designer of the system in question can determine through a Poisson analysis the number of counts per pulse required to accomplish communications.

Beginning with the first term on the right hand side of the communications model shown in Figure 1, there are 1.33×10^{18} UV photons per joule of radiated energy. The term in the brackets represents the total energy radiated per second per micron from the transmitter lamp. The energy radiated is directly proportional to the average electrical power consumed W_{IN}, the conversion efficiency η to radiation at wavelength λ and the wavelength interval $\Delta\lambda$. The fraction of the

energy transmitted which reaches the vicinity of the detector is represented by the atmospheric transfer function N_{ATM}. The atmospheric transfer function is a complex function depending on the scattering and absorbing characteristics of the atmosphere, the detector field of view function, the angular distribution $S(\Omega)$ of radiation from the transmitter lamp and the detector to source angle. The nature of the atmospheric transfer function will be described below.

The final item in the communications model is the figure of merit which represents the combined effects of the detector aperture area, the filter transmission, the photomultiplier tube quantum efficiency and the pulsing frequency. It is intuitively obvious that the counts per pulse will increase in direct proportion to the detector aperture area, the peak filter transmission and to the phototube quantum efficiency. Likewise, it is obvious that the counts per pulse will be inversely proportional to the pulse frequency. It is important to realize that in any pulsed communications system, the higher the pulse repetition rate, the more energy is required to obtain the communication. Thus, if one doubles the pulse repetition rate, it is also necessary to increase the power consumed by a factor of two.

One of the most important features of an ultraviolet voice communications system is the range which can be obtained for a given electrical power W_{IN} consumed. It has been shown in References 2 and 3 that the atmospheric transfer

function for most weather conditions is strongly dependent on distance and typically varies by several orders of magnitude over just a few kilometers. Thus, large increases in the figure of merit and/or the electrical conversion efficiency are needed to obtain reasonable increases in the range of the UV communications system.

2.2 Measurements of Ultraviolet Scattering and Propagation

A complete description of the measurements carried out under this contract and several previous contracts with the Office of Naval Research, the Air Force Avionics Laboratory and Naval Electronic Systems Command are presented in a massive four volume report[3] entitled "Atmospheric Propagation of Ultraviolet Radiation Through the Lower Atmosphere," A.R.A.P. Report No. 374b, November 1978. A complete description of the equipment used, the procedures followed, the data obtained, and the analysis of that data would be so lengthy that it is unreasonable to repeat the information in this report. Thus, a brief overview of the measurement program will be presented here and the reader is referred to the above mentioned report for a more detailed description.

As mentioned in the introduction, the measurements which were carried out can be divided into two general categories. The first category involved ground to ground propagation and scattering measurements while the second category involved documentation of prevailing atmospheric conditions. Attenuation (extinction) coefficients and the nonaxisymmetric radiant

intensity fields were measured along ground to ground paths for wavelength regions corresponding to the 225-245, 245-265, and 265-285 nm regions. The single scattering phase functions at various wavelengths within the solar blind portion of the ultraviolet spectrum were also measured using a scanning polar nephelometer.

The atmospheric documentation measurements included the barometric pressure, temperature, humidity, ozone concentration and aerosol particle size distribution. The ozone concentrations were measured with a Bendix Model 8002 ozone analyzer. The analyzer works on the chemiluminescence process between atmospheric ozone and ethylene. Aerosol concentrations and size distributions were measured with a Particle Measuring Systems, Inc. (Knollenberg) analyzer over a size range between .075 and 16 microns radius. The humidity was measured using a Bendix psychron aspirated psychromator which is a wet/dry bulb instrument. Ground level photographs were taken using a Miranda Sensorex 35 mm camera with a 50 mm lens and a Soligor 450 mm telephoto lens and Kodacolor 400 film. Other ground level photographs were taken using a Kodak Instamatic camera with Kodacolor II film.

The ultraviolet radiation source used for most atmospheric propagation measurements was a 200 watt mercury xenon lamp which was calibrated both in angular distribution and absolute intensity. The radiometer used to make the ground level measurements and the measurements of the single scattering

phase function utilizes a rubidium telluride photomultiplier tube with a 1 inch diameter photocathode operating in the pulse counting mode. Other ground level measurements were made with a radiometer which uses a cesium telluride tube with a 1.75 inch diameter photocathode obtained from the EMR Company. This detector used a spherical sighting device for finding the polar and azimuthal angle at which the detector was pointed relative to the source to detector line of sight and to the vertical direction. This second radiometer also utilized a collapsing field of view feature for measuring attenuation coefficients. The collapsing field of view was accomplished with an iris located in a focal plane of the collecting lens. Thus, the field of view function of the detectors changed as a function of the iris setting. Attenuation coefficients were made with the rubidium telluride radiometer by looking at the radiation source through a long cylindrical tube with a small hole at each end which restricted the total field of view angle to a very small steradiancy.

The absolute intensity calibration of the various detectors was accomplished with an ultraviolet standard deuterium lamp. The relative intensity calibration T_{VAC} for the various radiometers was measured in terms of the overall detector count rate which would be obtained for direct line of sight viewing of each particular radiation source at a distance of 1.0 km under vacuum conditions. In reality, the intensity calibrations were made over sufficiently short distances that

atmospheric attenuation is effectively zero. These relative intensity calibrations were used to normalize both scattered and directly transmitted radiation measured in the field. Thus, the resulting normalized scattered radiances and directly transmitted radiation were independent of the lamp and detector characteristics.

Wavelength discrimination filters with nominal bandpasses of 225-245, 245-265, and 265-285 nm were used together with the rubidium telluride radiometer to obtain spectral discrimination. These filters are shown in Figure 2. A special solar blind filter constructed by Ed Barr Associates was used for the 2 inch diameter cesium tube which is shown in Figure 3. Wavelength discrimination filters which could be used together with the solar blind filters shown in Figure 3 are shown in Figure 4.

A scanning polar nephelometer was used to measure the single scattering phase functions. The reader is referred to Reference 7 for a complete description of the operation of the scanning polar nephelometer. A schematic of the nephelometer is shown in Figure 5. The source of the ultraviolet radiation was a Model 6111 Oriel Universal Arc Source which incorporates a 200 watt mercury xenon lamp. An Oriel Model 6207 ultracollimator which was specially modified by the Oriel Corporation to operate in the ultraviolet has been added to the lamp to provide a clean incident beam. The lamp was mounted on the end of a rotatable four foot aluminum

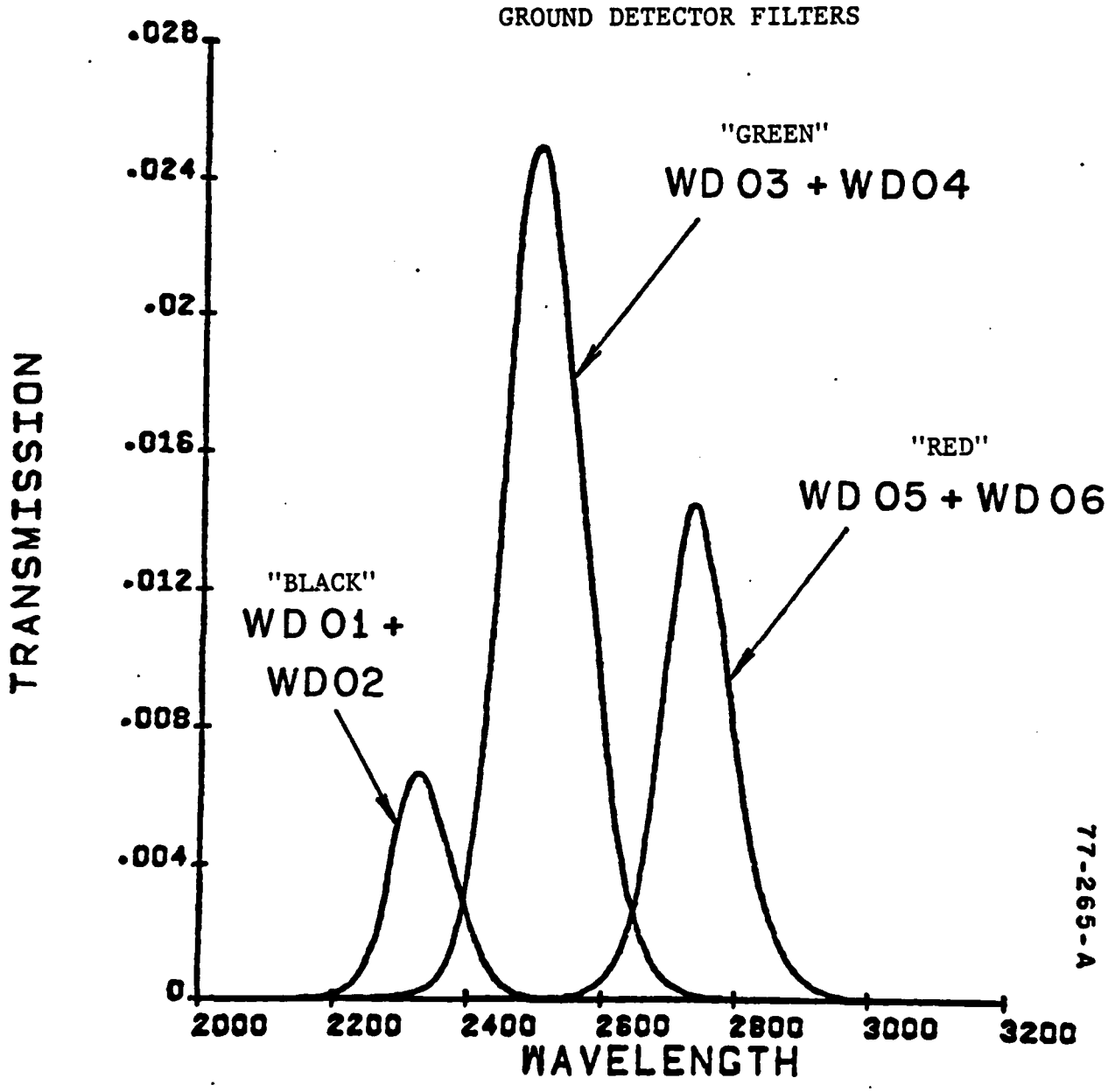

Figure 2. Transmittance of one inch diameter solar blind filters.

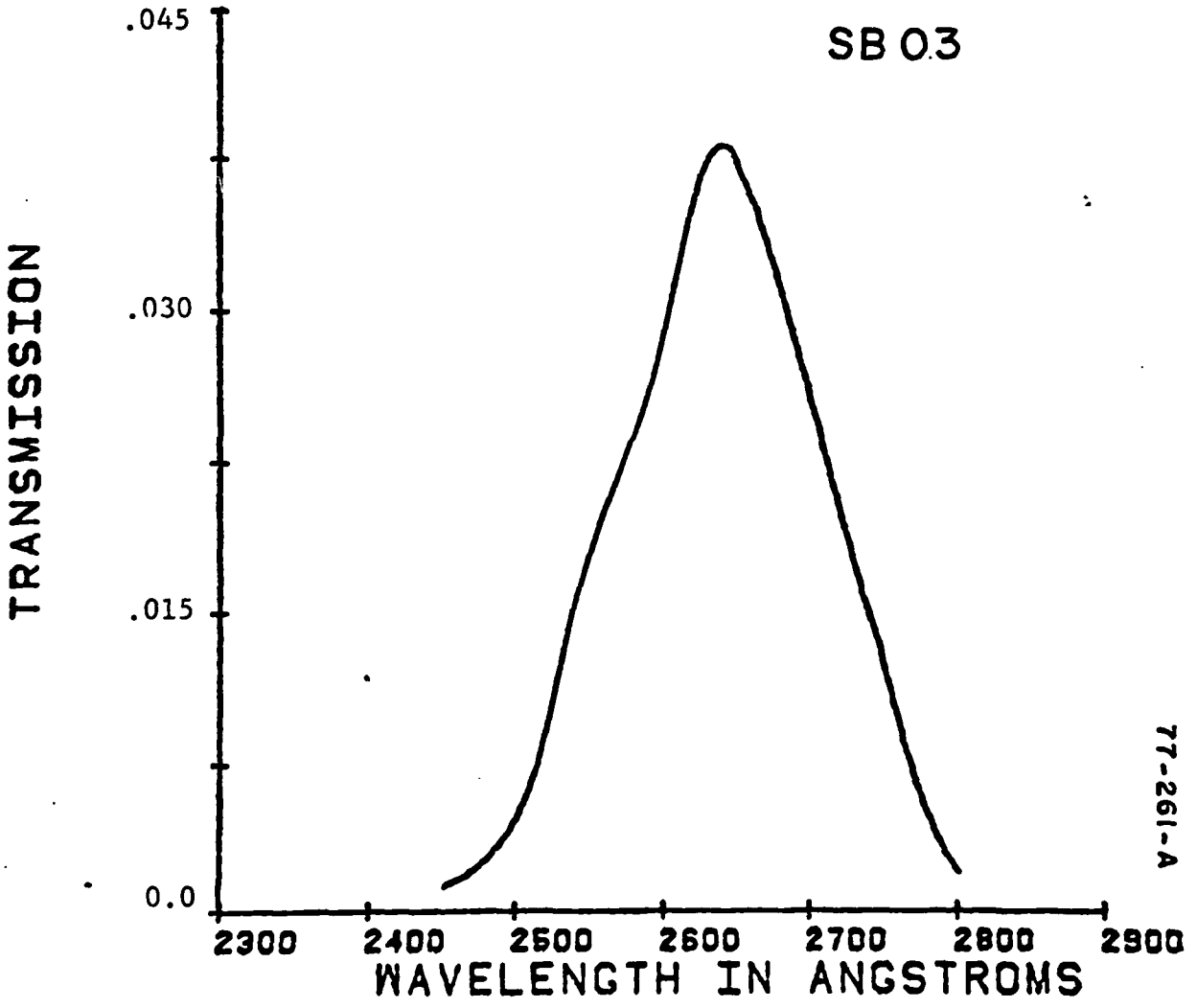

Figure 3. Transmittance of two inch diameter solar blind filters.

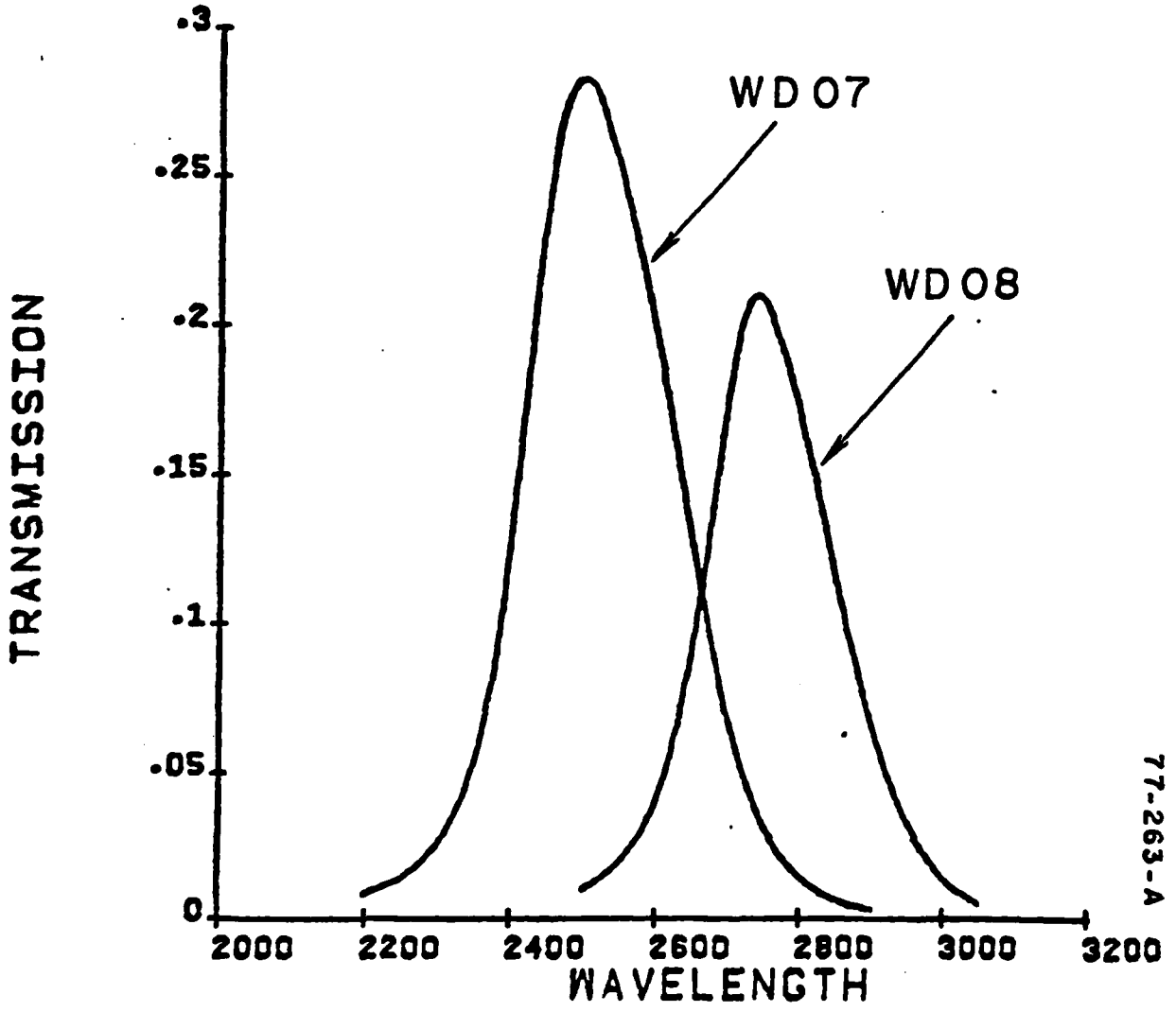

Figure 4. Transmittance of two inch diameter wavelength discrimination filters.

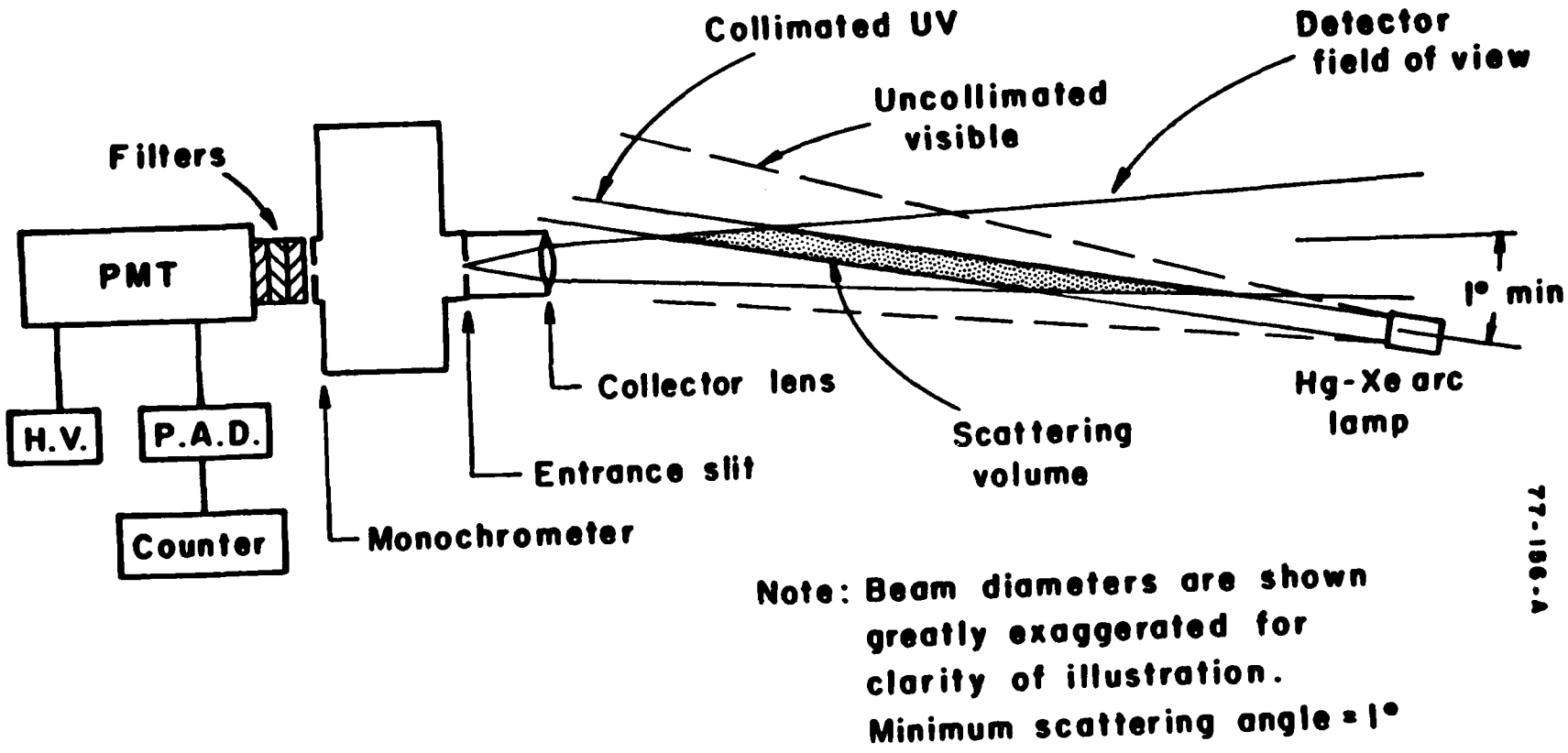

Figure 5. Schematic of Ultraviolet Scanning Polar Nephelometer.

channel that allows for any scattering angle from 0 to 170°. The detector assembly consisted of a Jarrell Ash Model 82-410 quarter meter monochromator and a collecting lens which was mounted on the front of the entrance slit of the monochromator at a distance equal to its focal length. A rubidium telluride photomultiplier tube was used as a detector.

On each given day for which measurements were carried out, both the directly transmitted radiation, which leads to the attenuation or extinction coefficient, and the scattered radiation as a function of angle were measured at several detector locations. The scattered radiances, which are typically normalized with respect to the vacuum transmission of the lamps T_{VAC} are sometimes referred to as scattering footprints since they represent the scattered radiation arriving from various positions in the sky.

The transmission and scattering measurements were carried out at three different geographic locations under the present contract. Measurements were carried out at the Wayside Laser Test Range at Ft. Monmouth, New Jersey, at A.R.A.P.'s Princeton location and on San Nicolas Island, off the west coast of the United States. A summary of the measurements made under the present program are given in Table 1. This table indicates the date, general weather conditions, visibility, and average temperature, humidity and ozone concentration measured on the day in question. Also shown are the scattering coefficients obtained by integrating the single scattering

SUMMARY OF DATA

DATE	WEATHER	VIS (km)	TEMP (°F)	HUM (%)	OZONE		TOTAL $k_{SCAT}(km^{-1})$			
					PPM	$k_{ABS}(km^{-1})$ λ=265NM	230NM	250NM	265NM	275NM
7/26	clear	25	75	71	.007	.18	-	.622	.60	-
7/28	rain, haze	8	79	73	.02	.50	-	-	1.34	-
8/31	rainy day; high mist	8	78	83	.04	1.00	-	-	1.41	-
9/22	cloudy-hazy	12	74	84	.005	.13	-	-	1.35	-
10/11	variable fog	1.5	63	89	-	-	1.19	1.42	1.49	1.15
10/12	clear, sunny a.m. - heavy fog p.m.	15 to 1.5	65	86	.082	2.06	1.19	1.09	.81	.87

TABLE 1.

phase functions measured with the scanning polar nephelometer.

A summary table for each day's measurements are shown in Tables 2 through 7. These tables indicate the site location, the altitude of the detector with respect to the source, the time of day, the source to receiver range in kilometers, the angle which the source to receiver line of sight makes with the horizontal, the temperature in degrees Fahrenheit, the total number density of particles within the 0.1 to 0.2 micron radius range, the measured attenuation coefficients for the solar blind (S), red (R), blue/green (B/G), and black (BL) filters. Also tabulated are the logs of the normalized radiances measured at an elevation angle of 15^{o} above the source to receiver line of sight. The filter symbols correspond to the filter transmission curves shown in Figures 2 and 3. Photographs showing prevailing weather conditions on the days for which measurements were carried out are shown in Figures 6 through 11, respectively.

Samples of the scattered radiance measurements made at the Wayside Laser Test Range at Ft. Monmouth, New Jersey are shown in Figures 12 through 18. In all cases, data is shown by solid lines or solid lines connecting data points. The dashed lines represent theoretical calculations carried out using the A.R.A.P. phenomenological scattering model which will be described below. The vertical axes of these plots represents the log of the absolute magnitude of the scattered radiation normalized with respect to the directly

FORT MONMOUTH, NJ
GROUND BASED AND HELICOPTER #2 DETECTORS
LAMP #3
(#2 Helicopter Detector Used in Air)

Date July 26, 1978

Site*	Alt* (km)	Time†	Range (km)	α* (deg)	Temp (°F)	$Log_{10}(N(r))$ ($cc^{-1}\mu m^{-1}$)	Attenuation Coeff.** (km^{-1})				Log_{10}(Normalized Radiance at 15°)***			
							S	R	B/G	B1	S	R	B/G	B1
FM2	.37	14.40	.883	23.5	68	1.51	.87	-	-	-	-.30	-	-	-
FM2	.37	15.00	.883	23.5	68	2.57	-	-	-	-	-.62	-	-	-
FM5	.91	14.70	2.75	19.1	60	2.52	1.26	-	-	-	-1.48	-	-	-
FM4	.82	14.8	1.97	24.0	62	1.79	1.44	-	-	-	-1.20	-	-	-
.81G	-.014	15.45	.81	-.99	-	-	.53	-	-	-	-.27	-	-	-
1.9G	-.007	16.00	1.9	-.21	-	-	+1.1	-	-	-	-.86	-	-	-
2.6G	-.007	16.25	2.6	-.15	-	-	-	-	-	-	-1.10	-	-	-

* See Figure 24

† Decimal Time

** Text Attenuation Coeff. Def.

*** Text Normalized Rad.

Table 2. Summary of Data for July 26, 1978 Measurements at Fort Monmouth, N.J.

FORT MONMOUTH, NJ
GROUND BASED AND HELICOPTER #2 DETECTORS
LAMP #3
(#2 Helicopter Detector Used in Air and on Ground)

Date July 28, 1978

Site*	Alt* (km)	Time†	Range (km)	α* (deg)	Temp (°F)	$Log_{10}(N(r))$ $(cc^{-1}\mu m^{-1})$	Attenuation Coeff.**(km^{-1})				Log_{10}(Normalized Radiance at 15°)***			
							S	R	B/G	B1	S	R	B/G	B1
FM2	.37	14.20	.883	23.47	70	-	1.27	-	-	-	-.69	-	-	-
FM5	1.21	14.33	2.86	24.74	63	-	1.8	-	-	-	-2.33	-	-	-
FM4	.91	14.70	2.01	26.4	68	-	2.2	-	-	-	-1.72	-	-	-
FM1	.18	14.80	.481	20.57	77	-	.94	-	-	-	-	-	-	-
FM3	.64	14.90	1.44	25.7	70	-	2.3	-	-	-	-	-	-	-
FM5	.01	16.20	2.6	-.15	79	-	1.97	-	-	-	-1.80	-	-	-
.81G	-.014	14.00	.81	-.99	-	-	-	-	-	-	-.57	-	-	-

* See Figure 24

† Decimal Time

** Text Attenuation Coeff. Def.

*** Text Normalized Rad.

Table 3. Summary of Data for July 28, 1978 Measurements at Fort Monmouth, N.J.

PRINCETON, NJ
#2 HELICOPTER DETECTOR USED ON GROUND
LAMP #3

Date August 31, 1978

Site*	Alt* (km)	Time†	Range (km)	α* (deg)	Temp (°F)	$Log_{10}(N(r))$ $(cc^{-1}\mu m^{-1})$	Attenuation Coeff.**(km^{-1})				Log_{10}(Normalized Radiance at 15°)***			
							S	R	B/G	B1	S	R	B/G	B1
1.2G	-.038	15.92	1.2	-1.8	82	-	.87	-	-	-	-.70	-	-	-
2.3G	-.038	16.33	2.3	-.94	82	-	2.23	-	-	-	-2.57	-	-	-
1.2G	-.038	16.75	1.2	-1.8	82	-	1.7	-	-	-	-.49	-	-	-
.55G	-.032	17.08	.55	-4.4	82	-	1.5	-	-	-	-.21	-	-	-
.17G	-.032	17.33	.169	-10.99	82	3.35	1.7	-	-	-	.11	-	-	-

* See Figure 21

† Decimal Time

** Text Attenuation Coeff. Def.

*** Text Normalized Rad.

Table 4. Summary of Data for Aug. 31, 1978 Measurements at Princeton, N.J.

PRINCETON, NJ
#2 HELICOPTER DETECTOR USED ON GROUND
LAMP #3

Date Sept. 22, 1978

Site*	Alt* (km)	Time†	Range (km)	α* (deg)	Temp (°F)	$Log_{10}(N(r))$ $(cc^{-1}\mu m^{-1})$	Attenuation Coeff.**(km^{-1})				Log_{10}(Normalized Radiance at 15°)***			
							S	R	B/G	B1	S	R	B/G	B1
2.3G	-.038	16.05	2.3	-.94	67	2.56	.53	.56	.60	-	-.09	-.15	-.44	-
1.2G	-.038	15.52	1.2	-1.8	67.5	-	.44	.42	.46	-	+.09	+.01	-.12	-
.55G	-.032	16.50	.55	-4.4	67.0	-	.23	.13	.13	-	-.20	-.04	-.28	-
.17G	-.032	16.83	.169	-10.99	68.0	-	.81	-1.6	.18	-	-	-	-	-

* See Figure 21

† Decimal Time

** Text Attenuation Coeff. Def.

*** Text Normalized Rad.

Table 5. Summary of Data for Sept. 22, 1978 Measurements at Princeton, N.J.

SAN NICOLAS ISLAND
#2 HELICOPTER DETECTOR USED ON GROUND
LAMP #3

Date Oct. 11, 1978

Site*	Alt* (km)	Time†	Range (km)	α* (deg)	Temp (°F)	$Log_{10}(N(r))$ $(cc^{-1}\mu m^{-1})$	Attenuation Coeff.** (km^{-1})				Log_{10}(Normalized Radiance at 15°)***			
							S	R	B/G	B1	S	R	B/G	B1
SN2	0.0	13.25	2.5	0.0	64	2.38	1.15	-	-	-	-1.12	-	-	-
SN2	0.0	13.50	2.5	0.0	64	2.79	1.46	-	-	-	-1.92	-	-	-
SN2	0.0	13.58	2.5	0.0	64	2.79	1.75	-	-	-	-1.89	-	-	-
SN2	0.0	13.70	2.5	0.0	64	2.79	1.53	-	-	-	-1.90	-	-	-
SN2	0.0	13.77	2.5	0.0	64	2.79	1.60	-	-	-	-1.47	-	-	-
SN2	0.0	13.91	2.5	0.0	64	2.79	1.52	-	-	-	-1.52	-	-	-

* See Figure 25

† Decimal Time

** Text Attenuation Coeff. Def.

*** Text Normalized Rad.

Table 6. Summary of Data for Oct. 11, 1978 Measurements at San Nicolas Island.

SAN NICOLAS ISLAND
#2 HELICOPTER DETECTOR USED ON GROUND
LAMP #3

Date Oct. 12, 1978

Site*	Alt* (km)	Time†	Range (km)	α* (deg)	Temp (°F)	$Log_{10}(N(r))$ $(cc^{-1}\mu m^{-1})$	Attenuation Coeff.**(km^{-1})				Log_{10}(Normalized Radiance at 15°)***			
							S	R	B/G	B1	S	R	B/G	B1
SN2	0.0	21.25	2.5	0.0	60	2.93	1.33	-	-	-	-1.31	-	-	-
SN2	0.0	21.30	2.5	0.0	60	2.93	1.33	-	-	-	-	-	-	-
SN3	0.0	21.92	4.0	0.0	60	2.91	1.33	-	-	-	-2.45	-	-	-

* See Figure 25

† Decimal Time

** Text Attenuation Coeff. Def.

*** Text Normalized Rad.

Table 7. Summary of Data for Oct. 12, 1978 Measurements at San Nicolas Island.

WEATHER DOCUMENTATION FOR JULY 26, 1978

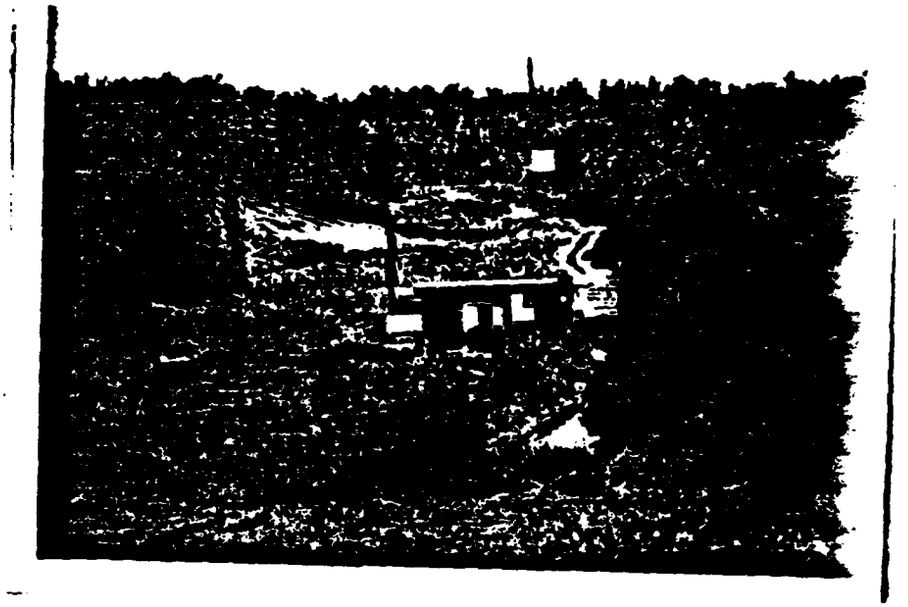

Looking Downrange From Source (Telephoto Lens)

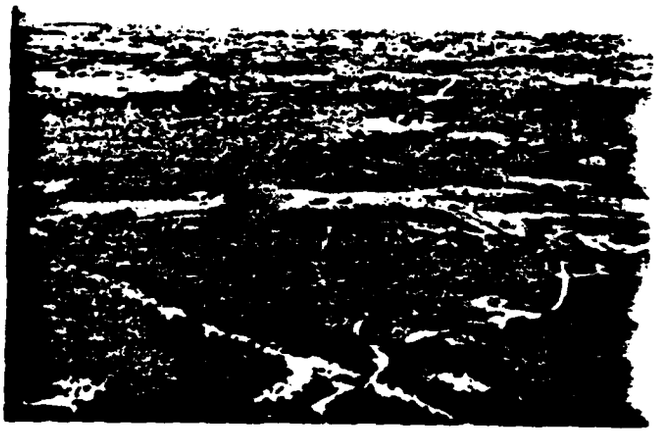

Airborne Photograph. Laser Range at Bottom.

Figure 6. Photographs taken on July 26, 1978.

WEATHER DOCUMENTATION FOR JULY 28, 1978

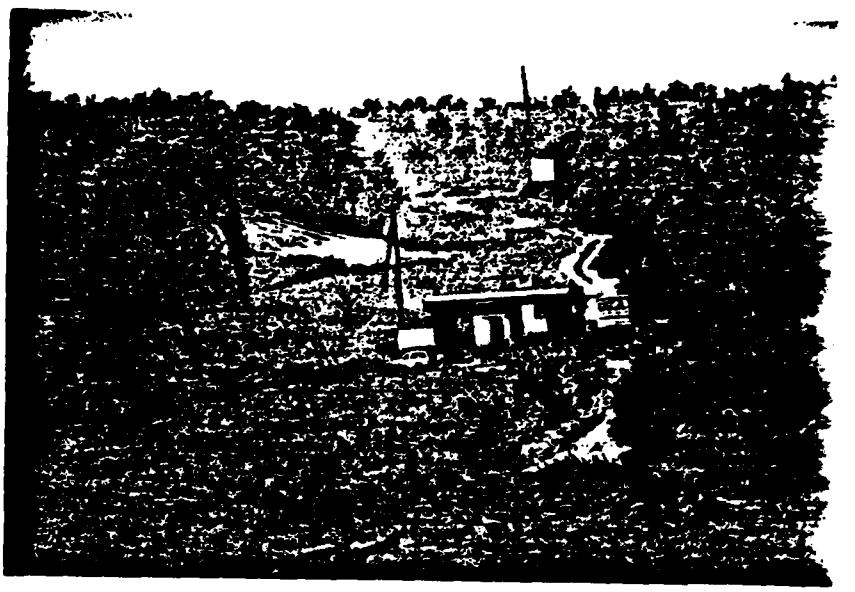

Looking Downrange From Source (Telephoto Lens)

Airborne Photograph. Laser Range at Bottom Right.

Figure 7. Photographs taken on July 28, 1978.

Looking at Source from 1.2 km Site

Ground Level Photograph

Figure 8. Photographs taken on Aug. 31, 1978.

Looking at Source from 1.2 km Site

Ground Level Photograph

Figure 9. Photographs taken on Sept. 22, 1978.

View to the Northwest

View of SN2 Site from Source

Figure 10. Photographs taken on Oct. 11, 1978.

View to the Northwest

View of SN2 Site from Source

Figure 11. Photographs taken on Oct. 12, 1978.

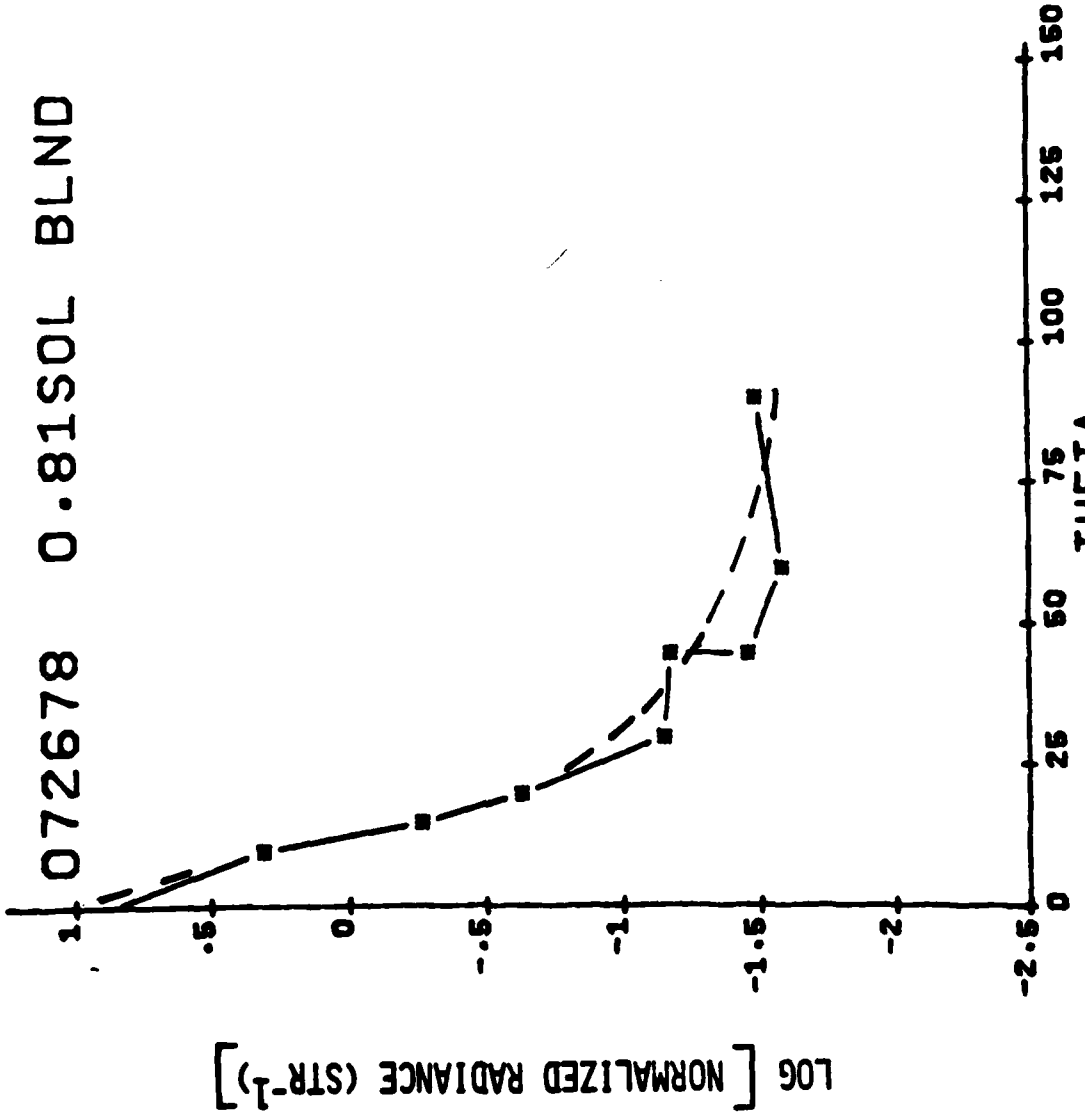

Figure 12. Comparison of Data with Theory at .81 Km Site Using Solar Blind Filter on 7/26/78.

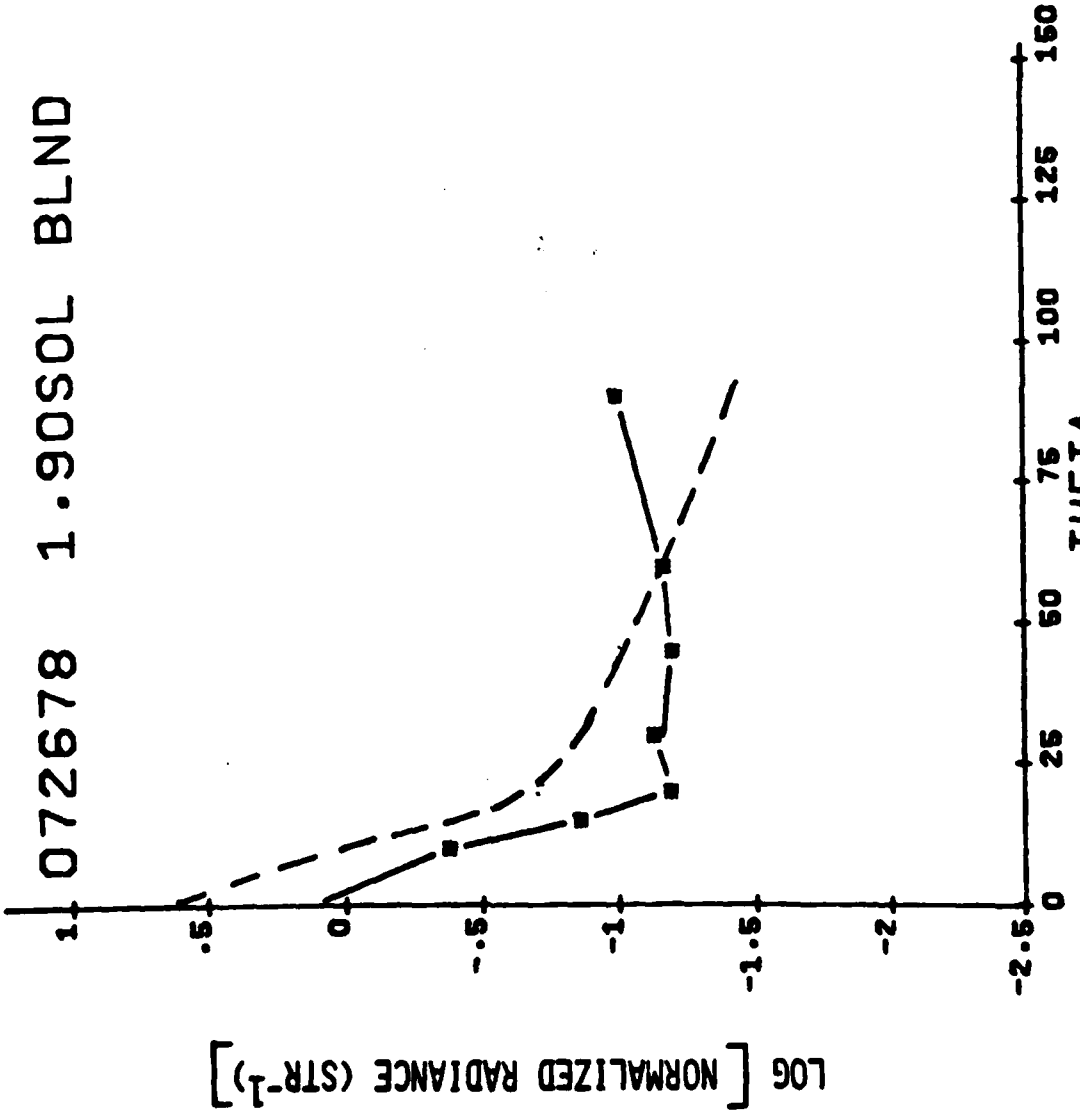

Figure 13. Comparison of Data with Theory at 1.9 Km Site Using Solar Blind Filter on 7/26/78.

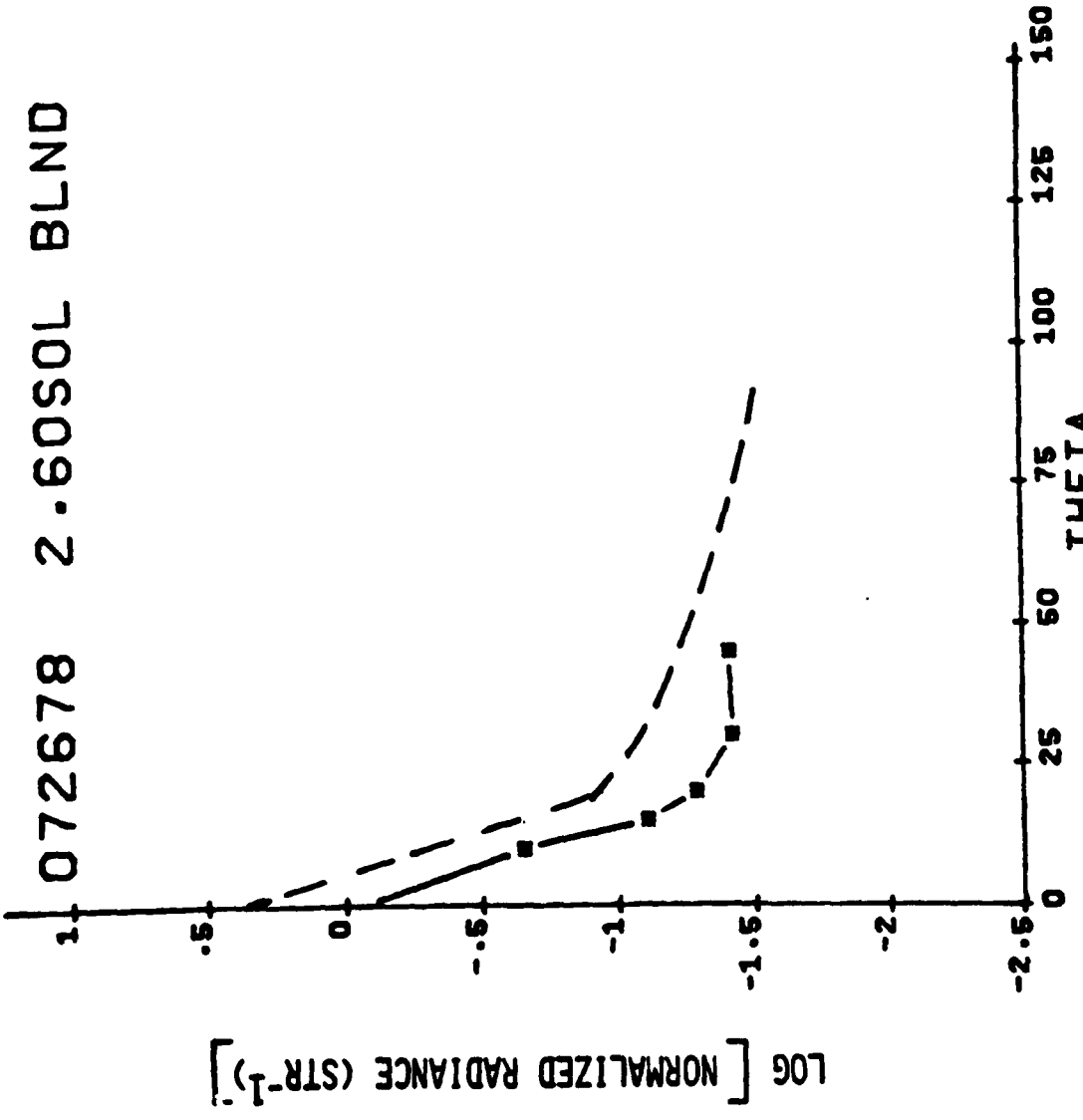

Figure 14. Comparison of Data with Theory at 2.6 Km Site Using Solar Blind Filter on 7/26/78.

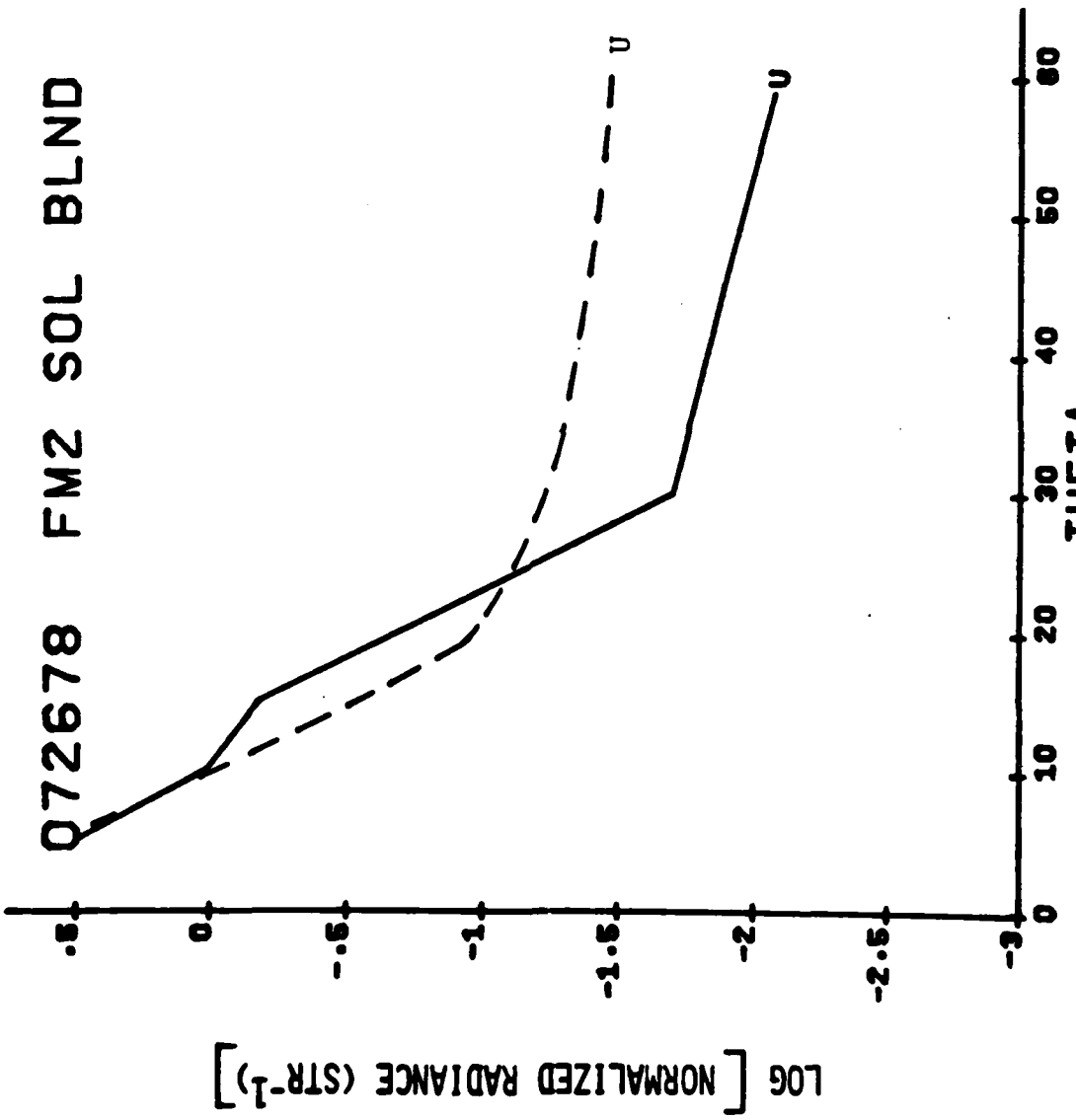

Figure 15. Comparison of Data with Theory at FM2 Site Using Solar Blind Filter on 7/26/78.

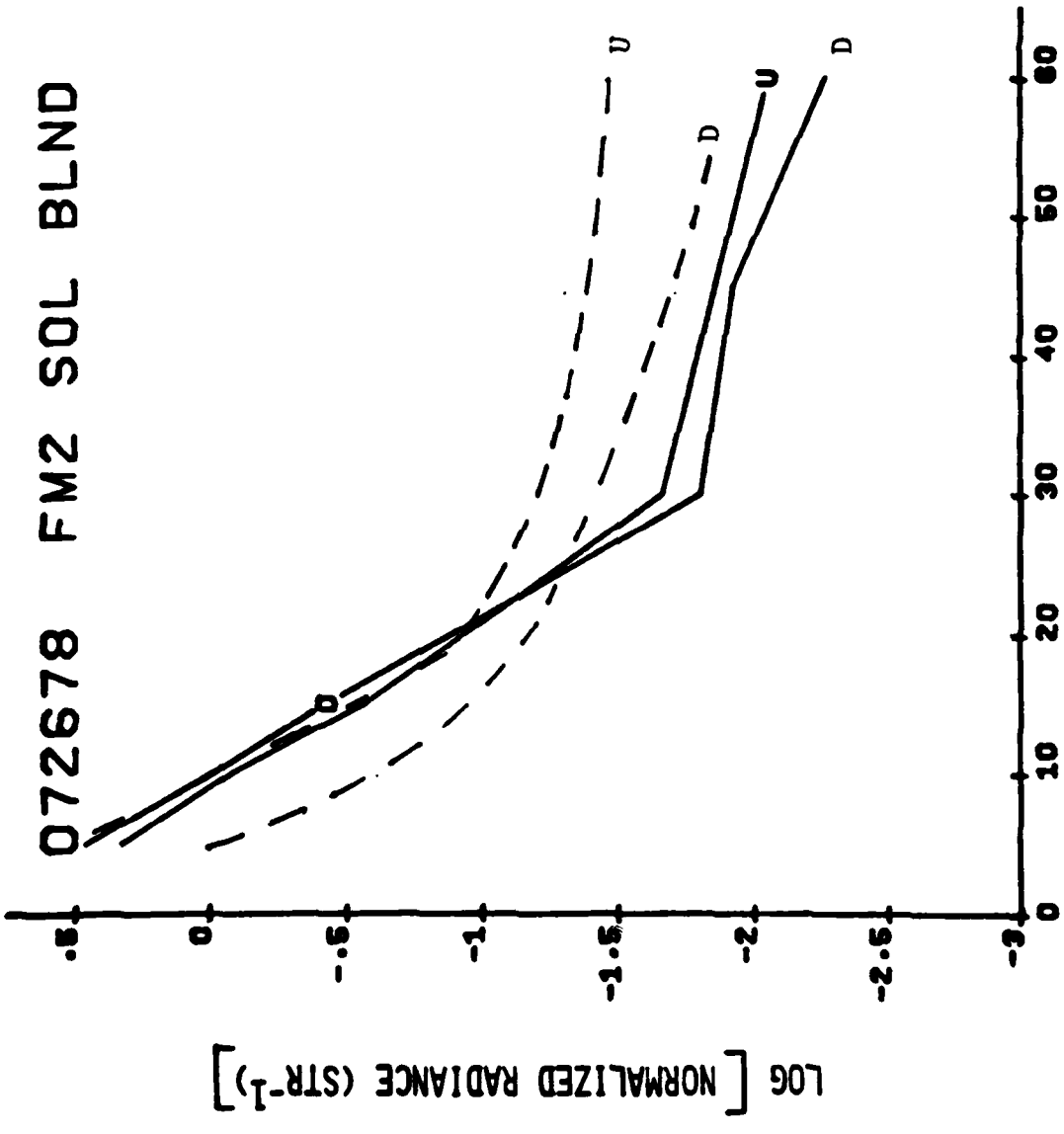

Figure 16. Comparison of Data with Theory at FM2 Site Using Solar Blind Filter on 7/26/78.

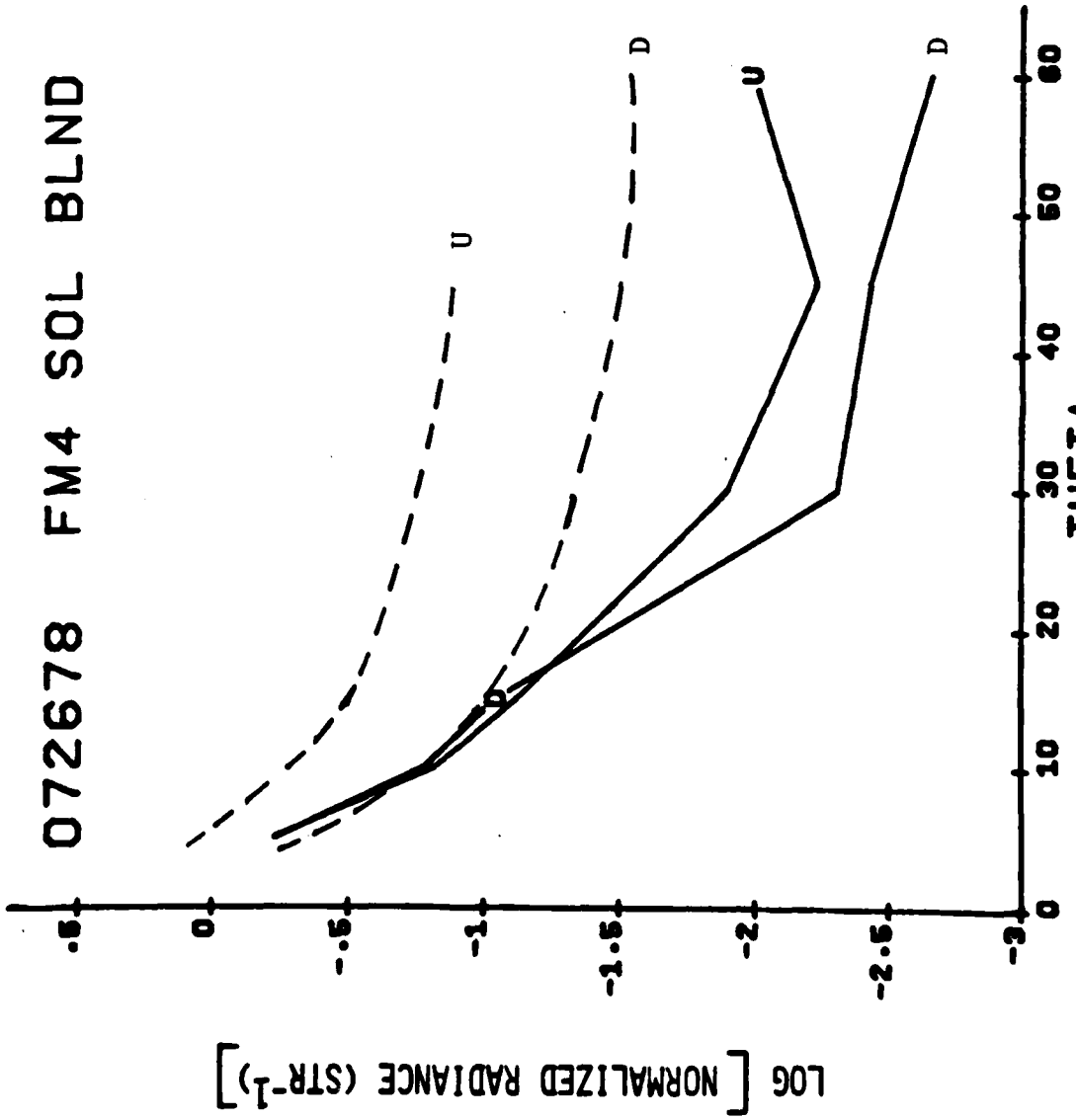

Figure 17. Comparison of Data with Theory at FM4 Site Using Solar Blind Filter on 7/26/78.

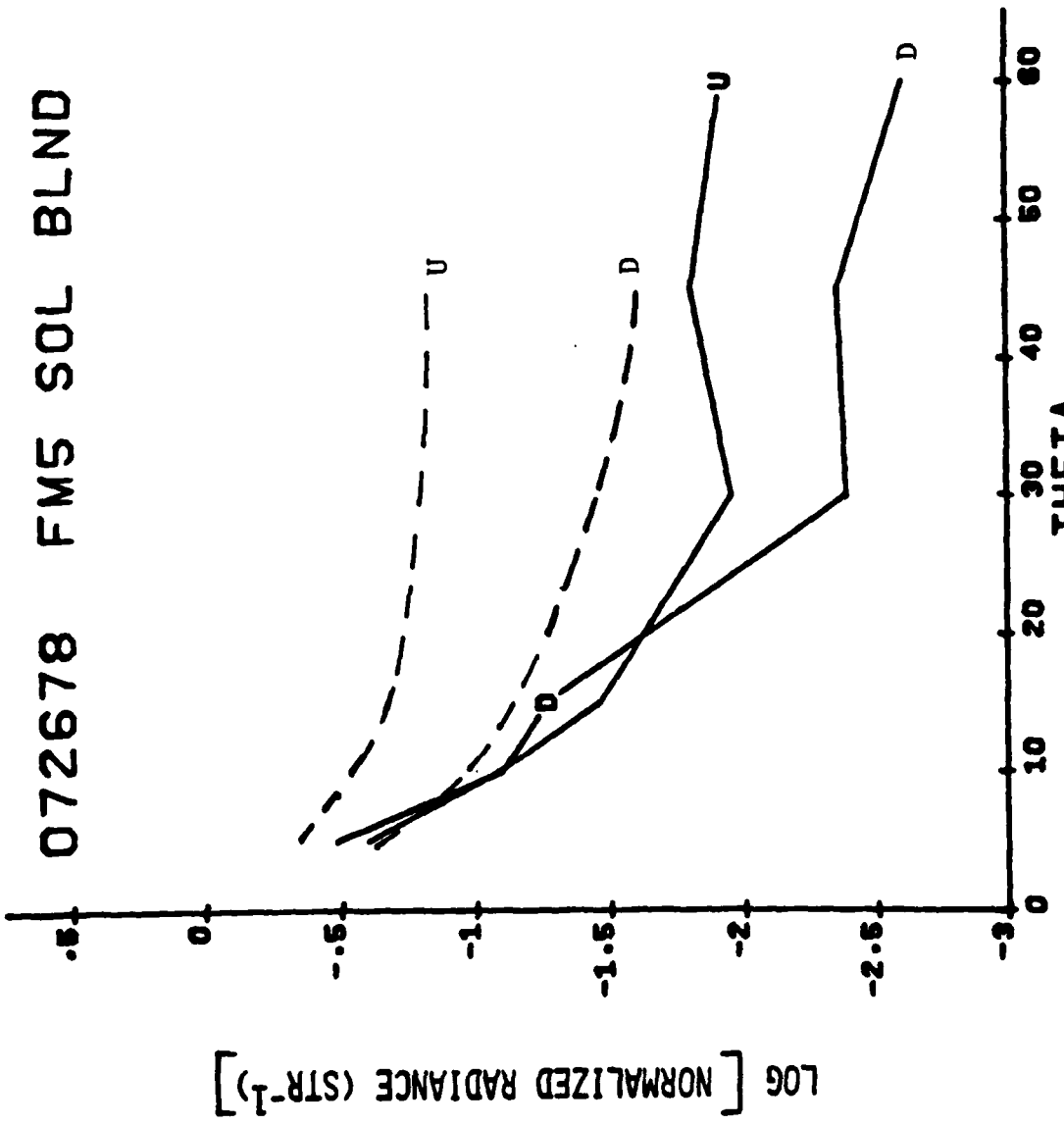

Figure 18. Comparison of Data with Theory at FM5 Site Using Solar Blind Filter on 7/26/78.

transmitted radiation T_{VAC} which would have been measured in a vacuum at the same range. The horizontal axis in these figures represents the elevation angle which the detector optical axis makes with respect to the source to receiver line of sight. Some of the measurements shown in Figures 12 through 18 were taken from a helicopter platform along a 30^{o} slant path with the horizontal. For these cases, the elevation angle between the detector optical axis and the source to receiver line of sight has been measured both in the upward and downward direction corresponding to the U's and D's on the figures.

As can be seen from Figures 12 through 14, reasonable correlation is obtained between data and theory for ground level measurements. Comparisons between measured and predicted scattered radiances for various airborne locations are shown in Figures 15 through 18. The comparison of radiation in the upper direction U is generally quite good at low values of θ and rapidly diverge at higher angles. This result is not totally unexpected since no measurements (Figure 19) were made at altitudes above the maximum helicopter altitude to determine the aerosol concentrations which should be used in the scattering calculations. Consequently, the slope of the increasing aerosol concentration shown in Figure 19 has been extrapolated to represent the atmospheric scattering at higher altitudes.

In contrast, comparisons of measured and predicted

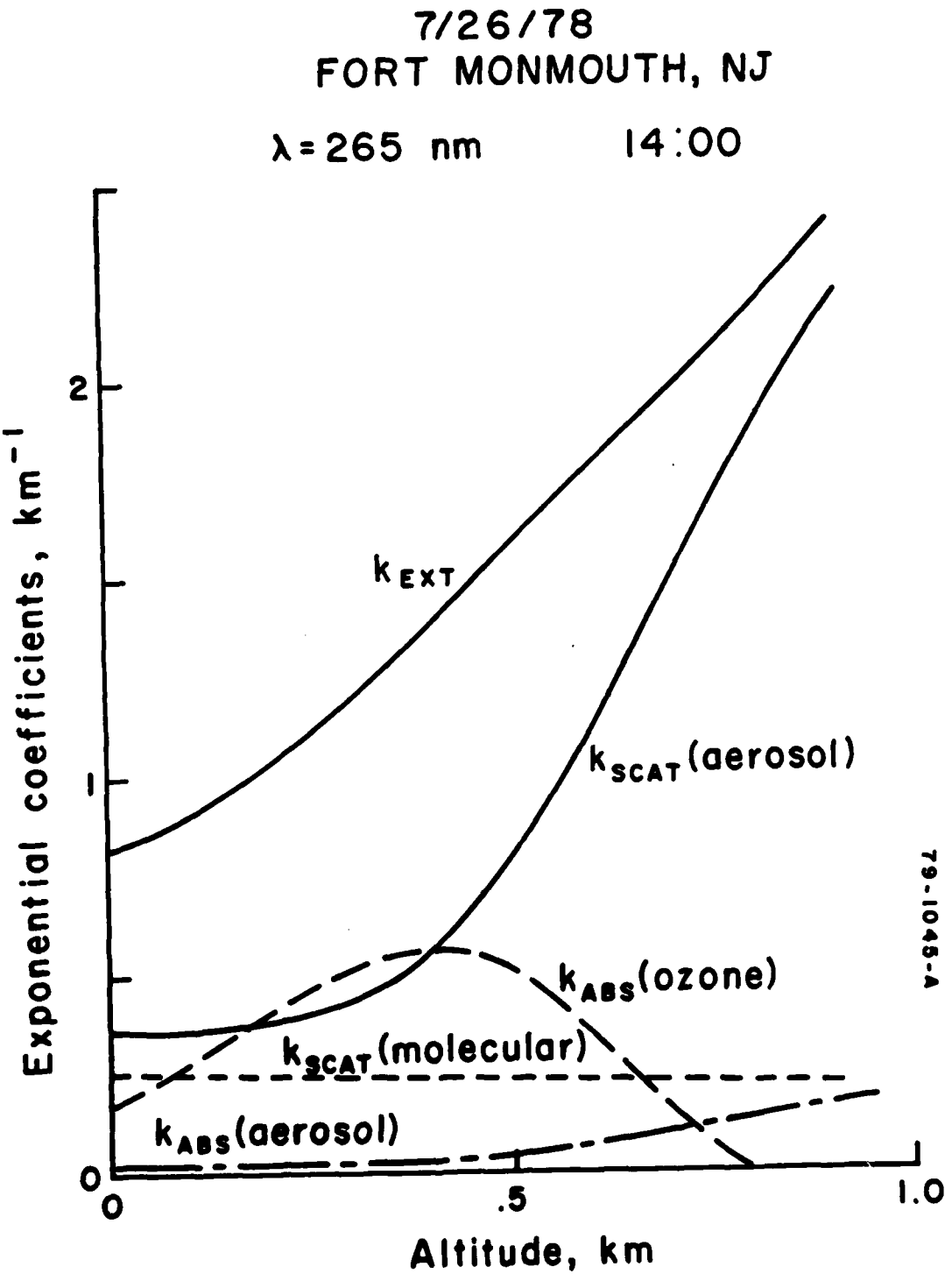

Figure 19. Altitude Variation of Atmospheric Optical Properties on July 26, 1978.

scattering for the downward direction D are generally better for lower angles, but diverge at higher angles. These results are not totally unexpected because of the flight path flown by the helicopter. As shown in Figure 6, the Wayside Laser Test Range is basically a long, narrow clearing in a heavily wooded area. The circular arcs flown by the helicopter generally started over the opening in the woods and proceeded to approximately a 45^{o} angle past the opening. While the lamp was always visible from the helicopter, much of the potential scattering volumes were shaded by the trees. In addition, the helicopter pilot did not have carefully laid out ground locations to fly over and consequently, the slant path ranges tended to increase with time as he flew away from the clearing. The general procedure followed during the airborne measurements was to make measurements for low elevation angles while the helicopter was immediately over the clearing and to make measurements at successively higher elevation angles as the helicopter flew away from the clearing. Considering the experimental difficulties encountered in the measurements made on July 26, the overall agreement between data and theory is quite good.

Another example of the measurements made under the current contract are shown in Figures 20 through 22 for ground level measurements made on September 22, 1978. Photographs showing the prevailing weather conditions on September 22 are shown in Figure 9. The weather conditions could generally be

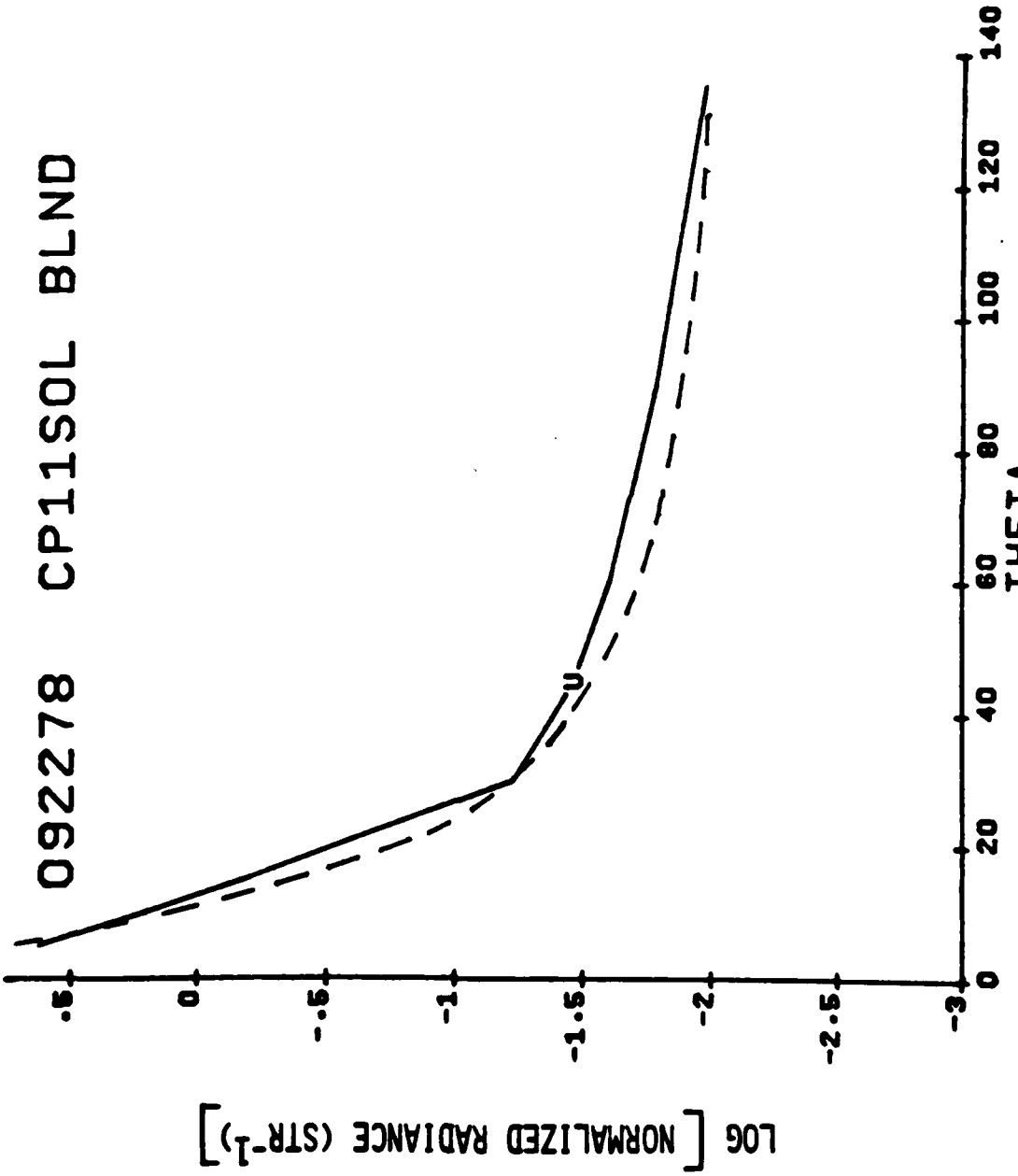

Figure 20. Comparison of Data with Theory at CP11 Site Using Solar Blind Filter on 9/22/78.

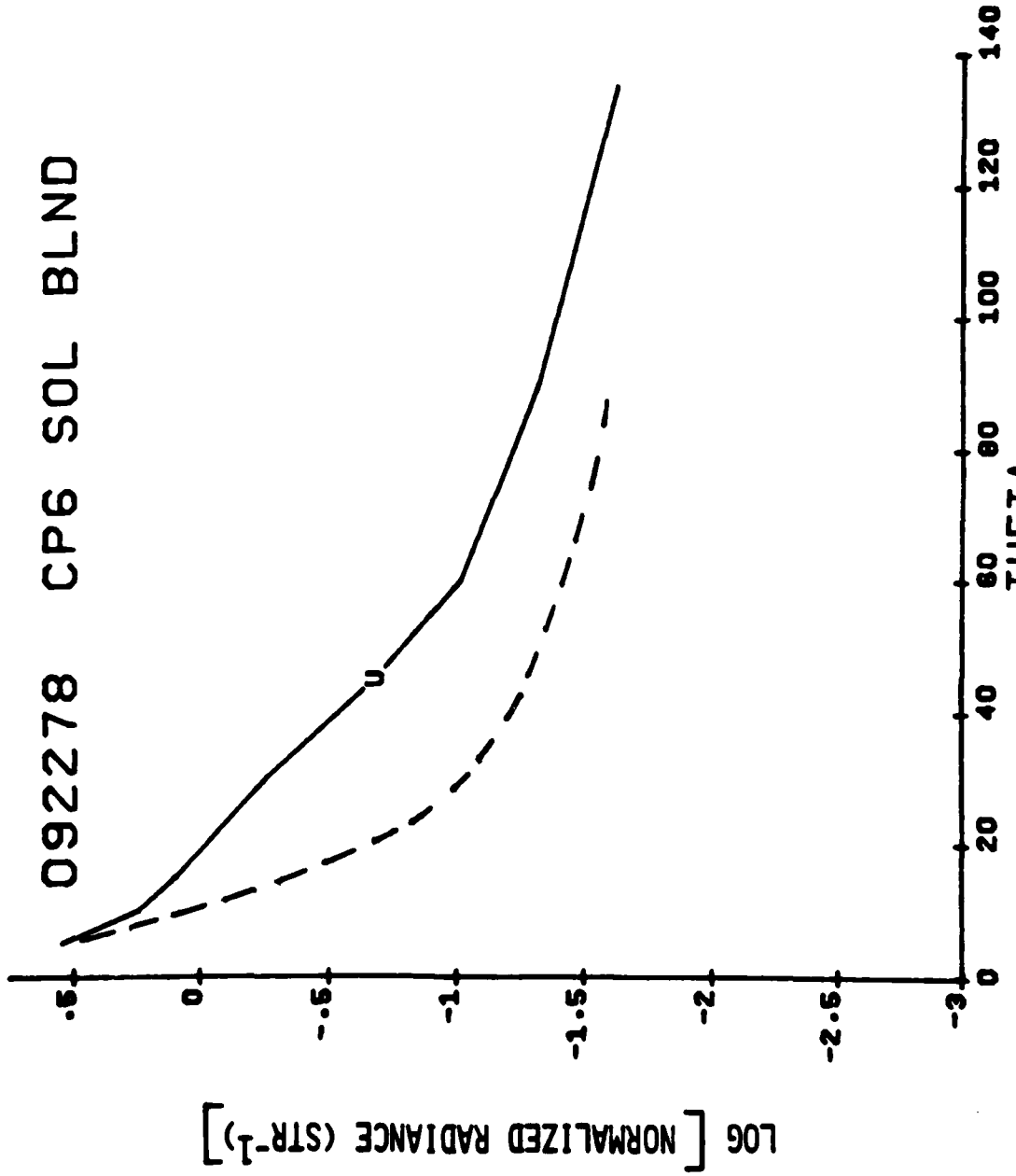

Figure 21. Comparison of Data with Theory at CP6 Site Using Solar Blind Filter on 9/22/78.

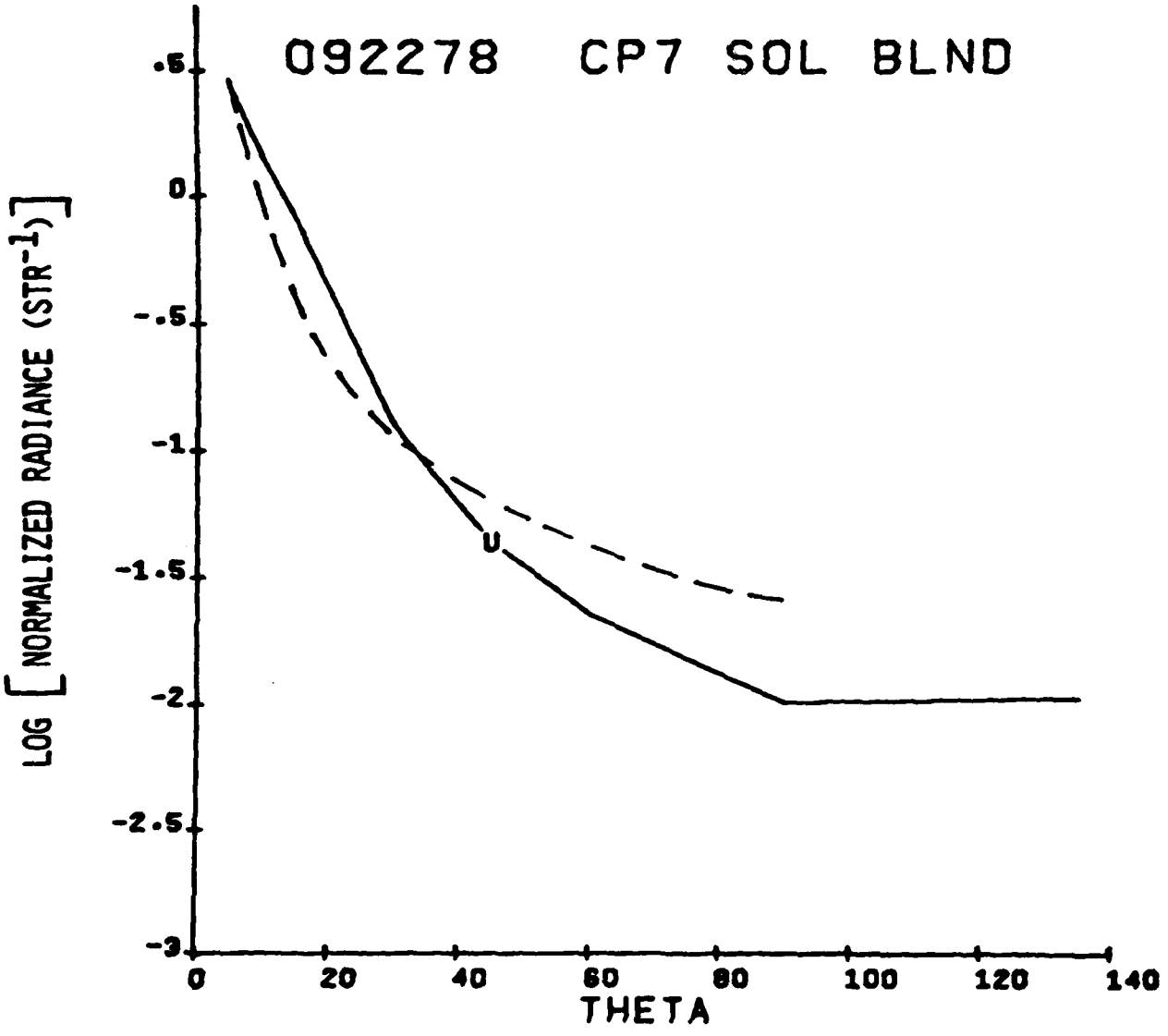

Figure 22. Comparison of Data with Theory at CP7 Site Using Solar Blind Filter on 9/22/78.

described as cloudy and hazy with a temperature of 74° and generally high scattering and low ozone. The CP11, CP6 and CP7 sites shown in Figures 20 through 22 correspond to .55, 1.2 and 2.3 km ranges. Comparisons between data and theory are reasonably good except for some angles at the CP6 location.

A subjective survey of all the comparisons between data and theory shown in this report and in Reference 3 has resulted in the following conclusions. The agreement between data and theory for both airborne and ground level measurements can be classified as good or excellent, approximately 65% of the time. The model used to predict values of the scattered radiance (which will be discussed below) are quite sensitive to the atmospheric input parameters such as ozone concentration and aerosol size distribution. The discrepancy between the extinction coefficients measured optically and those predicted from ozone and aerosol concentrations is more than sufficient to account for the observed discrepancies in the measured and predicted scattered radiance fields.

It is the opinion of the authors of this report that the phenomenological atmospheric propagation and scattering model compares quite well with the measured data. Discrepancies between measured and predicted data show no consistent trends or patterns. Most of the discrepancies between data and theory can be explained or at least associated with the general uncertainties in the atmospheric optical properties which are used as input to the model.

2.3 Atmospheric Propagation Model

Two atmospheric scattering and propagation models are currently in use at A.R.A.P. One is a Monte Carlo scattering program[8] originally developed at Radiation Research Associates in Fort Worth, Texas. To the best of our knowledge, this Monte Carlo scattering code is the most sophisticated code of its kind in existence. The Monte Carlo code can treat all the complexities of the ultraviolet propagation problem. Unfortunately, the code requires large amounts of storage space and is relatively slow. The other model is a phenomenological scattering model originally developed at A.R.A.P. (References 1, 2, and 3) and modified under this contract.

Any computerized model used to solve the atmospheric propagation problem associated with wide field of view ultraviolet detectors must be sophisticated enough to treat the real world complexities and fast enough to solve the entire multi-dimensional problem in a reasonable time. The real world complexities of the problem include the aspect angle dependence of the ultraviolet radiation from the plume, non-alignment of the plume to detector line of sight with either the detector optical axis or the lamp axis of symmetry, wide field of view detectors with complex angular response functions, steep vertical gradients in the concentrations of aerosols and ozone, an absorbing ground plane and a strong dependence on a wide range of weather conditions. The problem is multi-dimensional because there are often multiple detectors, the

transmitter to receiver geometry changes with time, radiation at each wavelength within the bandpass propagates differently and the intensity of the lamp radiation is a strong function of wavelength and aspect angle relative to the lamp axis of symmetry.

The phenomenological scattering model is ideally suited to solving the real world multi-dimensional problems discussed above. The phenomenological model represents an attempt to model the physics of the ultraviolet atmospheric propagation problem as observed in the extensive measurement program. The approach taken in developing the phenomenological model has been much different than the usual procedure of finding mathematical solutions to the radiative transport equations through a series of simplifying assumptions. The accuracy of the model has been verified both by comparison with measured data and by comparison with other models[9,10] currently in use. The only other model we know of which can handle problems of equal complexity is the Monte Carlo code described above which requires an order of magnitude more computer time and enormous amounts of computer storage space.

A detailed description of the phenomenological scattering and propagation computer code has been presented in Reference 3 and is beyond the scope of this report. While the reader is referred to Reference 3 for a complete description of the model, a comparison of the model with other models will be presented here.

A comparison of the Monte Carlo scattering code[8] in use at A.R.A.P. and the A.R.A.P. phenomenological model[3] with the models of Riewe and Green[10] and Zacor[9] is shown in Figure 23 for the baseline condition shown in Table 8. Riewe and Green utilize a Monte Carlo technique while Zacor utilizes a multiple recursion formula. The calculations have been carried out for a uniform infinite atmosphere using modified Henyey-Greenstein phase functions originally proposed in Reference 1. As can be seen from Figure 23, all four models give nearly the same results. The "normalized radiance" shown in Figure 23 is defined differently than throughout the rest of the report. The "normalized radiance" has been multiplied by the sine of the angle from the source in order that the area under the curve be proportional to the total field of view transmittance N_{TOT} . This form of the normalized radiance was originally used in Reference 9 for the case of an infinite uniform atmosphere. In real world situations in which the scattered radiance fields are asymmetric about the source to receiver line of sight, this form of the normalized radiance is inappropriate. The symbol τ shown in these figures represents the product of the extinction coefficient and the source to receiver distance. In realistic nonuniform atmospheres the normalized radiance cannot be scaled with such a parameter and thus, it is not used elsewhere in this report.

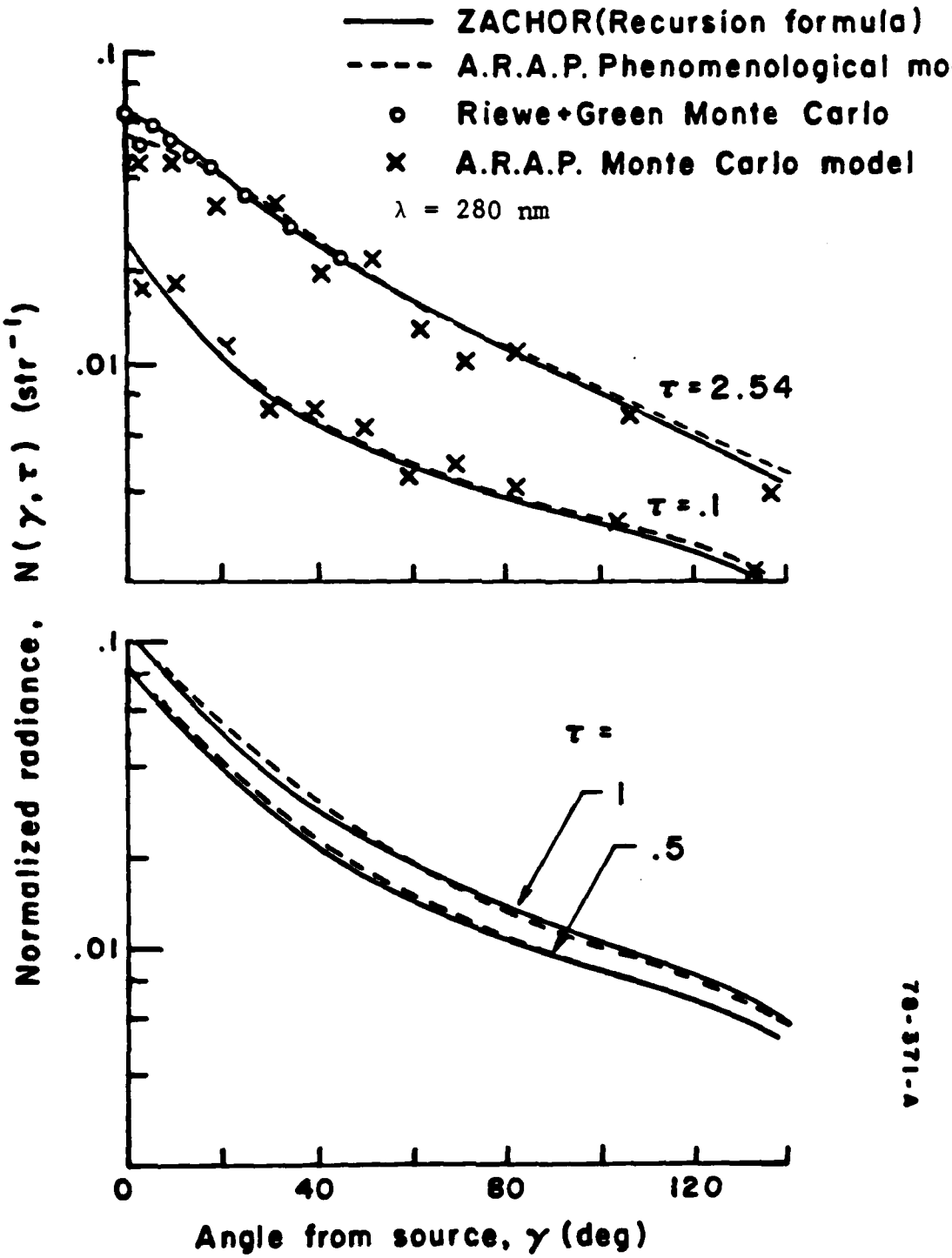

Figure 23. Comparison of Scattering Models.

TABLE 8.

MODEL SEA-LEVEL ATMOSPHERE USED IN COMPUTATIONS

λ (nm)	$k_{SCAT,M}$ (km^{-1})	$k_{SCAT,A}$ (km^{-1})	$k_{ABS,M}$ (km^{-1})	$\frac{k_{SCAT}^{*}}{k_{SCAT} + k_{ABS}}$	$\frac{k_{SCAT,A}}{k_{SCAT,M}}$	k_{ext} (km^{-1})
260	0.266	0.284	0.802	0.407	1.07	1.350
280	0.194	0.272	0.322	0.591	1.40	0.788
300	0.145	0.261	0.039	0.912	1.80	0.445
550	0.011	0.183	0	1.000	16.60	0.194

* $k_{SCAT} = k_{SCAT,M} + k_{SCAT,A}$

3. RESEARCH ORIENTED ULTRAVIOLET VOICE COMMUNICATIONS SYSTEM

A research oriented ultraviolet communications system has been designed and fabricated, incorporating the best available components. The research oriented communications system has been used to test new components as they have become available and to evaluate the UV communications model developed under the previous Navelex contract.[3]

3.1 General Description of Research Oriented Communications System

The research oriented communications system consists of one transmitter and one receiver. The new transmitter and receiver, when paired together with the original transmitter and receiver which was fabricated under a previous ARPA contract,[1] constitutes a two-way ultraviolet voice communications system. The new transmitter can be paired with the old receiver while the old transmitter is paired with the new receiver. Thus, the two systems can be used together, even though they utilize different carrier frequencies and slightly different modulation formats.

The new transmitter and receiver are modular in construction so that the various components can be easily removed, modified or replaced. The various modular components will be discussed in the next section. Both the transmitter and receiver each consist of three boxes which are shown schematically

in Figures 24a and 24b. The first box for both the transmitter and receiver are portable 12 volt power supplies with sufficient energy to operate the new transmitter and receiver for extended periods of time. These power supplies can also be plugged into 110 volt 60 cycle AC power outlets to generate the 12 volts DC required either to recharge the internal batteries or to run the transmitter and receiver directly. The second box of both the transmitter and receiver contain most of the electronic circuit cards, microphone, speakers and diagnostic meters required to achieve ultraviolet voice communications. These boxes also contain relatively small 12 volt rechargeable batteries so that they can operate for short periods of time independent of the main power supply boxes. In the case of the transmitter, the third box contains the high repetition rate ultraviolet flashlamp trigger module, triggering circuitry and the transmitting optics. In the case of the receiver, the third box contains the collecting optics, solar blind filter and photomultiplier tube. A more complete description of these various components is presented in the next section.

3.2 Individual Components

An attempt has been made to determine the best available components for use in the research oriented communications system. Wherever possible, existing components which were Government Furnished Equipment to this contract have been used for the new communications system. Many of these components are very close to being state-of-the-art. While no major

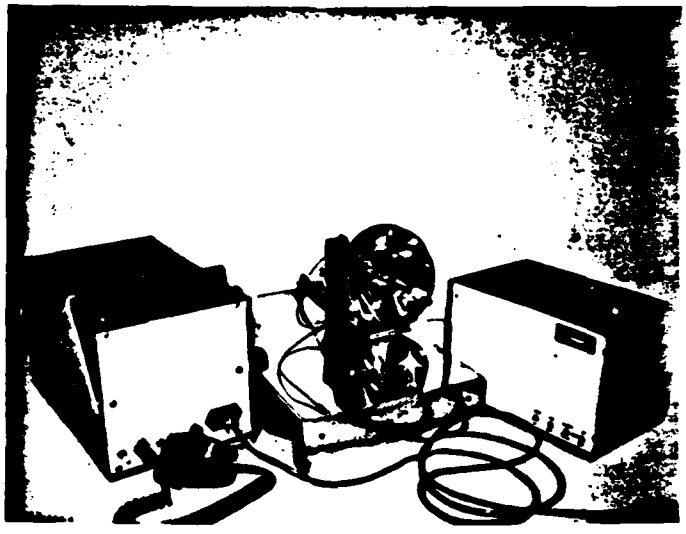

a) Transmitter with Parabolic Reflector in place

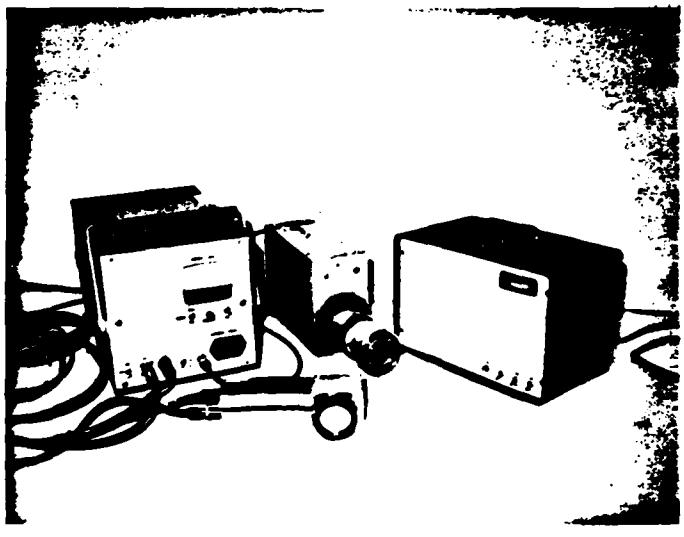

b) Receiver with Hamamatsu detector (front center) and EMR detector (back center).

Figure 24. Photographs of New Transmitter and Receiver.

component development efforts have been initiated under this contract, an attempt has been made to modify commercially available, off the shelf items to improve their performance in the ultraviolet system.

3.2.1 Flashlamps

Three different, high repetition rate hydrogen xenon flashlamps have been used in the present program. One of these is an 84 watt average power flashlamp shown in Figure 25a which was developed for A.R.A.P. by the EG&G Company. Included with the lamp is the necessary power supply and trigger circuitry so that only a small trigger pulse is required to flash the lamp. Originally, it had been hoped that this lamp would operate at approximately 300 watts average power and could be used to simulate a lower power, high efficiency flashlamp. The design specs on the lamp required a maximum pulse repetition rate of 10,000 Hz.

A second lamp was obtained from the USSI Corporation and is shown in Figure 25b. This lamp has a maximum average power rating of 50 watts and was used successfully in the original breadboard ultraviolet communications system built under the previous ARPA contract.[1] Since the total desired power to be expended by the ultraviolet voice communications system is on the order of 50 watts, this lamp is ideally suited to the power budget. The electronic triggering circuitry which has been developed for the USSI lamp is discussed below. The third lamp which was tested during this investigation was

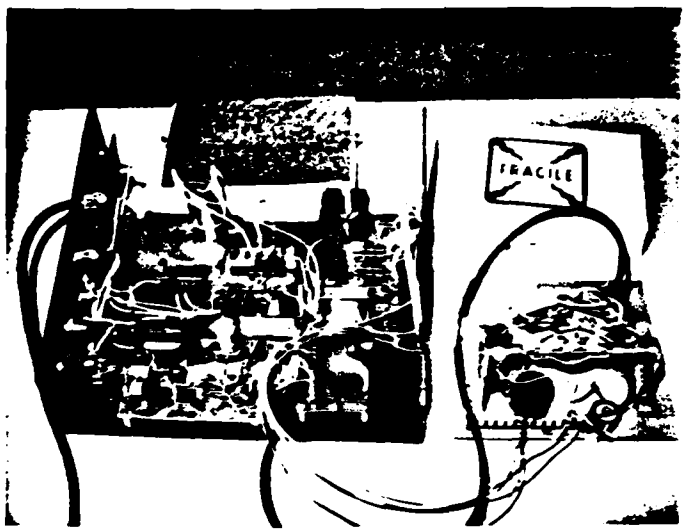

a) EG&G Lamp and Power Supply

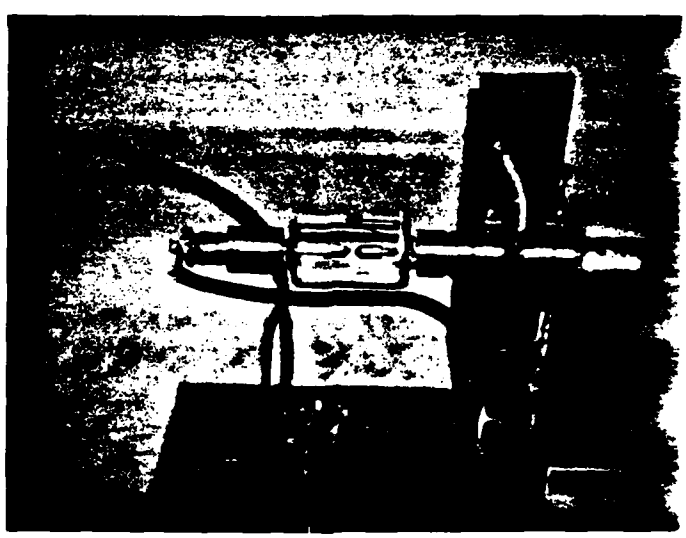

b) USSI Lamp

Figure 25. Transmitter Lamp.

another USSI bulb which together with its trigger circuitry was already available in the existing breadboard communications system.

3.2.2 Electronics

Power Supplies -- To facilitate both the testing of the individual components and the field testing of the completed communications system, the power supplies have been housed separately from the other transmitter and receiver components. Schematics of the receiver and transmitter power supplies are shown in Figures 26 and 27, respectively. The DC to DC converter shown within the dotted lines in Figure 26 converts 12 volts DC to +10, -25 and +25 volts DC. The 12 volts DC is obtained either from a 12 volt storage battery or from a battery charger and eliminator that operates on 110 volts AC. The power budget for the receiver electronics cabinet has been estimated at 10 watts. A 12 volt gel type storage battery with a 16 amp hour rating has been chosen which would give approximately 20 hours of continuous operation.

The transmitter power supply shown in Figure 27 is similar to the receiver power supply except that a second 30 watt DC to DC converter has been included to operate the flashlamp section of the transmitter. This 30 watt supply powers a 30 watt high repetition rate UV flashlamp from the USSI Company as opposed to the 84 watt lamp from the EG&G Corporation. A 16 amp hour 12 volt gel type storage battery is used for the transmitter power supply along with a battery

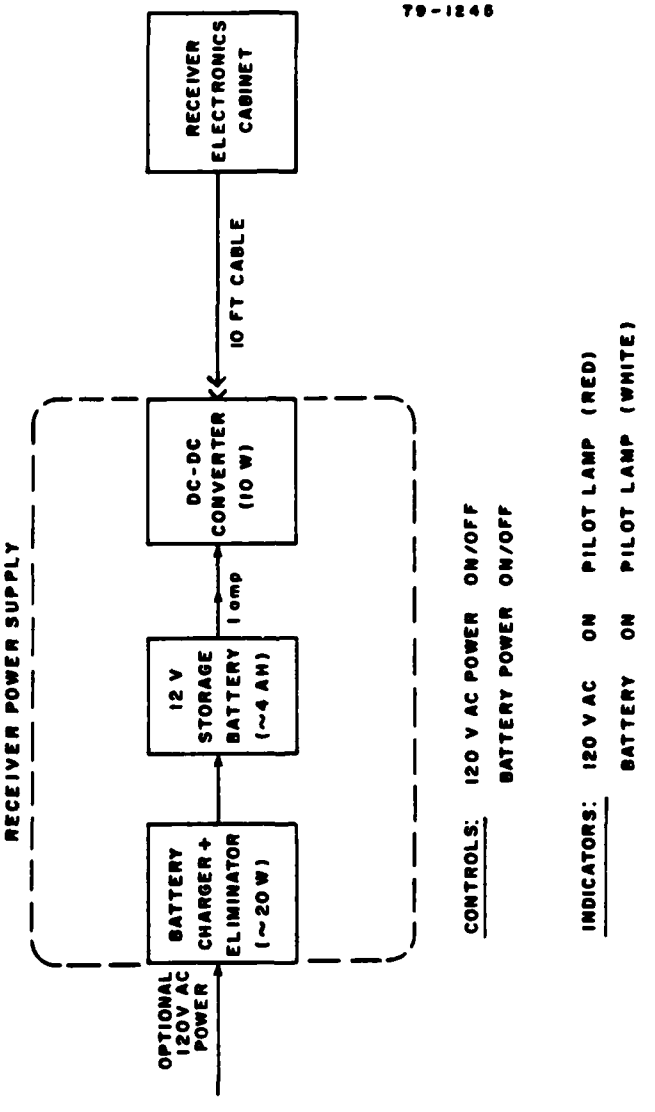

Figure 26. UV-1, Block Diagram of Receiver Power Supply.

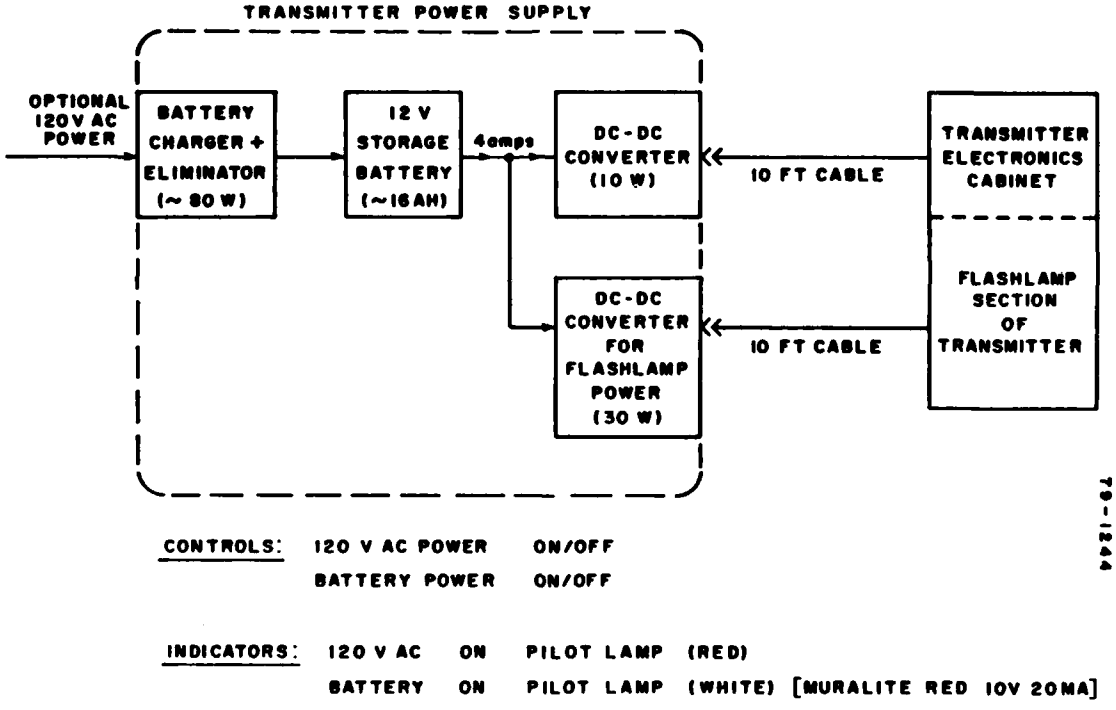

Figure 27. UV-2, Block Diagram of Transmitter Power Supply.

charger and eliminator rated at 80 watts for simultaneous charging of the battery and operation of the flashlamp.

Receiver Components -- A block diagram of the receiver for the new two-way voice communications system is shown in Figure 28. As can be seen from Figure 28, ultraviolet photons are focused on the photomultiplier tube by the receiver optics. Pulses from the photomultiplier tube are amplified by a pre-amplifier in the photomultiplier tube socket assembly and sent on to the first of seven circuit cards. The first card is a pulse amplitude discriminator which identifies pulses originating at the first dynode of the photomultiplier tube as opposed to those which originated in dynodes further down the line. The next card is a pulse pair gating system which distinguishes communication pulses from random background radiation. The next two cards are the pulse period demodulators which convert the time period between pulses into the voice waveform. The next card is a pulse demodulation filter which cuts out frequencies below 200 and above 2500 Hz corresponding to the voice bandwidths. The next card is a simple power amplifier for driving the speaker. The final card shown in Figure 28 is the power supply regulators which provide a constant +5 and $\pm$15 volts for operating the various circuit cards.

Schematics of the seven circuit cards denoted as card 10 through 70 are shown in Figures 29 through 35. Cards 10 and 20, shown in Figures 29 and 30, use low power Schottky transistor-transistor logic except for the first integrated

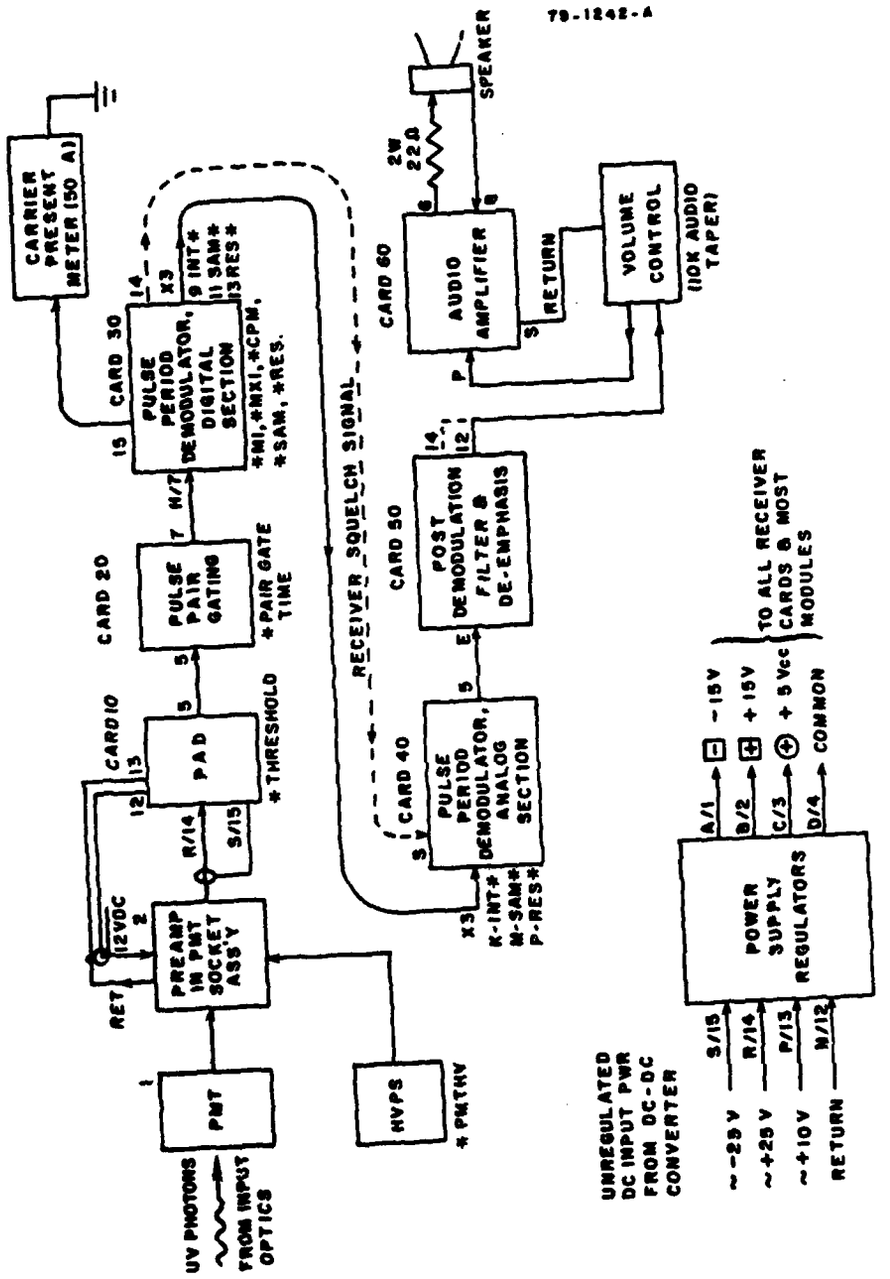

Figure 28. UV-100, Block Diagram of Receiver.

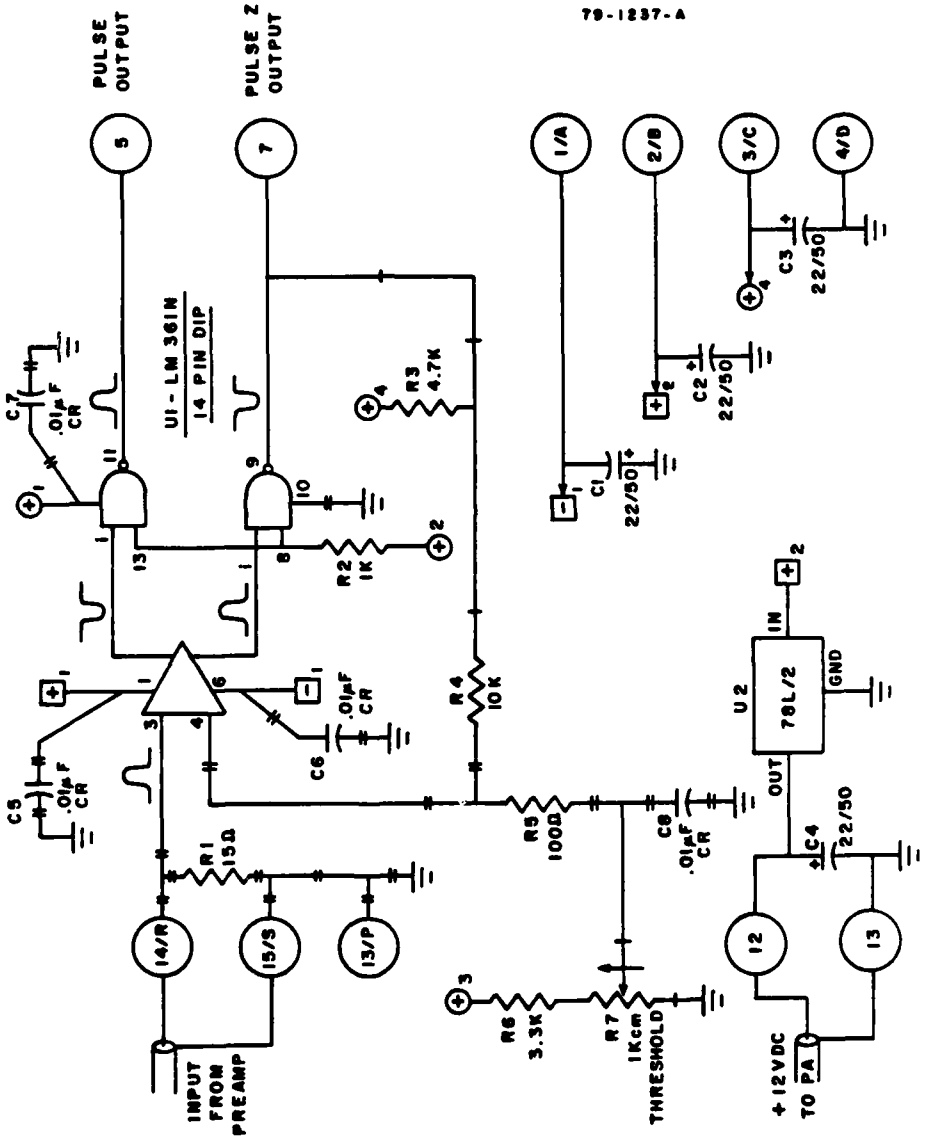

Figure 29. Card 10 or UV-110, Pulse Amplitude Discriminator.

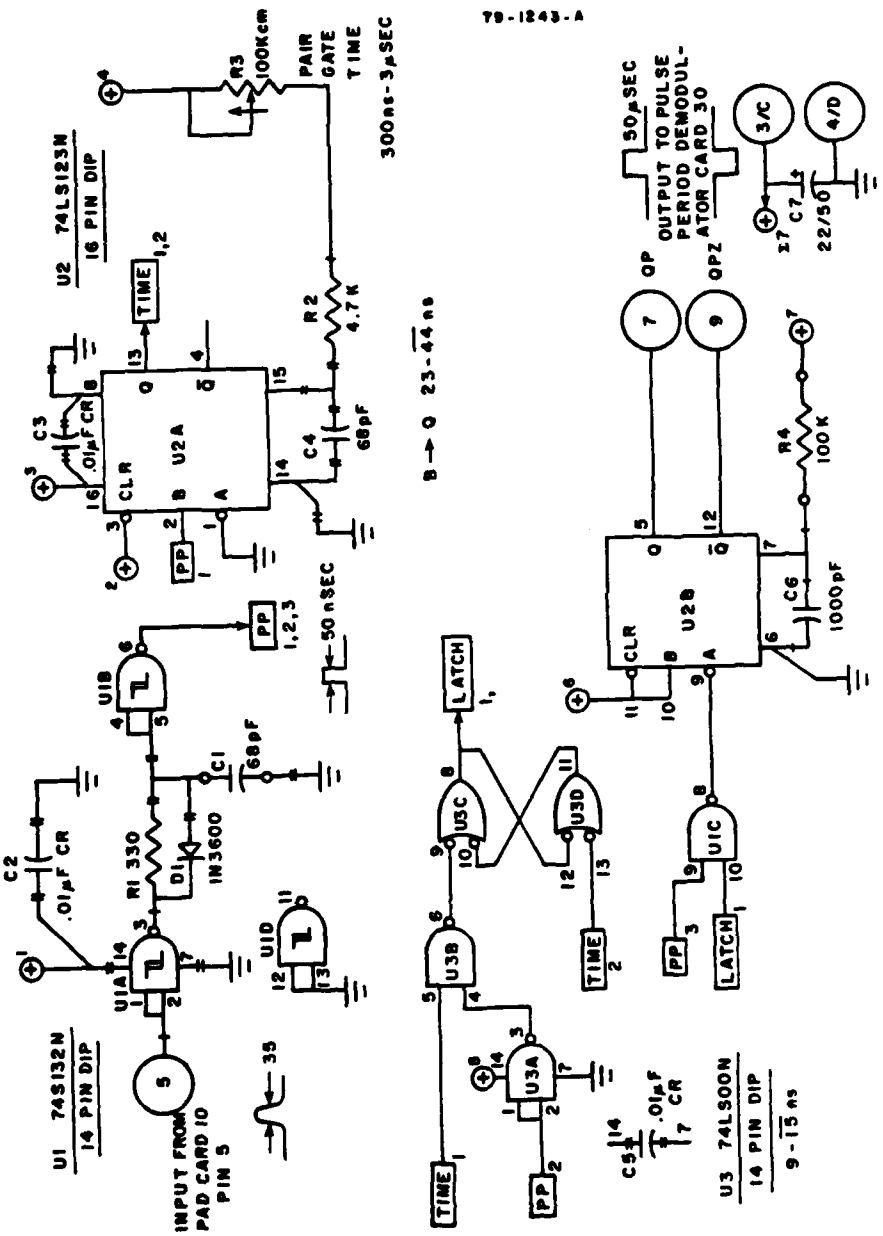

Figure 30. Card 20 or UV-120, Pulse Pair Gating.

circuit U1 which uses standard power Schottky transistor-transistor logic. From Card 30 on, CMOS logic is used. The TTL-LS logic is high speed, high power logic, while CMOS logic is much slower but requires only microwatts of power.

Card 10, shown in Figure 29, is the pulse amplitude discriminator which reduces the number of pulses coming from the photomultiplier tube which do not originate with photoelectric events. The output pulses from the pulse amplitude discriminator are approximately 35 nsec in length with a standard height of 3 volts. Card 20 is a pulse pair gating system used to reject random background radiation. The circuitry on this card is virtually identical to the electronic gating system developed under the previous Navelex contract with the exception that it does not have an analyze capability. Two or more photoelectric events occurring within a specified time period will result in a single pulse being sent forward to the pulse period demodulation cards.

Pulse period demodulation is accomplished on Cards 30 and 40 shown in Figures 31 and 32. Card 30 is the digital section of the pulse period demodulator which puts out five signals of various widths and timing which turn on and control the circuitry on card 40 which converts the variations in the incoming pulse period back to the analog signal. The signals from card 30 control the integrator including resetting it, starting it, turning it off and also includes a squelch signal that turns off the audio in the absence of a carrier. This

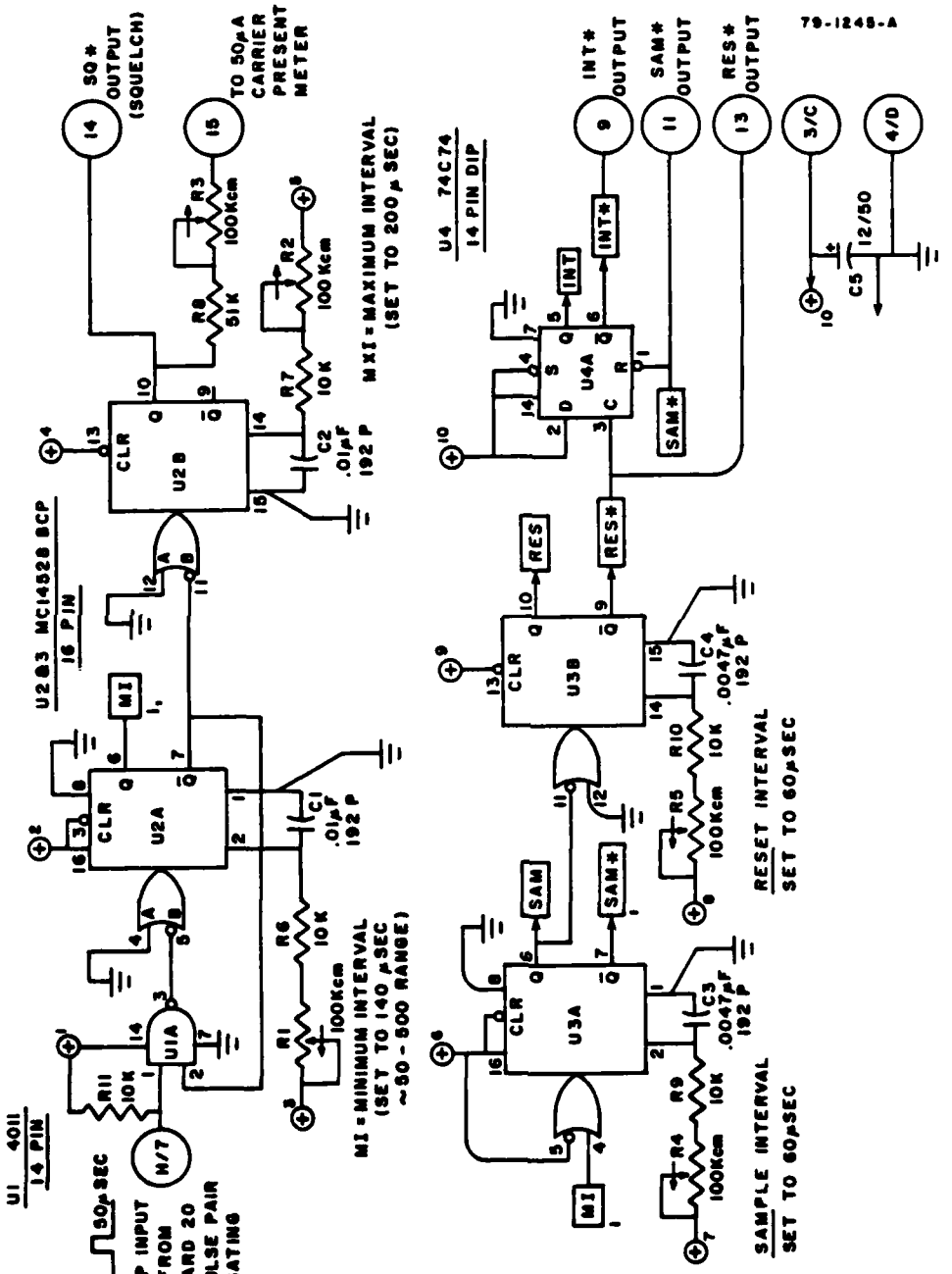

Figure 31. Card 30 or UV-130, Pulse Period Demodulator, Digital Section.

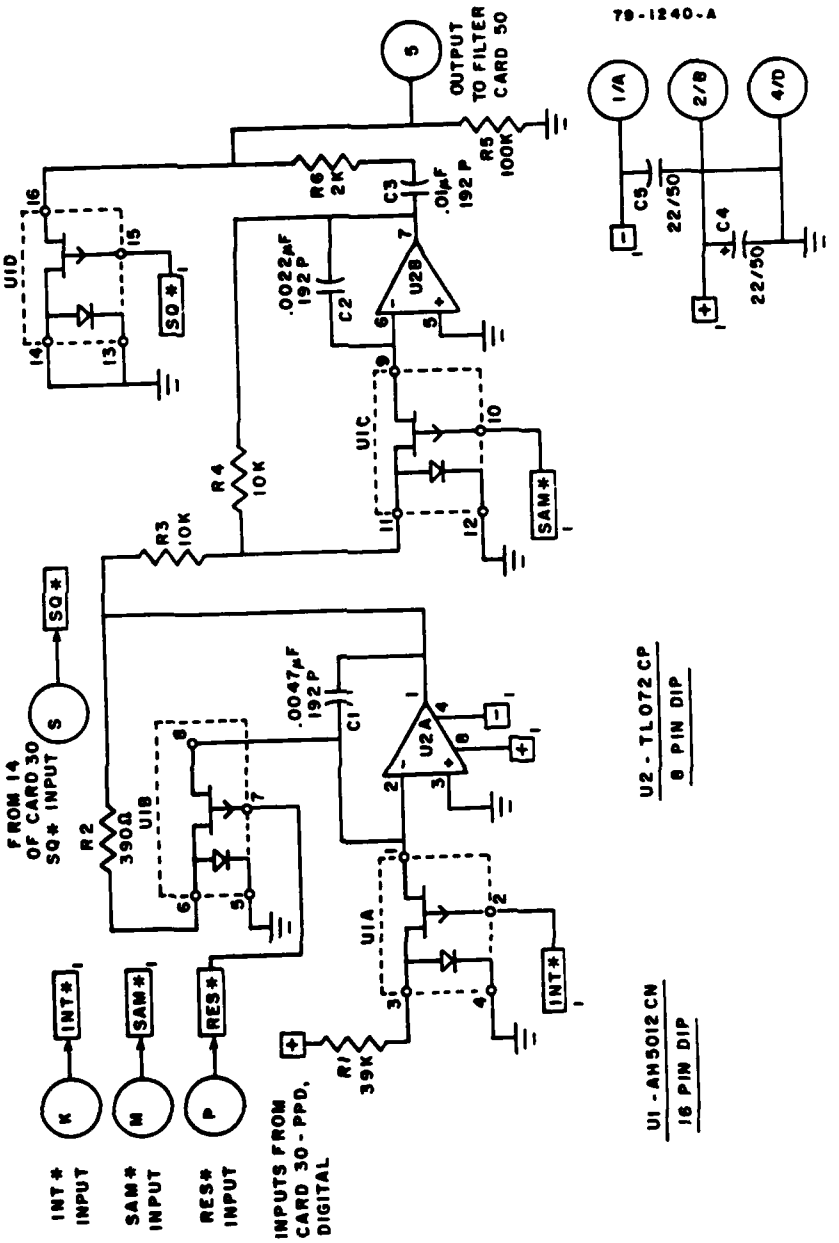

Figure 32. Card 40 or UV-140, Pulse Period Demodulator, Analog Section.

squelch minimizes noise or clicks from the speaker. Card 30 also contains an output for a carrier present meter which reads full scale when the carrier is strong and less than full scale when the carrier is weak. The carrier present feature is quite useful during field tests for determining whether sufficient signal intensity is present for accomplishing voice communications.

Schematics of cards 50, 60 and 70 are shown in Figures 33, 34 and 35, respectively. Card 50 is a post demodulation filter that cuts out frequencies below 20 Hz or above 2500 Hz which are outside of the voice bandwidth. Card 60 is a simple power amplifier for driving the speaker and Card 70 is a power supply regulator which converts the unregulated DC input power from the DC to DC converters into a uniform +5 and $\pm$15 volts DC.

Transmitter Electronics -- A block diagram of the various transmitter components are shown in Figure 36. Schematics of the four circuit cards denoted as cards 310, 320, 350, and 360 are shown in Figures 37 through 40, respectively. These various cards are basically mirror images of the receiver component cards described above. Card 310 is a preamplifier needed to raise the nominal 100 millivolt signal coming from the microphone to a nominal 20 volt peak to peak signal going into the anti-aliasing circuit. Thus, 20 volts is the peak to peak audio signal that is used in the transmitter. In addition to this approximate factor of 200 gain, the lower

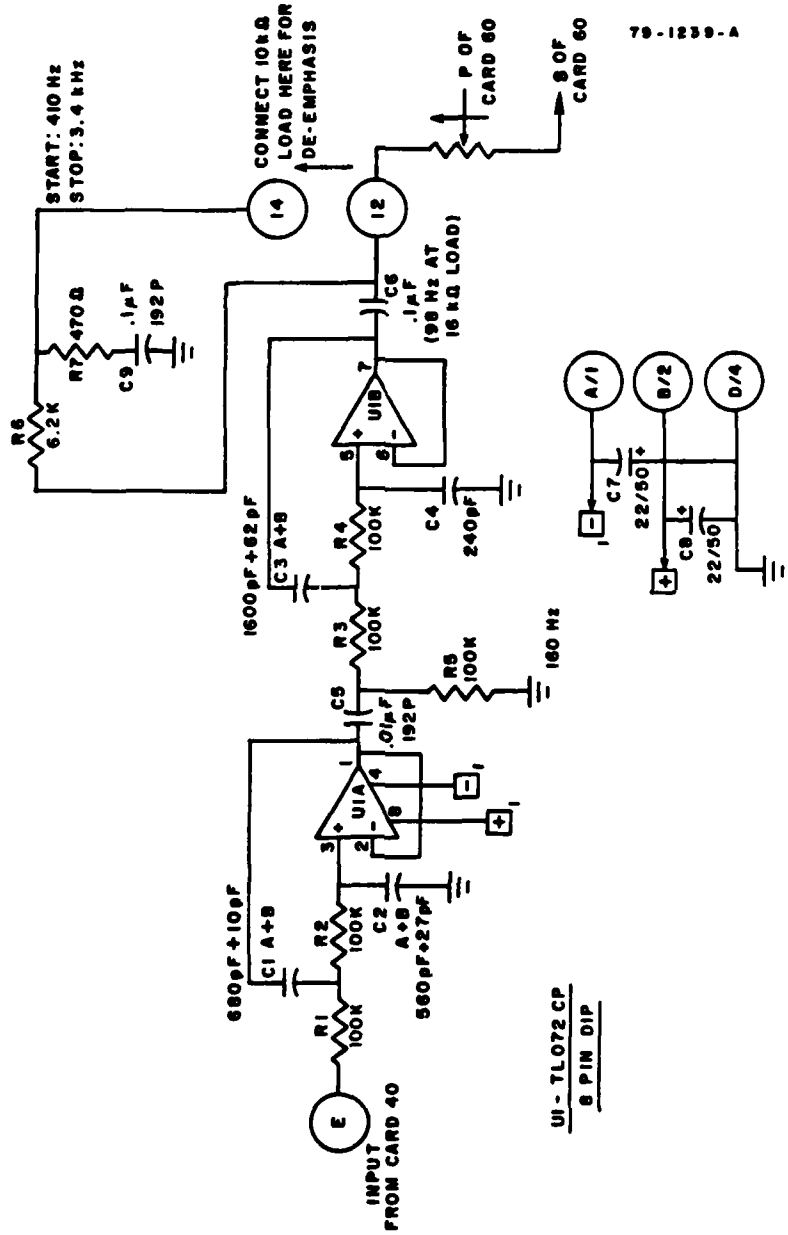

Figure 33. Card 50 or UV-150, Four Pole Post Demodulation Filter.

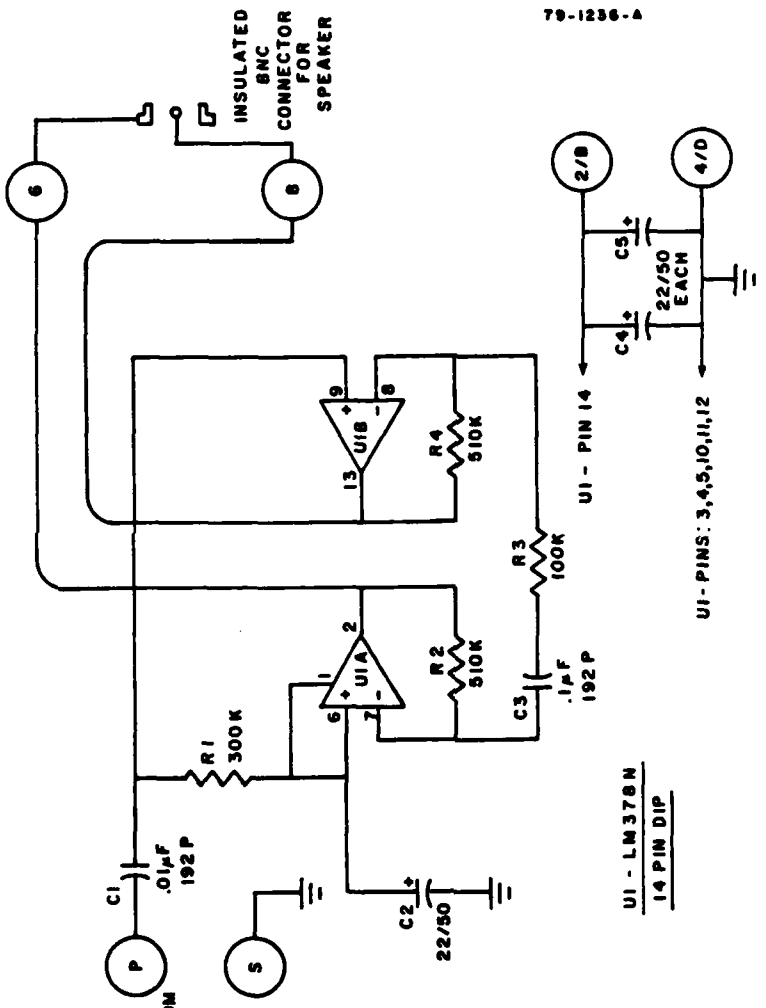

Figure 34. Card 60 or UV-160, Audio Power Amplifier.

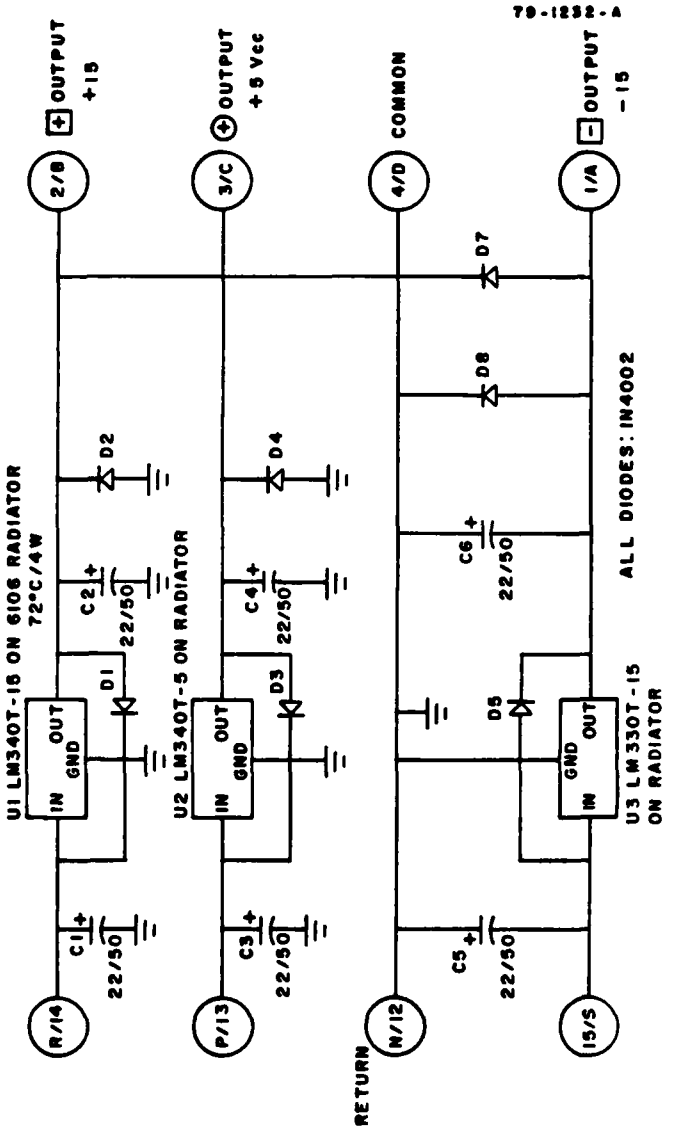

Figure 35. Cards 70 and 370 or UV-170 and UV-370, Power Supply Regulators.

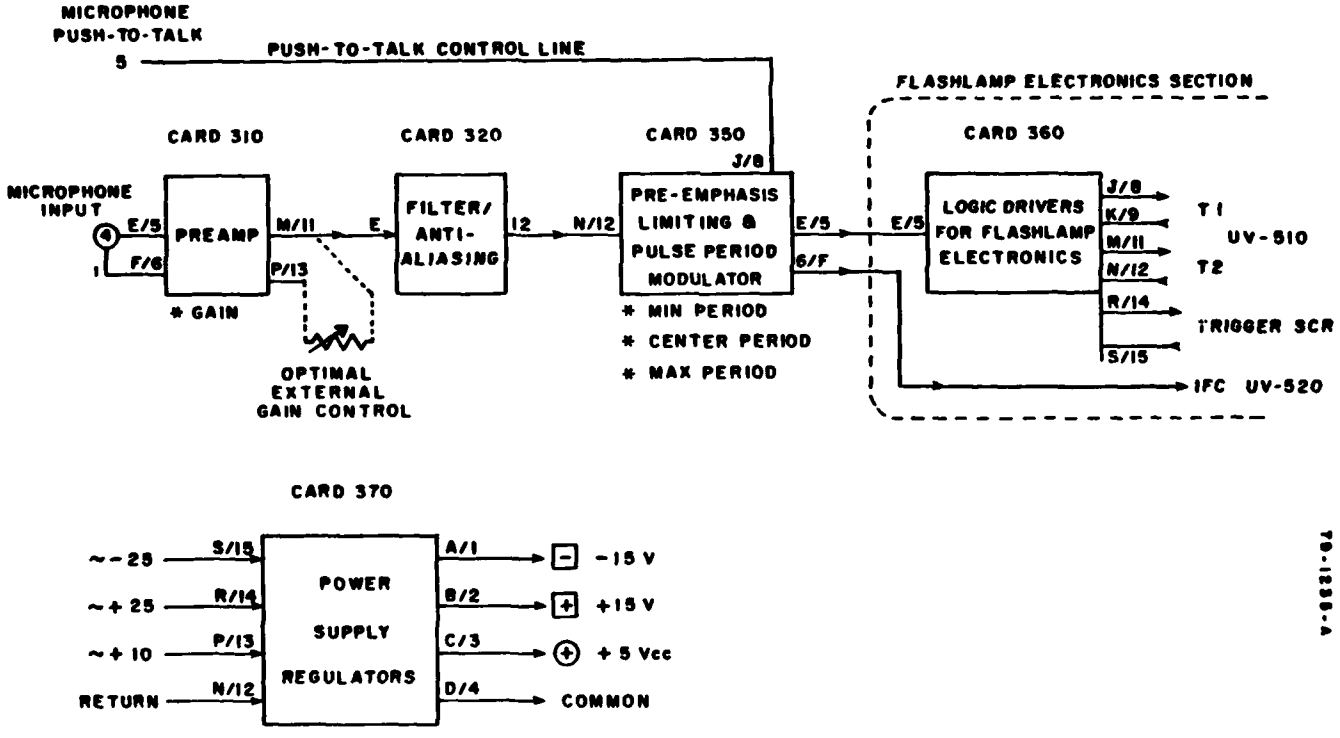

Figure 36. UV-300. Block Diagram of Transmitter.

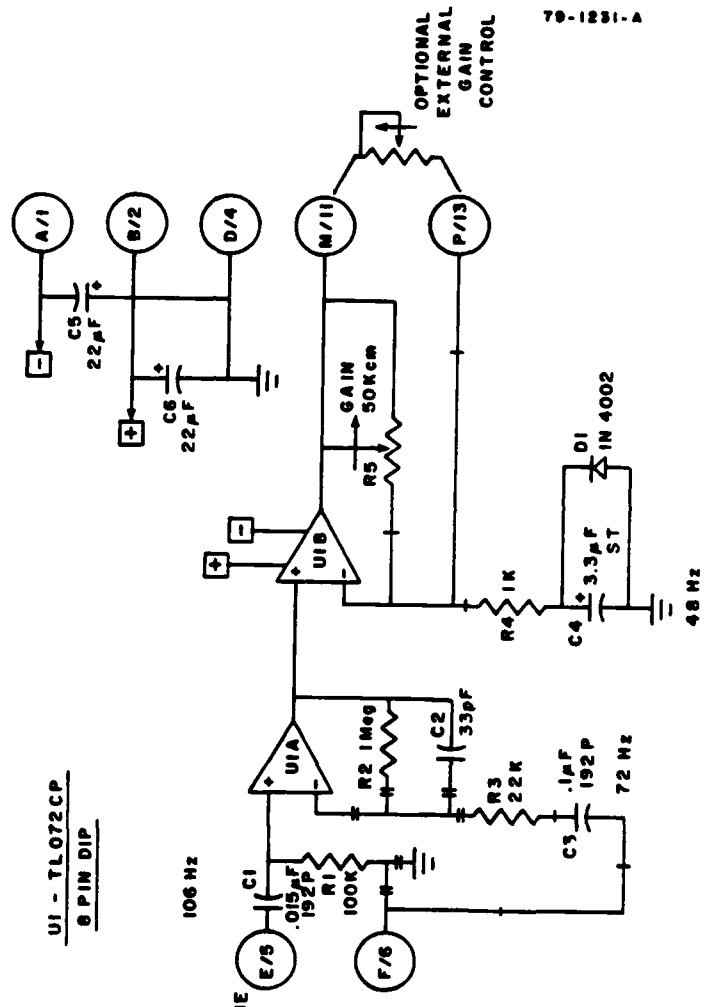

Figure 37. Card 310 or UV-310, Preamplifier.

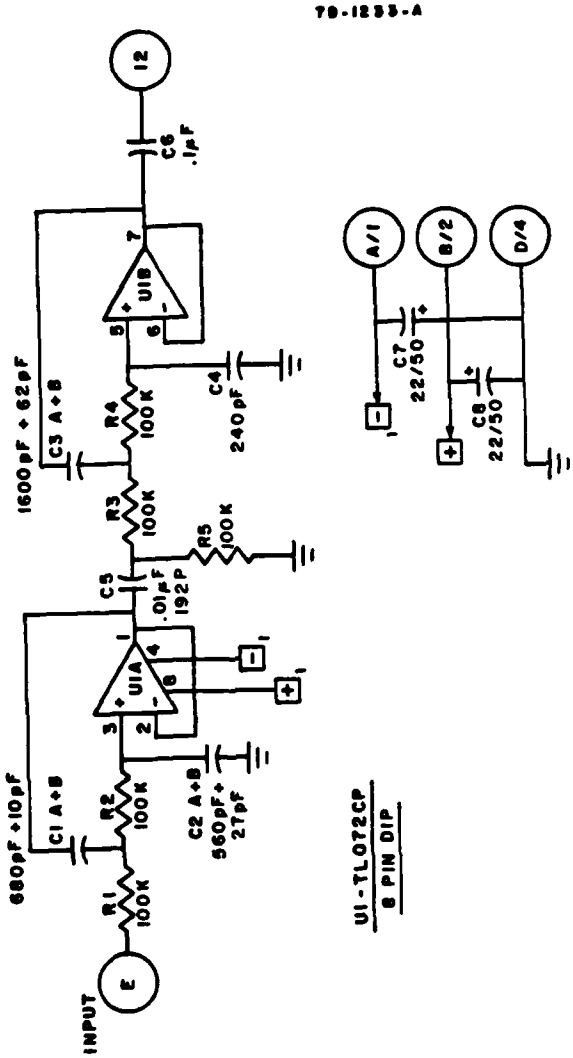

Figure 38. Card 320 or UV-320, Four Pole Anti-Aliasing Filter.

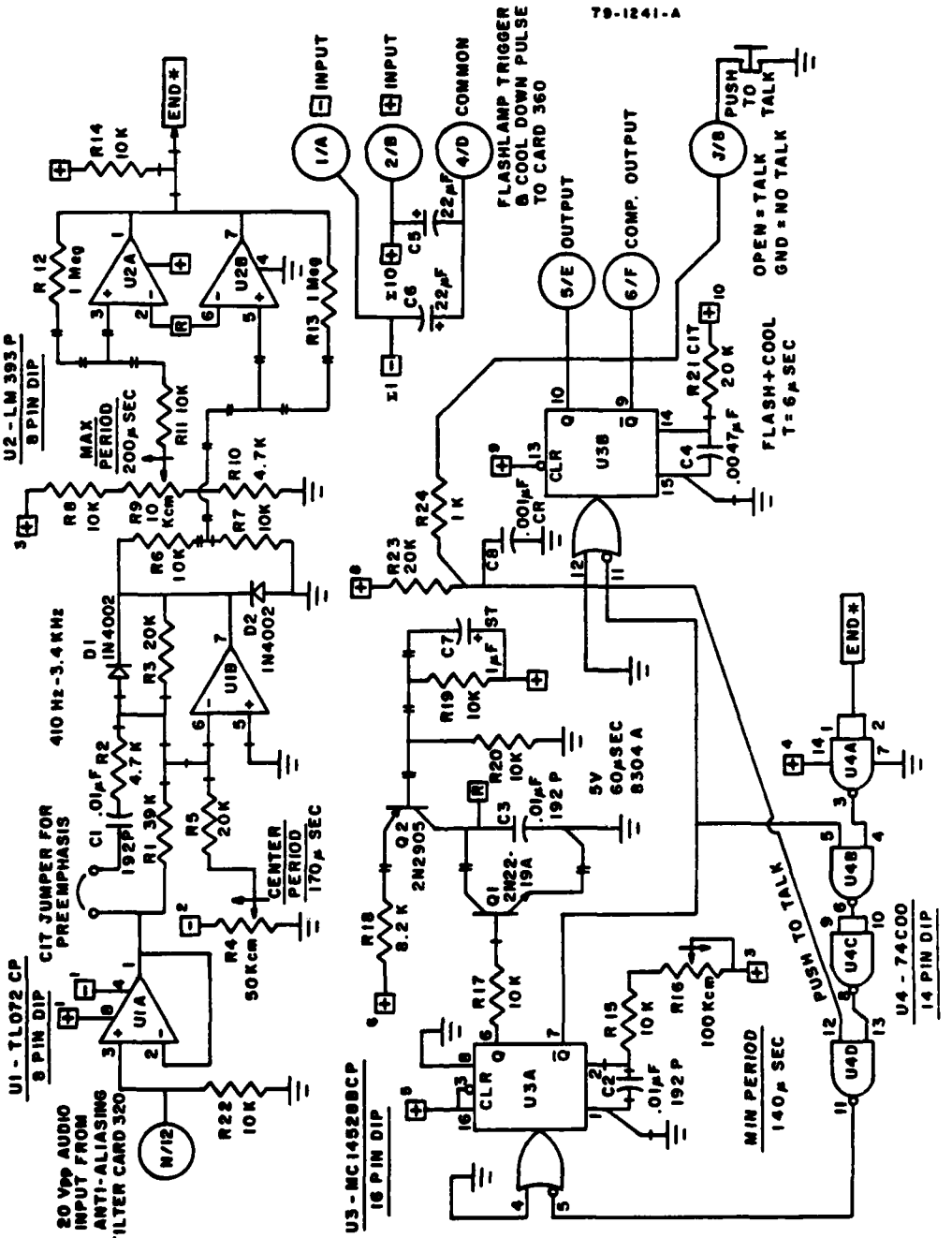

Figure 39. Card 350 or UV-350, Pre-emphasis, Limiting and Pulse Period Modulator.

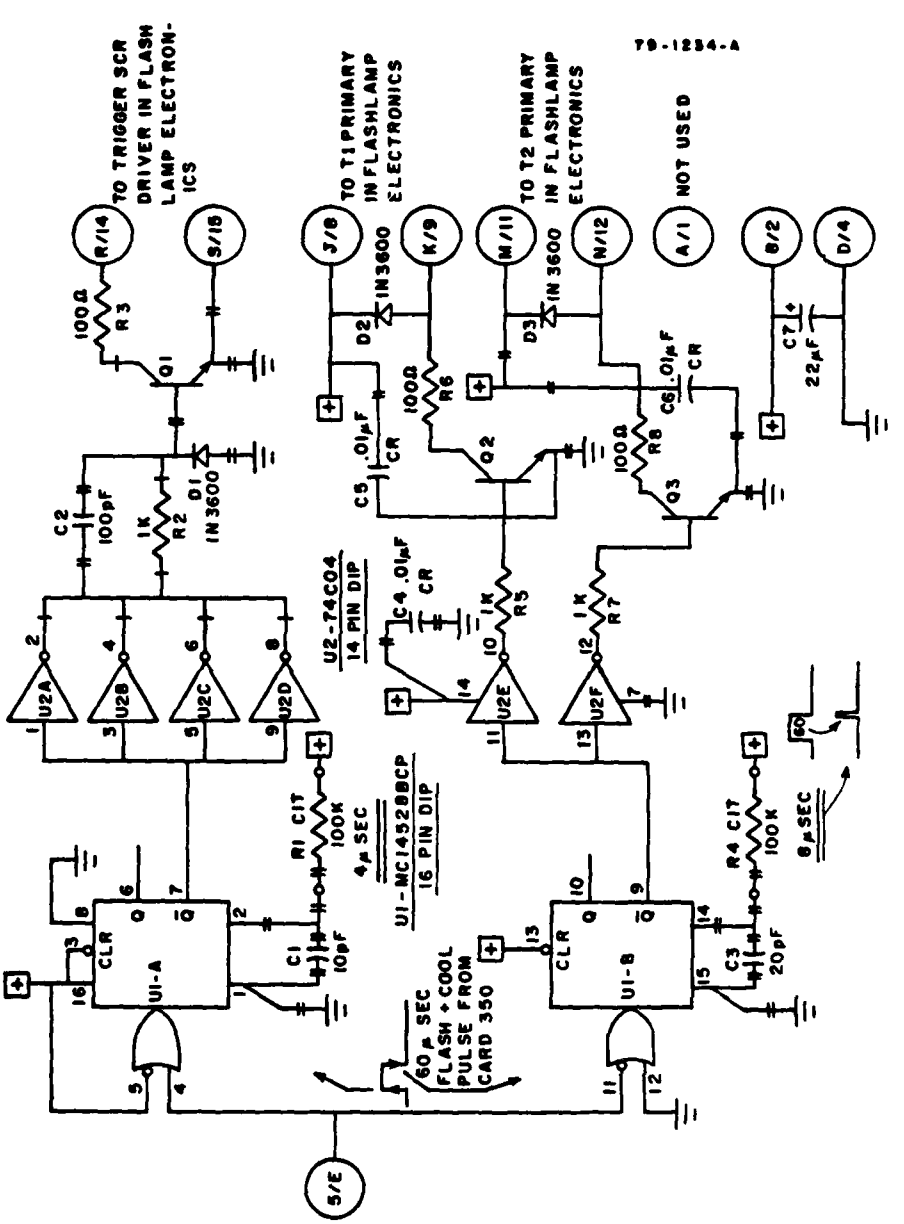

Figure 40. Card 360 or UV-360, Logic Drivers for Flashlamp Electronics.

frequencies in the speech tend to be attenuated and the higher ones tend to be boosted which makes the speech more intelligible without seriously reducing the fidelity. Card 320 is an anti-aliasing filter which provides a rather sharp attenuation for all frequencies above 2500 Hz. It also provides attenuations for frequencies below approximately 200 Hz. The main function of the filter is to provide a fairly steady response throughout the speech spectrum with a sharp roll off above 2500 Hz. The frequency response cutoff above 2500 Hz is required in order to eliminate alias components which are always shifted in frequency by plus or minus the carrier frequency or plus or minus twice the carrier frequency, etc. A standard way of avoiding alias components is to avoid transmitting frequencies which are more than half the minimum pulse rate, which in this case is approximately 5000 Hz.

Card 350 is a preemphasis, limiting and pulse amplitude period modulator. The purpose of the preemphasis circuitry is to amplify the high frequency components of the speech. At the receiver end, deemphasis circuitry is used to reduce the high frequency components and also automatically reduce high frequency background noise. The limiting circuitry prevents the voice signal from going below 0 volts or over 20 volts. The modulator circuit is a circuit that generates a ramp by charging a capacitor such that when the ramp voltage matches the speech voltage, the system puts out a pulse. Since the ramp is linear with time, the period between pulses

is linearly proportional to the speech signal and that is how the pulse frequency modulation is obtained.

Card 360 is actually a portion of the flashlamp electronics. The trigger pulse coming from the voice modulation electronics is used to generate a very strong 4 microsecond pulse that can be used to trigger the SCR which drives the flashlamp. Card 360 also generates an 8 microsecond pulse which drives another SCR that restarts the resonant charging after the lamp has flashed. The 8 microsecond pulse is not generated until 60 microseconds after the flashlamp pulse is generated. The 60 microsecond cooldown period is used to assure that the flashlamp arc has truly extinguished in order to prevent lamp holdover. The power supply regulators, Card 370, was already shown in Figure 35.

Flashlamp Electronics -- Schematics showing the electronic circuitry for triggering and powering the high repetition rate UV flashlamps are shown in Figures 41, 42 and 43. The gases within the flashlamp, which is shown schematically on the right hand side of Figure 41, are initially ionized by a high voltage spark between the lamp electrodes. The high voltage spark is initiated when the trigger pulse from the voice modulation electronics turns on a silicon controlled rectifier (SCR-3) which allows the 320 volts stored on capacitors C3A, C3B, and C3C to pass through the step up transformer in the lamp trigger module. These three capacitors are not recharged until a 60 microsecond cooldown period has elapsed after the lamp discharge.

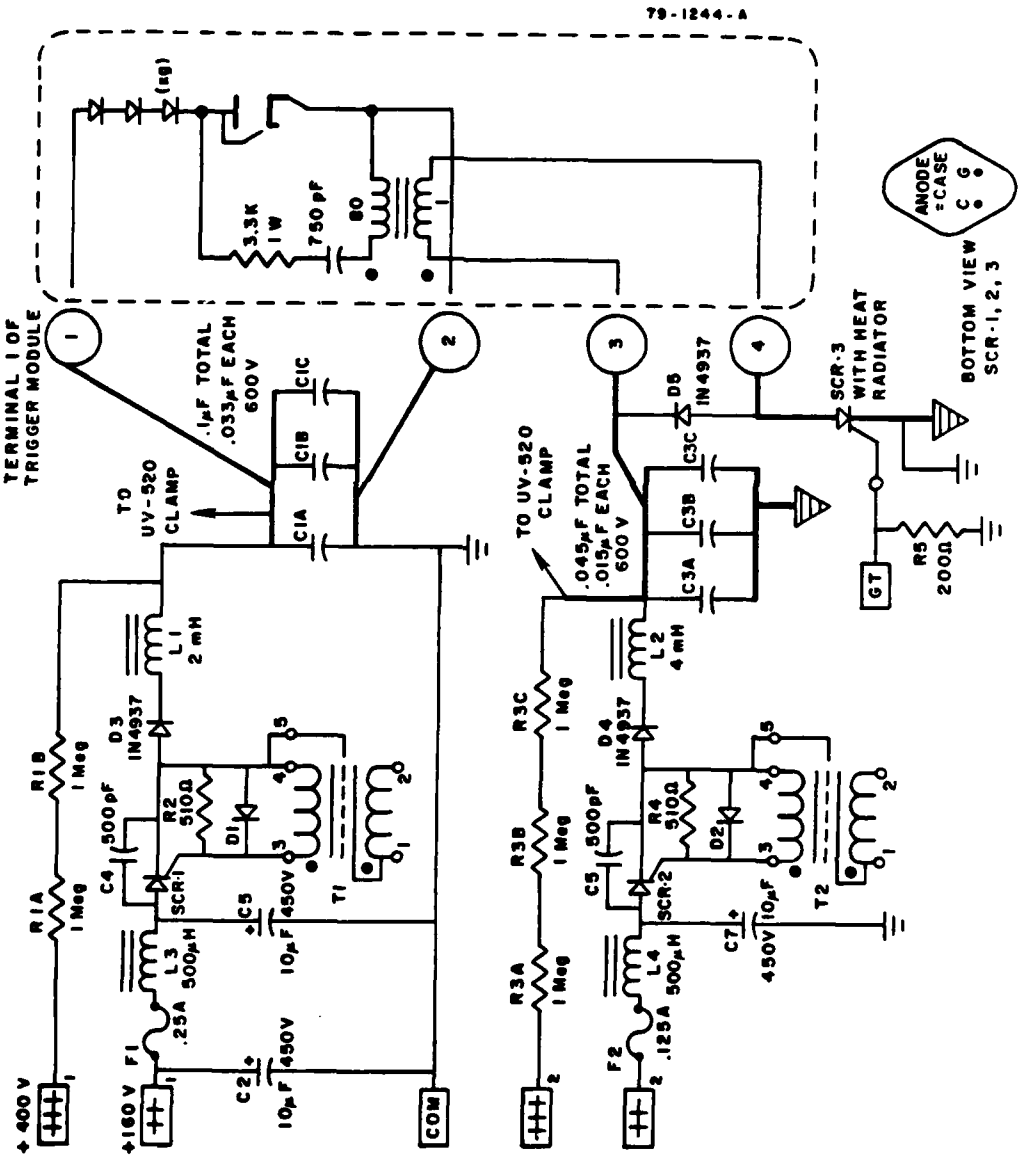

Figure 41. Circuit UV-510, High Voltage Section of Flashlamp Driver.

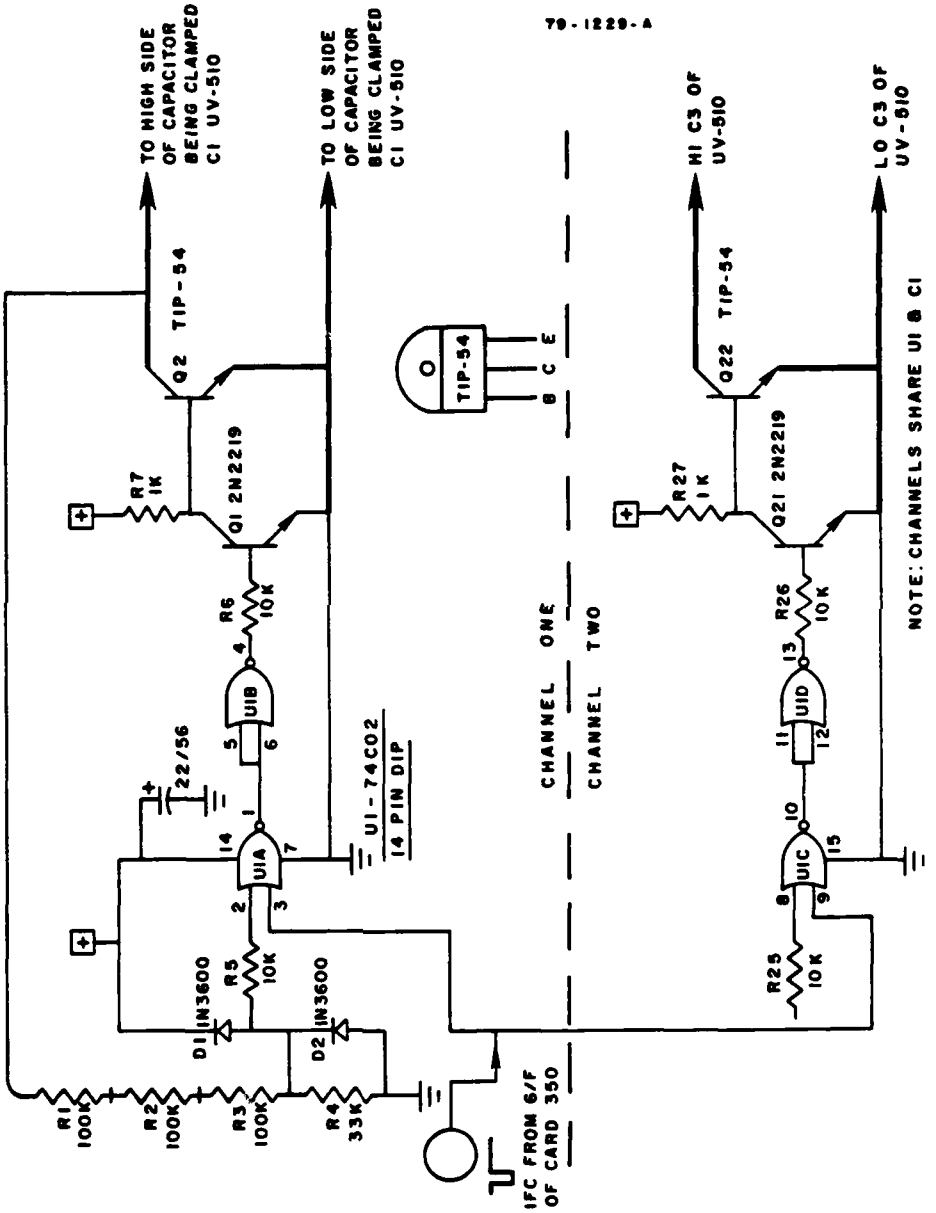

Figure 42. Circuit UV-520, Dual Channel Capacitor Clamps.

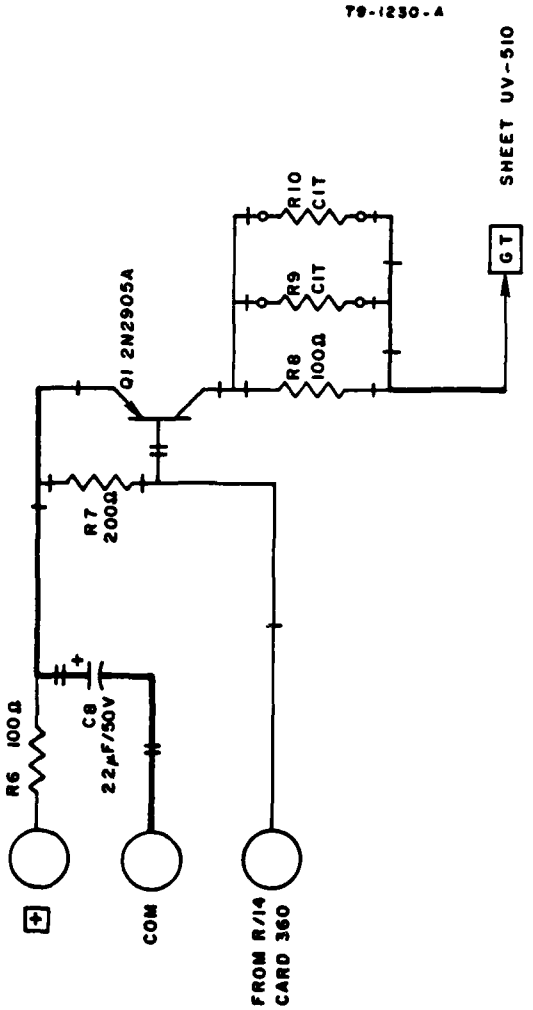

Figure 43. UV-511, Gate Trigger Stage for UV510.

AD-A080 319 AERONAUTICAL RESEARCH ASSOCIATES OF PRINCETON INC NJ F/G 17/2
THE DEVELOPMENT AND TESTING OF AN ULTRAVIOLET VOICE COMMUNICATI--ETC(U)
JUL 79 M E NEER, J M SCHLUPF N66001-78-C-0180
UNCLASSIFIED ARAP-394 NL

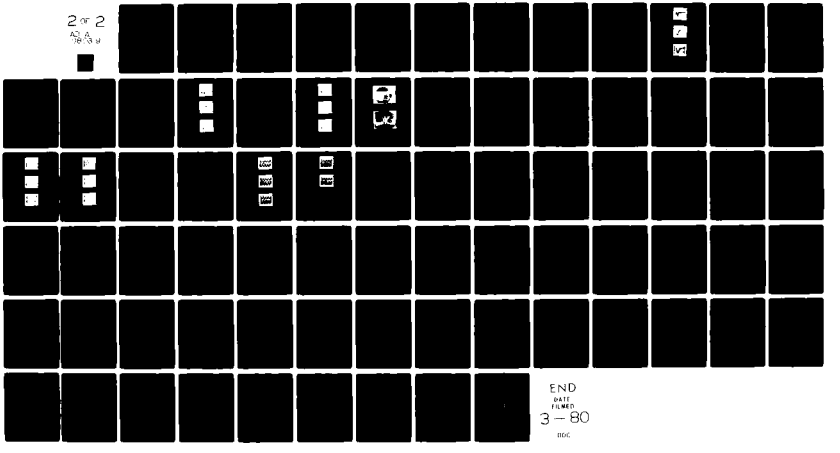

END
DATE FILMED
3-80
DDC

The upper part of Figure 41 is the resonant recharging path for the main energy storing capacitors C1A, C1B, and C1C. These capacitors also do not recharge until after the 60 microsecond cooldown period.

After the lamp has discharged, both sets of capacitors described above are clamped to zero voltage using the circuitry shown in Figure 42. The capacitors are clamped to zero voltage, because, in resonant charging circuits, the final voltage is dependent on the initial voltage of the capacitors. When relatively small residual voltages remain on these capacitors prior to recharging, the final voltages have been observed to vary by as much as 20% and therefore, the energy storage by as much as 40%. Since the range of the communications system is limited by the lowest energy pulses, these small residual voltages could result in the wasting of 20 to 40% of the available electrical energy. Figure 43 shows a power amplifier which boosts the power of the 4 microsecond gate pulse coming from the modulation electronics in order to open the silicon controlled rectifier (SCR) more quickly.

3.2.3 Detectors

Two different photomultiplier tube type detectors have been used in the present investigation. One of the photomultiplier tubes is a cesium telluride tube with a 1.75 inch diameter photocathode obtained from the EMR Corporation. A high voltage power supply and pulse amplitude discriminator are potted together with the tube which thus operates in a

photon counting mode. The second tube which has been used for this investigation is a cesium telluride side window Hamamatsu tube with a 1.0 cm by 2.5 cm active area. It has been necessary to utilize a high voltage power supply and a pulse amplitude discriminator (Figure 29) in order to operate this tube. The High Voltage Power Supply as well as the electronic components shown in the receiver and transmitter power supplies (Figures 26 and 27) have been supplied by Encore Electronics, Saratoga Springs, New York. A switch has been provided on the front of the receiver box to allow operation of either of these tubes. In the event that the EMR tube is used, the purpose of the switch is to bypass the high voltage power supply and pulse amplitude discriminator circuits.

3.2.4 Optics and Solar Blind Filters

Three different optical arrangements have been used in the present investigation. The first optical arrangement involves placing a 2 inch diameter solar blind filter directly in front of the photosensitive cathode. This arrangement, typical of ultraviolet warning receivers, provides the highest signal levels and widest field of view when observing purely diffuse scattering fields. The second optical arrangement also uses a solar blind filter directly in front of the photomultiplier tube. However, in this case an iris is placed in front of the solar blind filter and a 2 inch diameter quartz lens is placed in front of the iris at a distance equal to its focal length. By opening and closing the iris, the field

of view of the detector can thus be controlled. The main purpose of the lens iris arrangement is to limit the field of view of the detector without decreasing the total radiation observed from a point source. The field of view control is necessary for reducing background radiation due to fires, flares and other extraneous sources of ultraviolet radiation.

The third optical arrangement also involves the solar blind filter being placed directly in front of the photocathode, but in this case a large reflecting mirror is placed in front of the detector for gathering large amounts of radiation. Conventional mirrors with large collecting apertures are both heavy and expensive. A new lightweight mirror has therefore been designed using technology recently developed in the solar energy field. These mirrors utilize a lightweight acrylic honeycomb substrate and are either front silvered, aluminized, or gold plated. They are extremely lightweight and in production would cost on the order of $5 per square foot. While these mirrors are not of high enough quality for imaging, they are more than sufficient for gathering diffuse scattered radiation. The mirrors which have been used in the present investigation have a spherical surface, are approximately 6½" square and weigh approximately 3 ounces. The fields of view functions for these optical arrangments will be shown in Section 3.3.1.

3.2.5 Multi-Channel Operation

One feature which has been investigated but not included

in the present breadboard communication system is multiple channel operation. Several concepts have been investigated for obtaining multiple channel operation.

Most multi-channel operation in conventional radio wave communications involves changing the wavelength of the radiation. In the ultraviolet portion of the spectrum, this would correspond to transmitting and receiving radiation from individual spectral lines or very narrow spectral regions. However, this type of multi-channel operation is more complex in the ultraviolet than in the radio wave region of the spectrum due to the difficulty of obtaining transmitter lamps and receiver filters with discrete wavelength characteristics. While the ultraviolet voice communications system currently utilizes pulse frequency modulation, the wavelength of the transmitted radiation is not varied. In the future, perhaps the most promising mode of multi-channel operation will involve the use of high efficiency, tuneable lasers for generating the ultraviolet radiation. Combinations of narrow bandpass filters could then be used to obtain various channels.

At the present time, however, the only feasible mode of obtaining multi-channel operation through varying the wavelength appears to be putting wavelength discrimination filters on the front of both the transmitter and the receiver. Thus, if the solar blind bandpass region were divided into N different wavelength regions, then N single wavelength channels could be used. Another concept would be to use two

or more wavelengths k at a time. In this event, the number of channels which could be obtained would be according to the following formula

$$\binom{N}{k} = \frac{N!}{k!(N-k)!} \qquad \text{(Eq. 2)}$$

As can be seen from Equation 2, if the solar blind were to be divided into five spectral regions with two wavelength regions used simultaneously, then ten different channels could be obtained. Unfortunately, two transmitter lamps and two detectors would be required for each transmitter and receiver combination. The simultaneous detection of radiation in both wavelength regions would constitute the arrival of the intended communications pulse. The detection of a pulse in one or the other wavelength region alone would be interpreted as having come from a different communications system or background radiation.

Conventional background rejection electronics would be used to distinguish between random background radiation sources, such as fires and flares and the intended communication pulses. The proposed scheme, in addition to requiring additional transmitter lamps and receivers, would have a much shorter range because of all the ultraviolet radiation from the lamps which would not be utilized. In the case that the solar blind were divided into five discrete spectral regions, four fifths of the energy would be unused for each transmitter lamp. In addition, two transmitter lamps would be used so that the

total transmitted energy would be down by an order of magnitude for the same total of power consumed. In addition, it is unlikely that the narrow bandpass filters at the receiver would have as high a peak transmittance as the overall solar blind filters have. Thus, while the variable wavelength concept is possible for obtaining multi-channel operation, it does not appear to be feasible at the present time.

Another concept for obtaining multiple channel operation is time division multiplexing, in which pulse position modulation is used for each channel and the total time spectrum is divided into a number of time slots with a certain time slot devoted to each channel. In this case, however, much higher pulse repetition rates would be required and all the communication systems operating simultaneously must be synchronized. Since the method of accomplishing this synchronization is not immediately apparent and the pulse repetition rates of the lamps are currently limited to approximately 10 KHz, this method of multiple channel operation does not appear to be feasible at this time.

One concept which does appear to be promising for obtaining multi-channel operation involves using two flashlamps instead of one, with the second flashlamp transmitting a fixed period of time such as 4½ microseconds after the first transmitter lamp flashes. A gating system would be used at the receiver end which would test all incoming pulses as to whether a second pulse occurred exactly 4½ microseconds

after the first pulse. When such a pulse spacing did occur, the gating system would allow the second pulse through to the demodulating electronics. This gating system would be in addition to the gating system already used to discriminate against random background counts. In other words, a double gating system would be involved. Multiple channel operation would then be achieved by varying the time between the two flashes in units of perhaps 1 or 2 microseconds. The number of channels which could be obtained using this scheme is a complex statistical problem depending on both the original pulse width and the multi-path spread.

The main advantage of this particular multi-channel scheme is that only one half of the energy is thrown away. In other words, since two transmitter lamps must be used and the energy required to get each pulse to the detector is the same as if only one transmitter is used, then twice the energy must be expended to obtain each channel. However, this is much better than the previous concept where ten times the energy would be required to obtain each channel of the communications for a ten channel system.

The limiting factor in the number of channels which could be operated simultaneously using the double pulsing technique would be the accidental arrival of two communications pulses from two other channels at precisely the time interval required for the intended channel. While a complete statistical treatment of the problem is beyond the scope of this research

effort, it is apparent that approximately 400 ½-microsecond periods occur between consecutive pulses of the communications system. If there were ten systems operating simultaneously, then approximately ten pulse pairs would occur during each pulse period. The probability that any two pulses would overlap is fairly remote and since approximately 5 to 10% of the communications pulses can be lost without sacrificing good quality voice communications, it is likely that the ten channels could be operated simultaneously using this particular technique.

One feature of the ultraviolet voice communications system which should not be overlooked in discussing multiple channel operation is the inherent directionality of the UV communications system. When both the transmitter and receiver are used in the directional mode and aligned with each other, several simultaneous conversations could be carried on in the same area using the same channel as long as the transmitters and receivers for the various conversations were not directly aligned with each other.

3.3 Testing of Research Oriented Communications System

The testing of the individual components of the ultraviolet voice communications system as well as the testing of the system as a whole, has been carried out according to the "Test Plan" which was submitted to the Naval Ocean Systems Center in February of 1979. This Test Plan has been included as Appendix A of this report. This section describes the

results of that Test Plan.

3.3.1 Component Testing

The modular nature of the research oriented communications system has been very useful in testing individual components. The testing of various flashlamps, electronic circuit cards, detectors, optics, solar blind filters and so forth has been much more convenient due to the modular construction.

Flashlamps -- Experiments have been carried out to compare the pulse shapes, output power, and conversion efficiencies of the three transmitter lamps described in Section 3.2.1. The pulse shape of the lamp outputs were observed using an EMI cesium telluride photomultiplier tube and an oscilloscope with a 25 MHz bandwidth. The solar blind filter shown in Figure 3 together with several neutral density filters were placed in front of the photocathode so that the radiation was detected in the 245-285 nm wavelength range.

The pulse shape of the USSI lamp used in the original breadboard communications system developed under the ARPA contract[1] is shown in Figure 44a. The full width at half maximum of the pulse is approximately 350 nsec. The prominent spike in the early part of the trace is radiation from the trigger pulse. The pulse shape of the new 34 watt USSI lamp is shown in Figure 44b. The full width at half maximum of this pulse is approximately 400 nsec. The pulse shape of the EG&G lamp is shown in Figure 44c. The pulse shape is very similar to that of the 34 watt USSI lamp with a full width at

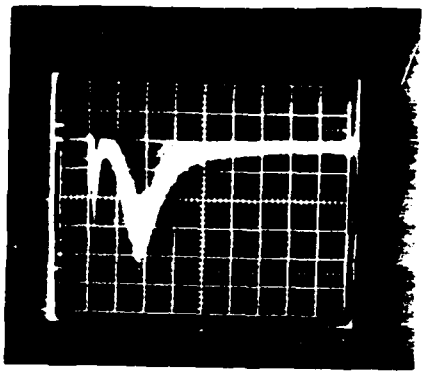

a) USSI Lamp from Original Breadboard System (18 watts)

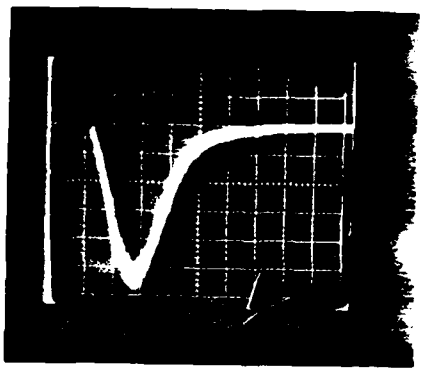

b) USSI Lamp from New System (34 watts)

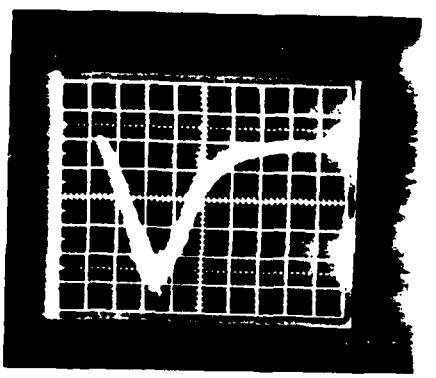

c) EG&G Lamp (84 watts)

Figure 44. Pulse Shapes of High Repetition Rate Flashlamps.

half maximum of approximately 400 nsec. All three pulse shapes approximate a gaussian profile with a slight trailing edge.

The conversion efficiencies and output powers of the various lamps were also determined. For these experiments, the EMR cesium telluride photomultiplier tube with the same solar blind filter and neutral density filters was used in a photon counting mode. The output of the various lamps was compared with the output from a deuterium standard lamp. The absolute intensity of the radiation reaching the photocathode was determined from the known filter transmission and standard lamp output. The average output powers of the three lamps in the bandpass of the solar blind filter were determined for several input parameters using this conversion factor. The conversion efficiency of electrical power in to usable solar blind radiation out was also determined with the results being tabulated in Table 9.

The new 34 watt transmitter lamp and associated circuitry is more efficient than the earlier 18 watt transmitter and the conversion efficiency appears good even at low input powers. The 18 watt unit is not only less efficient but does not run nearly as efficiently at low input powers. The EG&G lamp is somewhat lower in conversion efficiency than the 34 watt USSI lamp. While it was hoped that the EG&G lamp would have a maximum average power of 300 watts at a 5700 Hz carrier frequency, the lamp actually utilized only 84 watts of average power at the carrier frequency of 5700 Hz. The lower conversion

TABLE 9

Transmitter Lamp Output Comparison

Lamp	Repetition Rate (Hz)	Input Power (watts)	Output Power (watts)	Conversion Efficiency
34W (USSI) Lamp	5001	29.76	5.57×10^{-2}	.187%
"	"	26.70	5.01×10^{-2}	.188%
"	"	22.96	4.19×10^{-2}	.182%
"	"	19.76	3.42×10^{-2}	.173%
"	"	16.80	2.65×10^{-2}	.158%
"	"	14.30	1.89×10^{-2}	.132%
18W (USSI) Lamp	4545	14.52	1.58×10^{-2}	.109%
"	"	12.37	8.43×10^{-3}	.068%
"	"	10.49	4.01×10^{-3}	.038%
"	"	9.08	1.94×10^{-3}	.021%
"	"	7.94	1.24×10^{-3}	.014%
84W (EG&G) Lamp	500	7.36	1.29×10^{-2}	.175%

efficiency, of electrical energy in to UV radiation out, of the EG&G lamp has not yet been explained.

Electronics -- The triggering circuitry for the new EG&G flashlamp has so far proven to be unsatisfactory. The flashlamp could not be operated at the 5700 Hz carrier frequency for more than 1 or 2 seconds at a time. While the manufacturer reported that they were able to obtain sustained operation at 6000 Hz, they were unable to obtain sustained triggering at higher frequencies. Because the lamp could not be operated at the carrier frequency, it was not possible to test the lamp in the ultraviolet voice communications system. However, even if the lamp could have been pulsed at the carrier frequency, the output power per pulse was only a factor of two higher than a 34 watt USSI lamp and therefore would not have represented a significant increase in an ultraviolet communications system performance.

The new triggering circuitry for the new USSI bulb has performed very well. The 60 microsecond cooldown period between when the lamp flashes and the capacitors are recharged has apparently solved the holdover problem. Early in the testing of the new USSI lamp and associated triggering circuitry, the lamp was occasionally observed to extinguish itself. However, it was later found that an improperly designed, 160 volt power supply was overheating and causing the occasional shutdowns of the lamp. The power supply was repaired after which the lamp functioned properly.

The various receiver and transmitter cards have been tested according to the test plan given in Appendix A. After some initial adjustments and replacement of a few inoperative components, all cards have been found to operate according to design specifications. The 25 volt and 160 volt power supplies which were obtained as off-the-shelf items from Encore Electronics were all found to be defective in basic design. The defect was found and corrected by the manufacturer and now operate according to design specifications.

Detectors -- Both the EMR photomultiplier tube with its built-in PAD and high voltage power supply and the new Hamamatsu tube with the PAD and high voltage power supply constructed at A.R.A.P. have been successfully tested. While the pulse shape of the pulses coming from the anode of the EMR tube cannot be measured directly, it has been assumed based on the past performance of EMR tubes that the pulse height distribution is relatively uniform. The pulse height distribution of the Hamamatsu tube appears to be much less uniform in height from pulse to pulse. Thus, it is not easy to determine where the pulse amplitude discriminators should be set for the Hamamatsu tube. The EMR tube has a 1.75 inch circular photocathode which is approximately six times the area of the cathode of the side window Hamamatsu tube. This factor of six in the photocathode area is very important for nonline of sight communication where the radiation is diffuse and both the detector aperture size and field of view need

to be maximized.

The pulse amplitude discriminator of the EMR tube tended to undergo a "lock out" when the flux of photon counts got very high. The oscilloscope trace in Figure 45a shows output pulses coming from the PAD of the EMR tube in a continuous sweep mode. For each sweep, the oscilloscope has been triggered by the lamp trigger pulse. The time scale in Figure 45 is 0.5 microseconds per division. Figure 45a shows a dark spot occurring early in the pulse corresponding to the "lock out" of the pulse amplitude discriminator. The response of the EMR tube and pulse amplitude discriminator to five individual flashes of the lamp are shown in Figure 45b where the oscilloscope was operated in a single sweep mode and triggered by the lamp trigger pulse. Figure 45b shows that most of the photon counts are occurring more than one microsecond after the lamp trigger pulse. As can be seen from the pulse shapes of the lamp shown in Figure 44, most of the photon flux occurs during the first one microsecond after the lamp trigger pulse. In contrast, when a factor of ten neutral density filter is placed in front of the photomultiplier tube, the oscilloscope trace shown in Figure 45c results where it is evident that now most of the photon counts are occurring early in the pulse period indicating that the photomultiplier tube is no longer locked out. Unfortunately, communications are not easily accomplished when the input signals are low enough that the EMR tube is not in the lock-out mode.

a) Continuous sweep made without factor of 10 filter

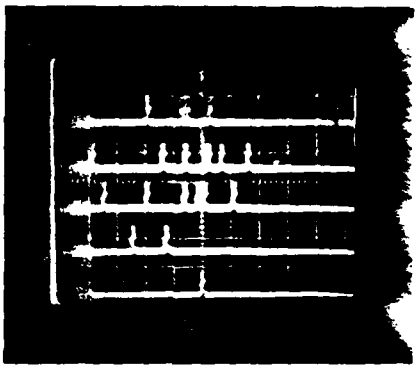

b) Single sweep made without factor of 10 filter

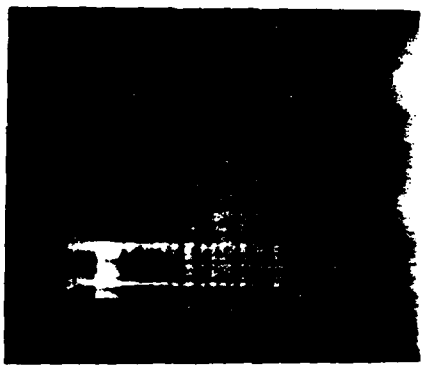

c) Continuous sweep made with factor of 10 filter

Figure 45. Output of EMR Photomultiplier Tube and Pulse Amplitude Discriminator.

Corresponding oscilloscope pictures for the Hamamatsu tube are shown in Figures 46a, b and c. Figure 46a shows the Hamamatsu tube with a very high photon flux while the photon counts associated with individual pulses obtained with the oscilloscope in the single sweep mode are shown in Figure 46b. Figure 46c shows the Hamamatsu tube with a factor of ten reduction. As can be seen from Figure 46b, lock out does not occur and the individual photon counts required to operate the two photon gating system are readily available.

Because of the lock out of the EMR tube at high photon flux levels, the EMR tube does not perform as well in direct line of sight communications as the Hamamatsu tube. Despite the factor of six smaller cross sectional area of the Hamamatsu tube, the Hamamatsu tube can operate at a line of sight range approximately 50% longer than the EMR tube. However, for nonline of sight communications using the front surface mirror, the narrower field of view resulting from the small Hamamatsu photocathode area resulted in the EMR tube working better at longer ranges. These experiments will be discussed further in a later section.

Optics and Solar Blind Filters -- The various 6" square hemispherical mirrors (Figure 47) were tested using a mercury penray lamp and the EMR detector with the solar blind filter in front of the photocathode. The ratio of the signal using the 6" square mirrors compared to when the detector was

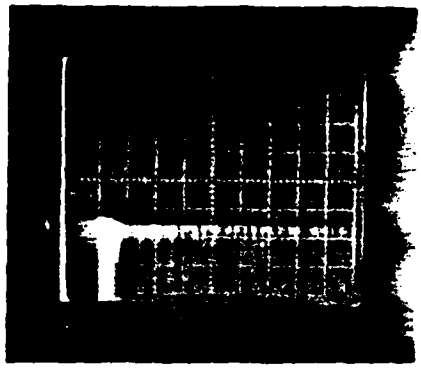

a) Continuous sweep made without factor of 10 filter

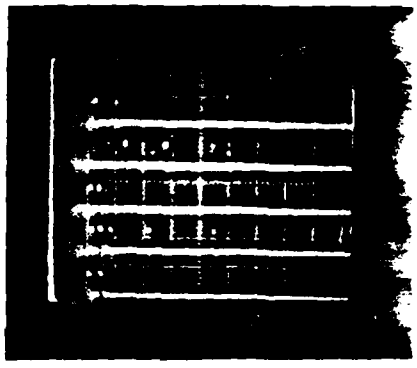

b) Single sweep made without factor of 10 filter

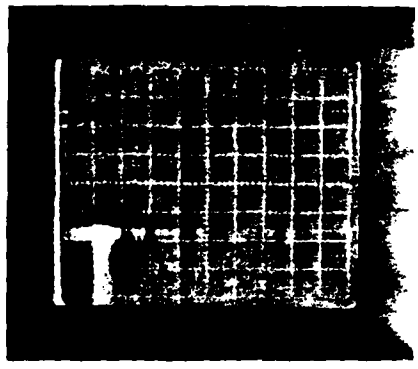

c) Continuous sweep made with factor of 10 filter

Figure 46. Output of Hamamatsu Photomultiplier Tube and Pulse Amplitude Discriminator.

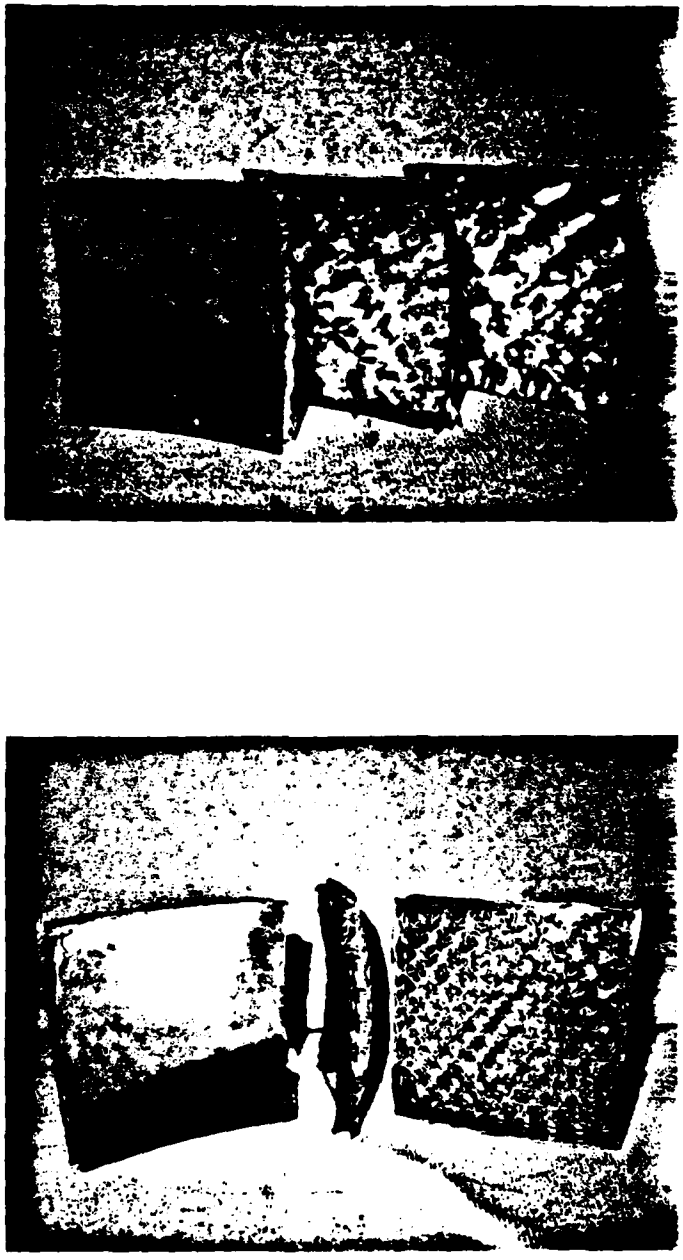

Figure 47. Lightweight Spherical Mirrors.

pointed directly at the mercury lamp without the mirrors was determined for each type of coating. The upper limit for the theoretical increase in total surface area between the mirrors and the photocathode was a factor of 15. The gold plated mirror achieved a ratio of 7.6 increase in signal, while the silvered mirror with a magnesium fluoride overcoat achieved a ratio of 8.5. The best ratio was obtained with the aluminum coated mirror giving a ratio of 14. The ratio of 14 increase using the aluminized mirror was checked on several occasions and found to be repeatable. While it seems unlikely that a factor of 14 increase should have been accomplished considering the geometry of the experimental arrangement, it has been hypothesized that certain areas of the photocathode are more sensitive than others so that by focusing the radiation with the mirror on the more sensitive area a higher peak signal could be obtained. Because of its high performance, the aluminum mirror was used throughout the rest of the test.

Experiments using the EMR detector with a solar blind filter only compared to using the EMR detector with a solar blind filter and collimating lens showed that, for direct line of sight, virtually no difference in the total received radiation could be observed. In the case of scattered radiation, the lens iris attachment proved to give much lower count rates than when the photomultiplier tube and solar blind filter alone were used. The angular field of view response

of the EMR detector with the solar blind filter only is shown in Figure 48. Likewise, the angular field of view responses for the EMR tube and solar blind filter when used together with either the aluminum reflecting mirror or the lens-iris arrangement are shown in Figures 49 and 50, respectively.

Comparisons of the two solar blind filters used in this project indicated that the peak transmittance of both filters was approximately the same. However, the two inch diameter solar blind filter (Figure 3) was observed to pass much more radiation in the nonline of sight communications mode than the older solar blind filters (Figure 51) which were approximately 1¼ inches in diameter.

3.3.2 Overall System Performance

Voice Quality -- In evaluating the performance of the ultraviolet voice communications system, it has been necessary to establish criteria by which the quality of the voice communications can be judged. When communicating between remote areas in the field, subjective evaluations of voice quality, such as excellent, good, fair, and poor, are sometimes the only standards which can be applied. The evaluation technique which has been used most often in this investigation involves the transmission of a sequence of numbers and verbal messages unfamiliar to the receiver operator. The receiver operator than records the number sequences and messages along with a subjective estimate of the clarity of the communications.

In order to more quantitatively document the quality of

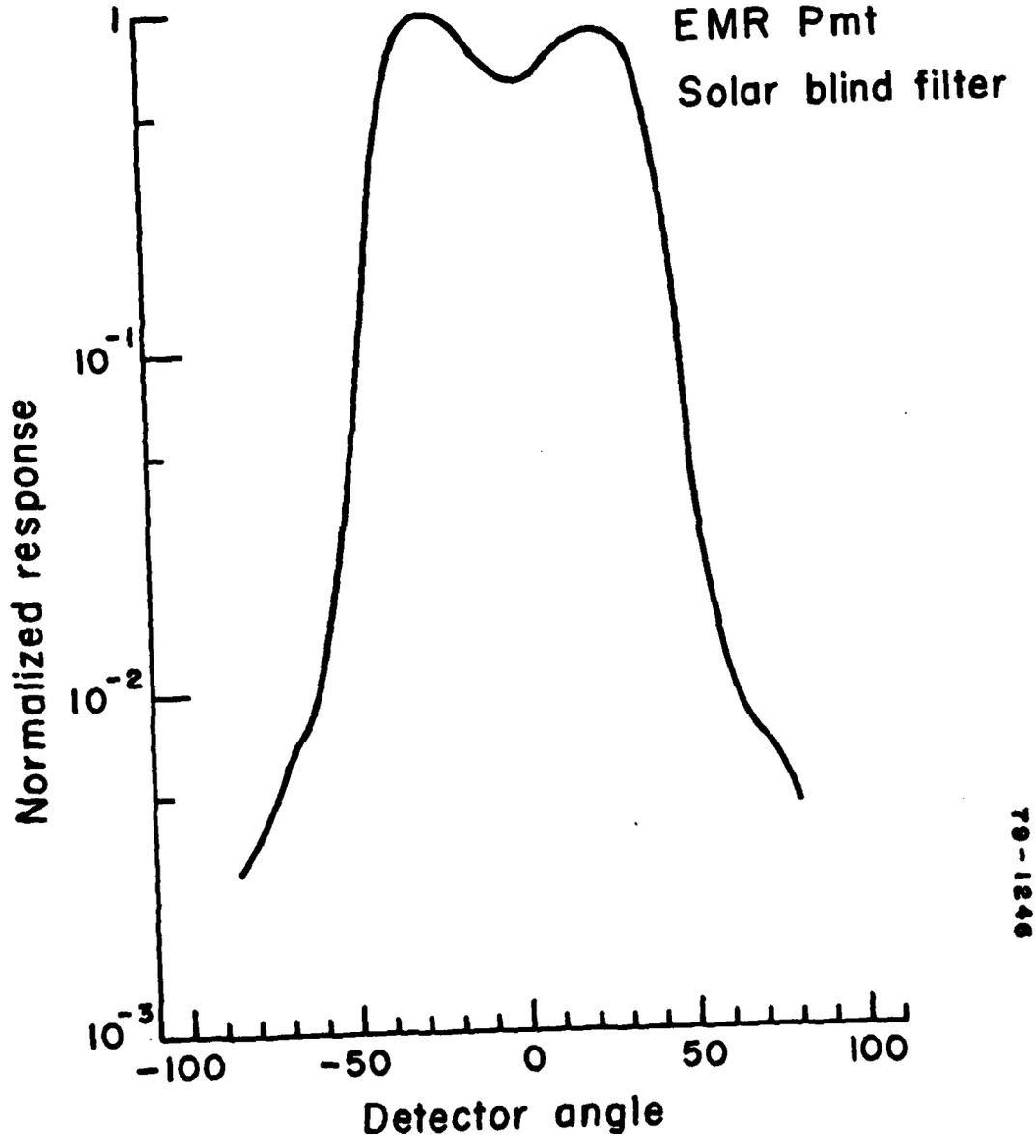

Figure 48. Angular Field of View Function of EMR PMT and Solar Blind Filter Only.

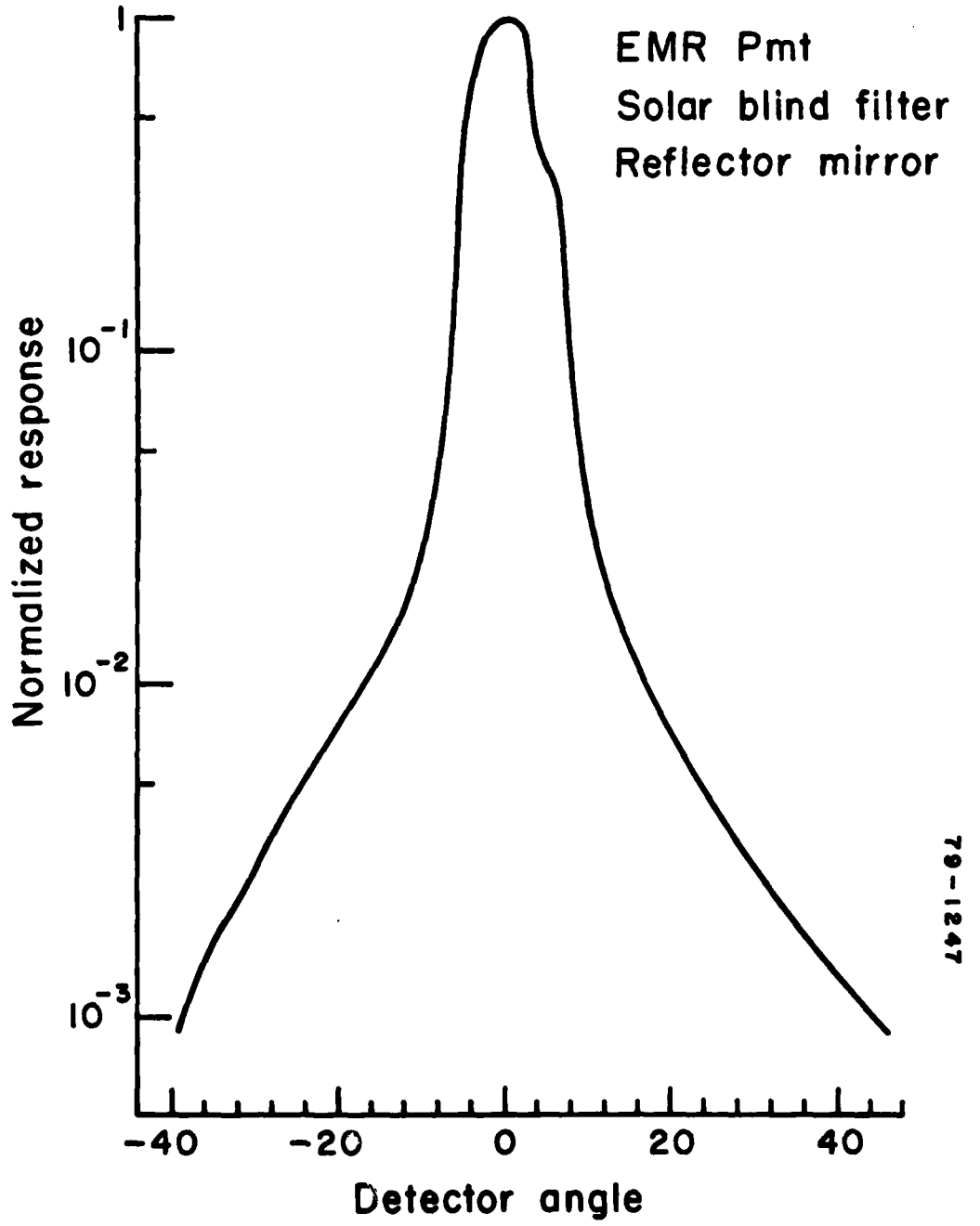

Figure 49. Angular Field of View Function of EMR PMT, Solar Blind Filter and Reflector Mirror.

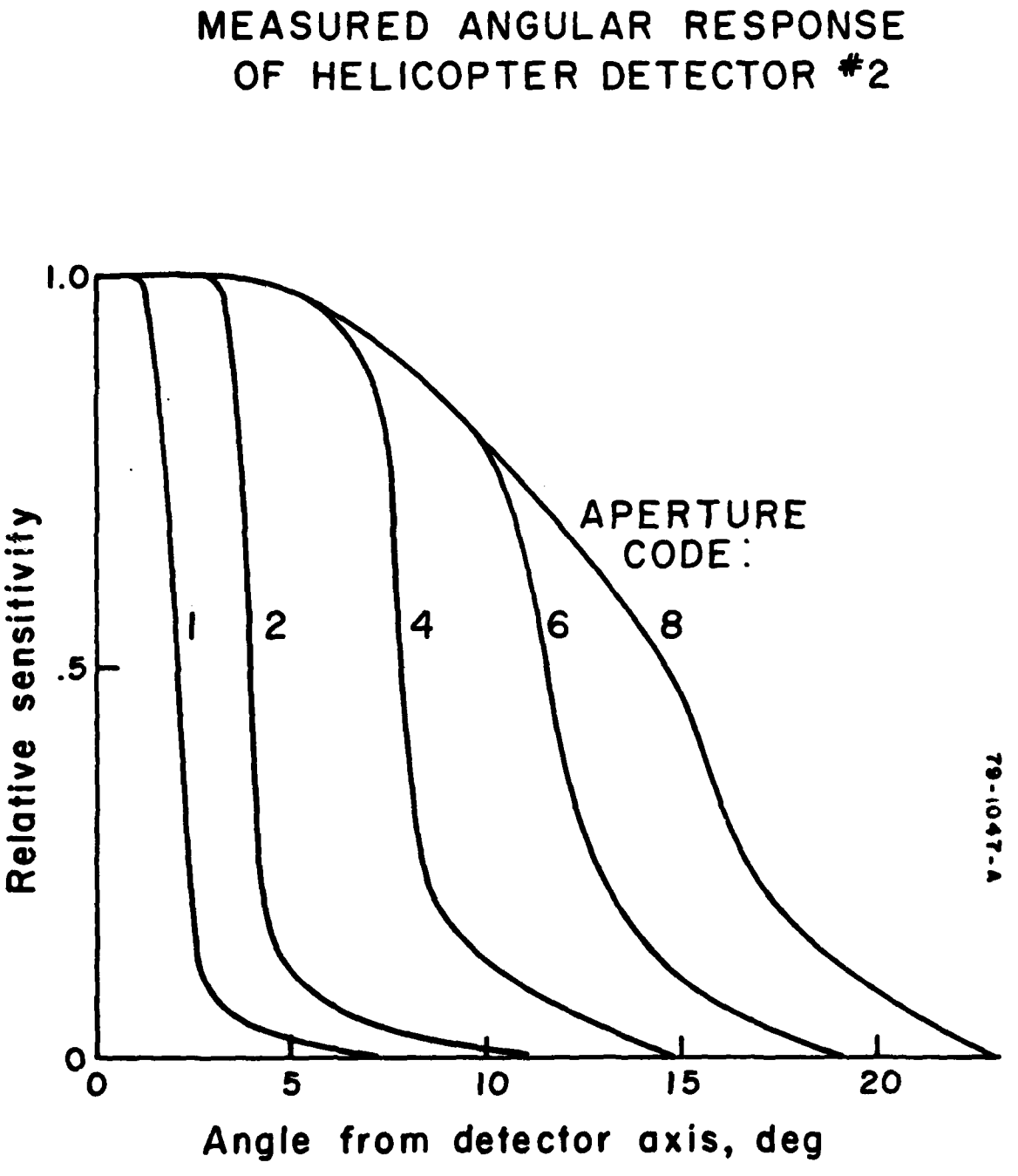

Figure 50. Measured Angular Response of EMR PMT and Solar Blind Filter with Lens Iris Attachment.

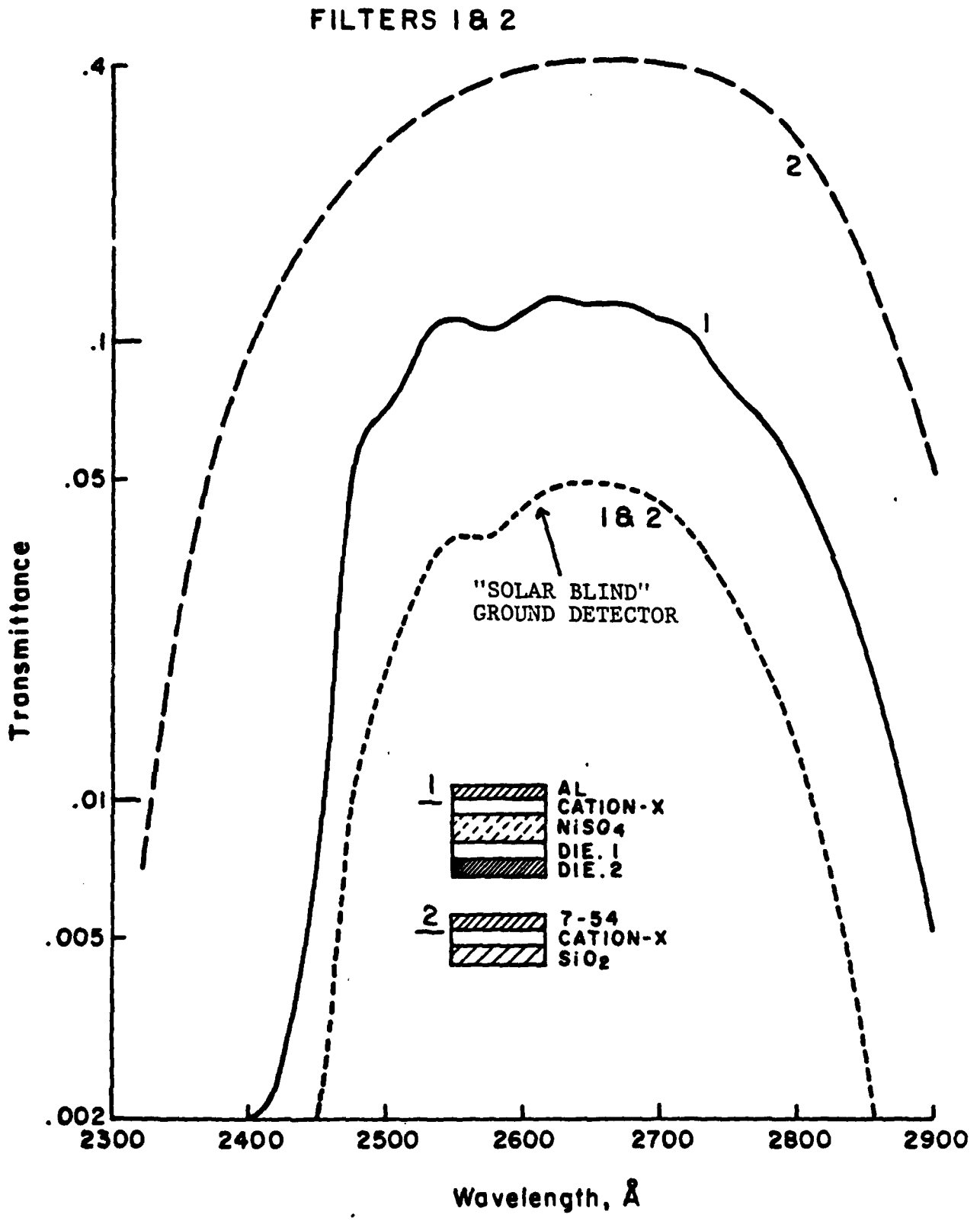

Figure 51. Transmission Characteristics of 1.25 inch Diameter Solar Blind Filters.

the voice communication, a function generator has been used in the place of the microphone as the input to the transmitter. An oscilloscope has then been used to observe the reconstructed waveform at the input to the speaker of the receiver. The results of these experiments are shown in Figures 52 and 53 where the top trace of each photograph shows a sine wave input to the transmitter and the lower trace shows the received signal at the input to the speaker. Figures 52a, 52b, and 52c correspond to input frequencies of 200, 500 and 1000 Hz respectively, while Figures 53a, 53b, and 53c correspond to input frequencies of 2000, 2200, and 2400 Hz, respectively. The voice waveform is faithfully reproduced at frequencies from 200 to 2000 Hz with some distortion observed between 2000 and 2400 Hz.

In Figures 52 and 53, the amplitude of the received signal has been adjusted in all cases to approximately equal the amplitude of the input signal on the oscilloscope traces. In reality, the amplitude of the input waveform was constant and the amplitude of the output waveform varied slightly as a function of frequency as shown in Figure 54.

In order to quantitatively display "voice quality," a series of experiments has been carried out in which the voice quality was varied from "excellent" to virtually "unintelligible." For this series of experiments, the frequency of the input sine wave was set to 2000 Hz and a propane flame was used to systematically degrade the voice. The results

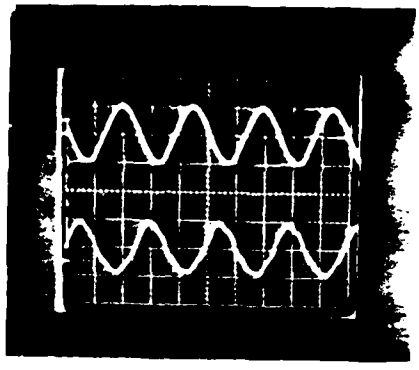

a) 200 Hz input

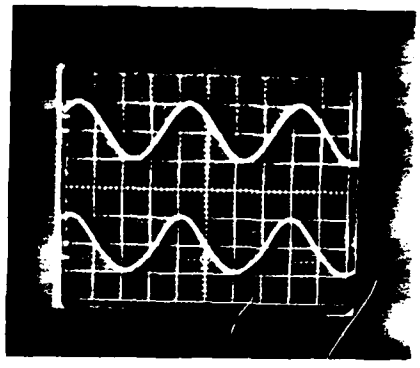

b) 500 Hz input

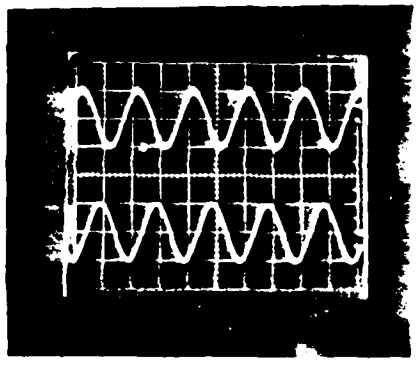

c) 1000 Hz input

Figure 52. Frequency Response of New Communication System (Top Trace is Input, Bottom Trace is Output).

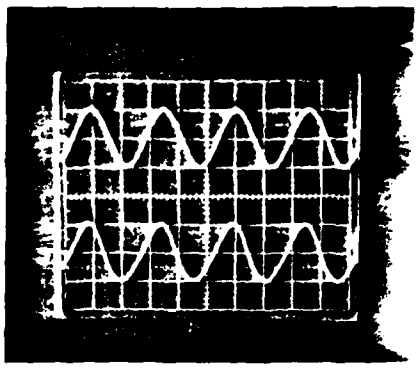

a) 2000 Hz input

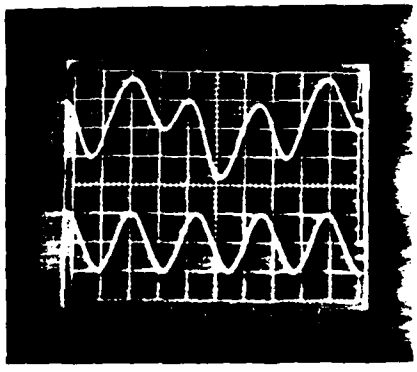

b) 2200 Hz input

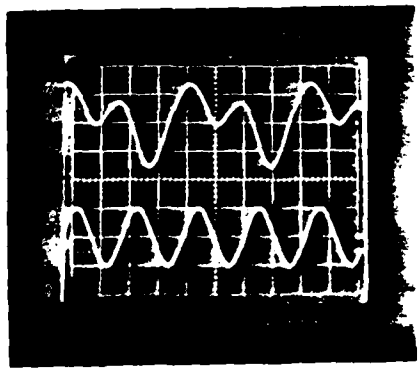

c) 2400 Hz input

Figure 53. Frequency Response of New Communication System (Top Trace is Input, Bottom Trace is Output).

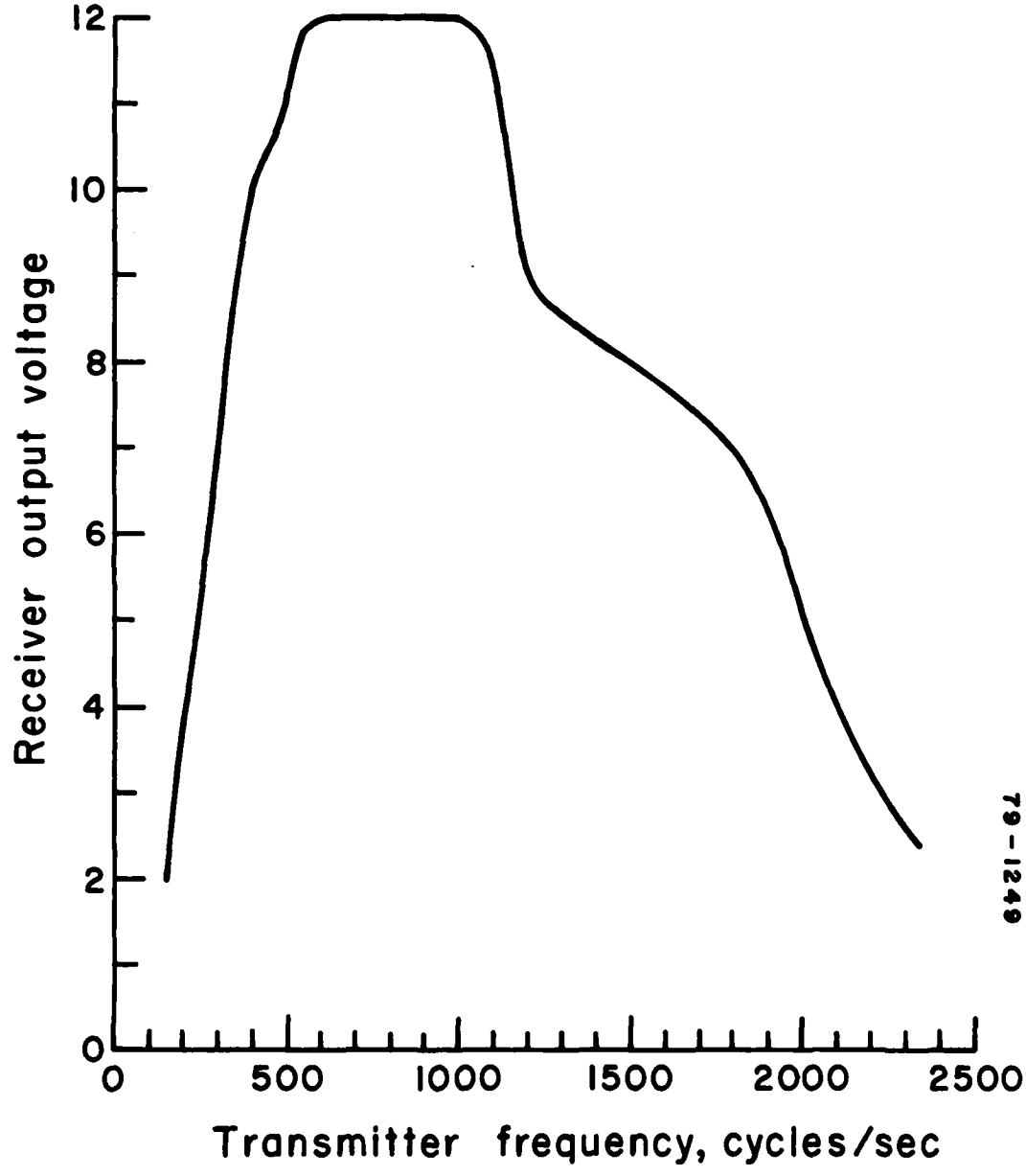

Figure 54. Amplitude-Frequency Response of New Transmitter and Receiver.

of these experiments are shown in Figures 55 and 56. The resulting voice communications was judged to be good, fair and poor in Figures 55a, 55b, and 55c, respectively. The voice was virtually unintelligible in Figure 56a.

Since the loss of voice quality in the experiment described above was due to the addition of extra pulses from the propane flame, the question arose as to whether the degradiation in voice quality due to the absence of intended pulses alone would look the same. Therefore, the above experiments were repeated in which the voice quality was degraded not with a propane flame but rather by closing down the receiver aperture, thereby reducing the received signal. The results of these experiments were virtually identical as can be seen in Figure 56b for which the voice was judged to be poor.

Background Rejection -- A series of experiments has been carried out to test the background rejection capabilities of the new research oriented voice communications system both in the laboratory and in the field. The results of these experiments indicate that background rejection can be quantized in a straightforward fashion by specifying the number of extraneous background "counts" which can successfully be rejected. In order to accomplish good quality voice communications approximately 95% or more of the transmitted pulses must be received.

The reception of a pulse requires two or more photon counts within a 0.5 microsecond period, assuming that the

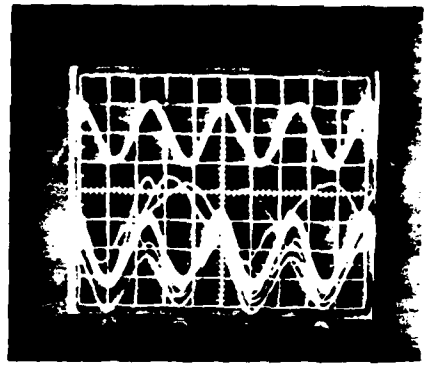

a) Good voice quality

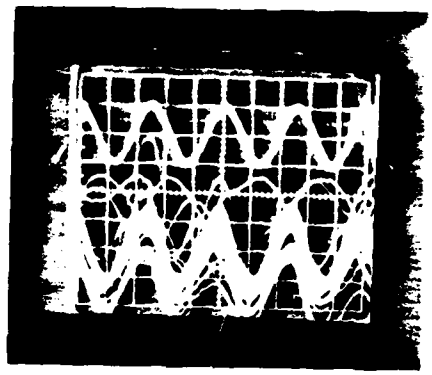

b) Fair voice quality

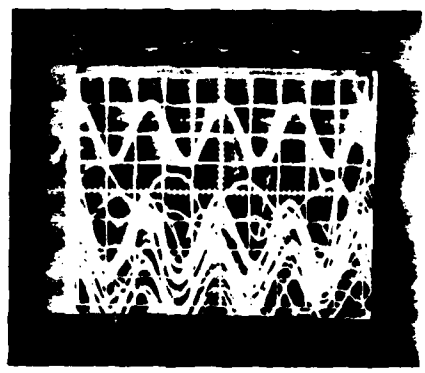

c) Poor voice quality

Figure 55. Voice Quality Tests; Top Trace is Input Waveform.

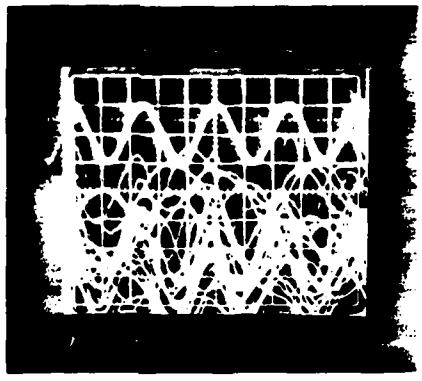

a) Unintelligible voice quality

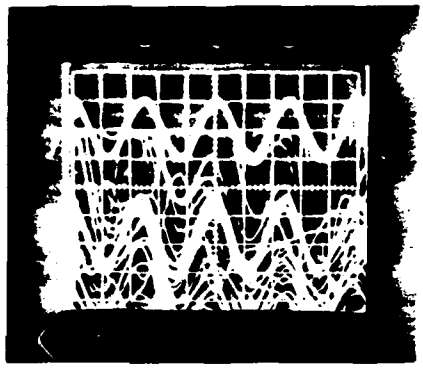

b) Poor voice quality

Figure 56. Voice Quality Tests; Top Trace is Input Waveform.

background rejection electronics are being used. It has been observed experimentally and predicted theoretically using Poisson statistics, that an average of approximately 5 photon counts per pulse is required to obtain good quality voice communication. Since the carrier frequency of the communications system is 5700 pulses per second, approximately 29,000 counts per second are required to obtain good quality voice communication. The number of counts per second which can be received depend on many things including the intensity of the transmitter lamp, the transmitter to receiver distance, the receiver aperture, the degree of directional transmitting, and the angular orientation of the receiver and transmitter optical axes. The 30,000 counts per second required to obtain good quality voice is thus the only baseline number by which the rejection of extraneous background radiation can be measured. The number of counts per second of background radiation which can be rejected must be compared to the 30,000 counts required for good quality voice as a measure of the background rejection capability of the system.

A series of laboratory experiments has been carried out to measure the background rejection capabilities of the new research oriented communications system. These experiments were carried out by establishing good quality voice communication using a 30,000 count per second signal from the voice communications transmitter. A propane flame was used to provide a variable background radiation count level. The

time gate on the background rejection electronics was adjusted to obtain the optimum background rejection. The experiment was carried out for both the EMR photomultiplier tube and the Hamamatsu tube.

The following results were obtained for the EMR photomultiplier tube. Excellent voice quality was maintained up through and including a background radiation level of 15,000 counts per second. Good quality voice communication was obtained up through and including a background of 30,000 counts per second. Fair quality voice communication was obtained up to approximately 40,000 counts and poor, barely intelligible voice quality was obtained up to 50,000 counts. While the gating system was originally designed to provide a background rejection of 60,000 counts, the lock out feature in the EMR photomultiplier tube discussed in Section 3.2 has prevented the full realization of the background rejection potential that could be obtained with the existing electronics.

The background rejection capabilities of the Hamamatsu tube were somewhat better than the EMR tube as expected. Since the Hamamatsu tube does not have the pulse amplitude discriminator lock out problem which the EMR tube has, the background rejection electronics performed as predicted. Unfortunately, some difficulty was encountered in actually measuring photon counts with the Hamamatsu tube due to the fact that the high voltage power supply and pulse amplitude discriminator are built directly into the communications receiver. There was

no easy way to switch over from voice communication to a conventional counter and the pulse amplitude discriminator was unable to drive both devices simultaneously. However, it was generally observed that the Hamamatsu tube was able to reject approximately twice as much background radiation for each category of voice quality.

Outdoor experiments of background rejection using the propane flame as a background radiation source were also carried out. These experiments essentially verified the results obtained in the laboratory. Good quality voice could be obtained at any time that the background radiation count was reduced to below the 30,000 count level using the EMR tube. In general, when the background radiation level from the flame was higher than 30,000 counts per second, the background level could be reduced to below 30,000 counts either by rotating the receiver away from the flame, by closing down the receiver field of view, or by increasing the transmitter intensity and decreasing the receiver aperture. Since the receiver field of view could be decreased to a half angle of approximately 1.0 degree, the background radiation source could almost always be rejected by pointing the receiver directly at the transmitter except when the propane flame was very nearly along the receiver to transmitter line of sight.

An additional series of experiments was carried out to determine the background rejection capabilities against a pulsed source. For these experiments, the transmitter from

the original breadboard communications system developed under the ARPA contract[1] was used as a background or jamming source. The background rejection electronics are essentially ineffective against a pulsed source because the pulse shape of the lamp flashes are equally narrow to that from the intended transmitter. However, the fact that the communications system shuts off for approximately 140 microseconds after having received a new communications pulse makes it somewhat effective in rejecting the pulsed jamming source. This limited background rejection capability is only effective when the jamming source is approximately a factor of 10 weaker than the intended communications source, thus allowing the receiver to lock on to the intended transmitter instead of the jammer.

Laboratory measurements, as well as field tests, showed that the pulsed jamming source could be rejected as long as approximately 500 or less pulses per second were detected by the communications receiver, which appears to correspond to approximately a 5% loss in the intended communications signal. The 500 detected pulses per second obtained from the jamming source correspond to approximately 3000 counts per second. In other words, approximately 3000 counts per second must be obtained in order that 500 pulse pairs will exist which will satisfy the pulse pair gating criteria of the background rejection electronics. Thus, the pulsed background or jamming source need only be approximately 10% as strong as the intended transmitter. However, once again, directional beaming

and directional reception can easily be used to avoid the jamming of the communications signal. Thus, the jamming source would virtually have to be along the source to receiver line of sight in order to be effective in jamming the communications signal.

Security and Covertness -- For the security and covertness tests, it has been assumed that the unintended receiver is identical to the intended receiver. Thus, we are assuming that the adversary is aware of the existence of the ultraviolet channel, knows how the system works, and has the technology to duplicate the receiver. Furthermore, we assume that his receiver is as good as, but no better than, our own.

It is important to realize that in the case of the ultraviolet voice communications channel, the word security does not refer to the encoding of the voice signal but rather to the combined exponential absorption and inverse square losses associated with atmospheric propagation. Thus, it is a spatial security, defined in terms of the locus of possible detector locations and orientations for which the received communications signal is no longer intelligible.

Field tests have shown that the communications signal is totally unintelligible when 25% of the transmitted pulses are undetected at the receiver location. The definition of covertness is more complex depending on the method used for detecting the signal. The strictest definition of covertness would be that the photomultiplier tube when used strictly in

the photon counting mode with an electronic counter would not sense any signal above the background level. Thus, if the detector had a typical dark count of 20 counts per second and absolutely no background radiation, then the covertness criteria would have to be defined as an additional 10 counts or less of radiation measured from the transmitter. If 30,000 counts are used as the measure of good voice communication, then the total signal would have to be decreased by 3 orders of magnitude before it could be defined as covert.

A less strict definition of covertness would be that no signal were detected with the communications receiver. Such a situation is observed to occur in the field if less than 1000 counts of radiation is present, meaning that less than 1% of the transmitted pulses are detected. During most of the field tests carried out in this investigation, spurious background sources were observed such that it was often difficult to determine whether noise coming from the receiver was due to an unintelligible voice transmission or due to some other background source. Only by transmitting continuously without interruption could the real communications system be separated from extraneous sources in the field.

In order to test for security and covertness in the case of isotropic transmission, the detector was moved to a distance such that good quality voice communication could be established if and only if the detector were pointed directly at the transmitter or, in the case of nonline of sight communication,

directly at that point on the horizon above the source to receiver line of sight. For the case that the solar blind filter and photomultiplier tube alone were used, the detector could be rotated through an angle of 40° before the communications signal became unintelligible. This angle corresponds to the field of view function of this particular detector configuration as shown in Figure 48. When the detector was rotated an entire 180° from the angle of peak signal, the transmitted signal was barely detectable in most cases. In the case that the large reflecting mirror was used, the maximum line of sight range increased but the angle of intelligibility became much tighter as shown by the field of view function of this configuration in Figure 49, and in most cases the signal was not detectable when the detector was rotated 180° from the peak signal. Similar results were obtained for the lens-iris system, which had a field of view function dependent on the iris setting as shown in Figure 50.

It is interesting to note that in the case of beamed transmission, the range increased substantially but very little difference was observed in the covertness and security limits for the various receiver configurations. This result is not inconsistent, however, with the strong forward peaking of scattered radiation in the ultraviolet. One instance in which isotropic transmission led to a wider range of angles for voice intelligibility and detectability was when the radiation source was relatively close to buildings or trees. The

buildings and trees sometimes acted as better reflectors of ultraviolet radiation than the atmospheric aerosols and molecular species.

For the case that the receiver was pointed directly at the transmitter, the range at which the voice communications became undetectable or covert, was generally approximately 2 km beyond that point at which good quality voice communications could be detected. This observation, however, is strongly dependent on the atmospheric absorption and extinction coefficients at the time the measurements were made. As will be shown in the next section, most of the communications system testing was carried out at a time when the atmospheric extinction coefficient was between 1.5 and 2.5. In very clear weather where the absorption coefficient was nearly zero, the covertness range for line of sight communications could be further.

Range -- As pointed out above, most of the communications system experiments were carried out at a time when the atmospheric extinction coefficient was on the order of 2.0 km^{-1} which represents almost a worst case condition for the ultraviolet voice communication channel. For the case of isotropic transmission, the maximum line of sight range for good quality voice communication was found to be approximately 1.6 km using the large aperture mirror configuration. For the case that the solar blind filter and photomultiplier tube alone were used, the maximum range was found to be approximately

.7 km. For nonline of sight communications with isotropic transmission, the maximum range was found to be approximately .3 km.

While these ranges are somewhat less than had been hoped for, several improvements should be made which could conceivably increase the isotropic transmission/nonline of sight range of future systems. The conversion efficiency of the present flashlamps is on the order of 0.2%. It is hoped in the future that this conversion efficiency can be raised appreciably. The second improvement would be to use state-of-the-art solar blind filters and photomultiplier tubes which have improved considerably since those in the existing communication system were manufactured.

Another improvement which could increase the range of the communications system is the use of a voice actuated transmission feature which would turn off the carrier frequency during pauses in the conversation even though the push to talk button had been pressed. It is estimated that approximately a 50% savings in energy could be obtained by using this method. Hence, the 50 watt limit imposed by the available transmitting power and by the average power rating of the transmitting lamps could be raised to an effective value of 100 watts, which is a factor of 3 higher than the 34 watts which is currently being used. This factor of 3 increase could result in a 40 to 70% increase in the range of the system.

Finally, it should be pointed out than when the transmitting

lamp was used in the isotropic mode, absolutely no reflectors of any kind were employed. Even in the event that truly omni-directional transmission is desired the radiation which is transmitted downward into the ground could be recovered by the use of a reflector under the transmitting lamp. Likewise, it has been shown in Reference 1 that radiation transmitted in the vertical direction is of very little value in accomplishing ground to ground communications. Therefore, a second reflector might very well be placed above the transmitting lamp so that the transmitted radiation would be broadcast in a doughnut shaped region with perhaps a factor of 2 or 3 increase due to the use of the reflectors. Another factor which reduces the range of the ultraviolet communications system at the present time is the lock out feature of the pulse amplitude discriminator of the EMR photomultiplier tube. Hopefully, the next design of this system will have a better pulse amplitude discriminator which should to some degree increase the range of the system.

In the case of beam transmission, the maximum line of sight range which was obtained was 4.7 km using the reflector mirror configuration for the detector. The maximum nonline of sight range obtained was 1.3 km over a large wooded area and several buildings. In all instances it was found that the maximum nonline of sight range could be obtained by pointing the beamed radiation source as close to the horizon as possible. Similarly, the maximum signal for the receiver

was always obtained when the optical axis was pointed directly at the horizon.

Comparison of System Performance Using the EMR and Hamamatsu Photomultiplier Tubes -- As mentioned above in the discussion of the Hamamatsu and EMR photomultiplier tubes, the Hamamatsu tube has a smaller cathode area by a factor of six. However, due to the lock out caused by the pulse amplitude discriminator of the EMR tube, the Hamamatsu tube performs approximately twice as well for line of sight communications, at least in the near field of the source.

In order to test the performance of the two photomultiplier tubes, a factor of ten neutral density filter was placed over the solar blind filter and both the systems were tested over relatively short distances. The EMR tube obtained excellent voice communication for isotropic transmission at a distance of 49 meters. The Hamamatsu tube with the same solar blind filter and factor of ten neutral density obtained excellent voice communication at a distance of 76 meters. For these tests, excellent voice communication was defined in terms of obtaining on the order of 99.9% of the transmitted radiation pulses.

Nonline of sight experiments were carried out at a distance of 1.2 km using both the Hamamatsu and the EMR photomultiplier tubes together with the solar blind filter shown in Figure 3 and the large aperture reflecting mirror. The EMR tube was observed to perform better in the nonline

of sight mode. It is postulated that this better performance was the result of the much larger photosensitive cathode which resulted in a much larger field of view or detector steradiancy. Since nonline of sight communications is accomplished primarily through the scattering mode the radiation source is more diffuse and therefore, the total field of view becomes very important. As mentioned above, it is anticipated that with a better design of the pulse amplitude discriminator, the EMR tube with the large photosensitive cathode would be better for communication purposes.

Verification of Communications Model -- In order to verify the communications model, a series of isotropic transmission communication experiments was carried out with documentation of the atmospheric optical properties. Knollenberg particle size analyzers were used to measure particle size distribution from .075 to 16 microns radius and a Bendix Model 8002 ozone analyzer was used to measure the ozone concentration. Mie scattering calculations were carried out for the measured particle size distributions to determine both the absolute single scattering phase function and the scattering and absorption coefficients due to atmospheric aerosols. The pressure and temperature were measured from which the single scattering phase function and scattering coefficient due to molecular species can be calculated using Rayleigh scattering theory. The ozone absorption coefficient was inferred from the ozone concentration reading. A sample

of these various exponential coefficients are shown as a function of time in Figure 57 for the evening of June 28, 1979.

The phenomenological atmospheric propagation and scattering model described in Reference 3 has been used to determine the total flux of directly transmitted and scattered radiation incident at various receiver locations. These fluxes constitute the atmospheric transfer function shown in the communications model in Figure 1. In evaluating the communications model using the parameters shown in Table 10, the maximum range for isotropic transmission was found to be 1.7 km. This range corresponds nearly exactly with the 1.6 km range that was determined. The communications model has also been used to predict that for isotropic transmission at a distance of .18 km, good quality voice communications should have been accomplished at all elevation angles up to 60 degrees. This prediction was also verified through experimentation.

It is interesting to note that not only has the communications model been proven to give accurate predictions of the range of the ultraviolet voice communications system, but a discrepancy which occurred in the initial attempts to verify the communications model was a major clue which led to the discovery that the pulse amplitude discriminator of the EMR photomultiplier tube was "locking out" at high signal levels.

Safety -- The determination of what is a safe level of ultraviolet radiation from an ultraviolet voice communications

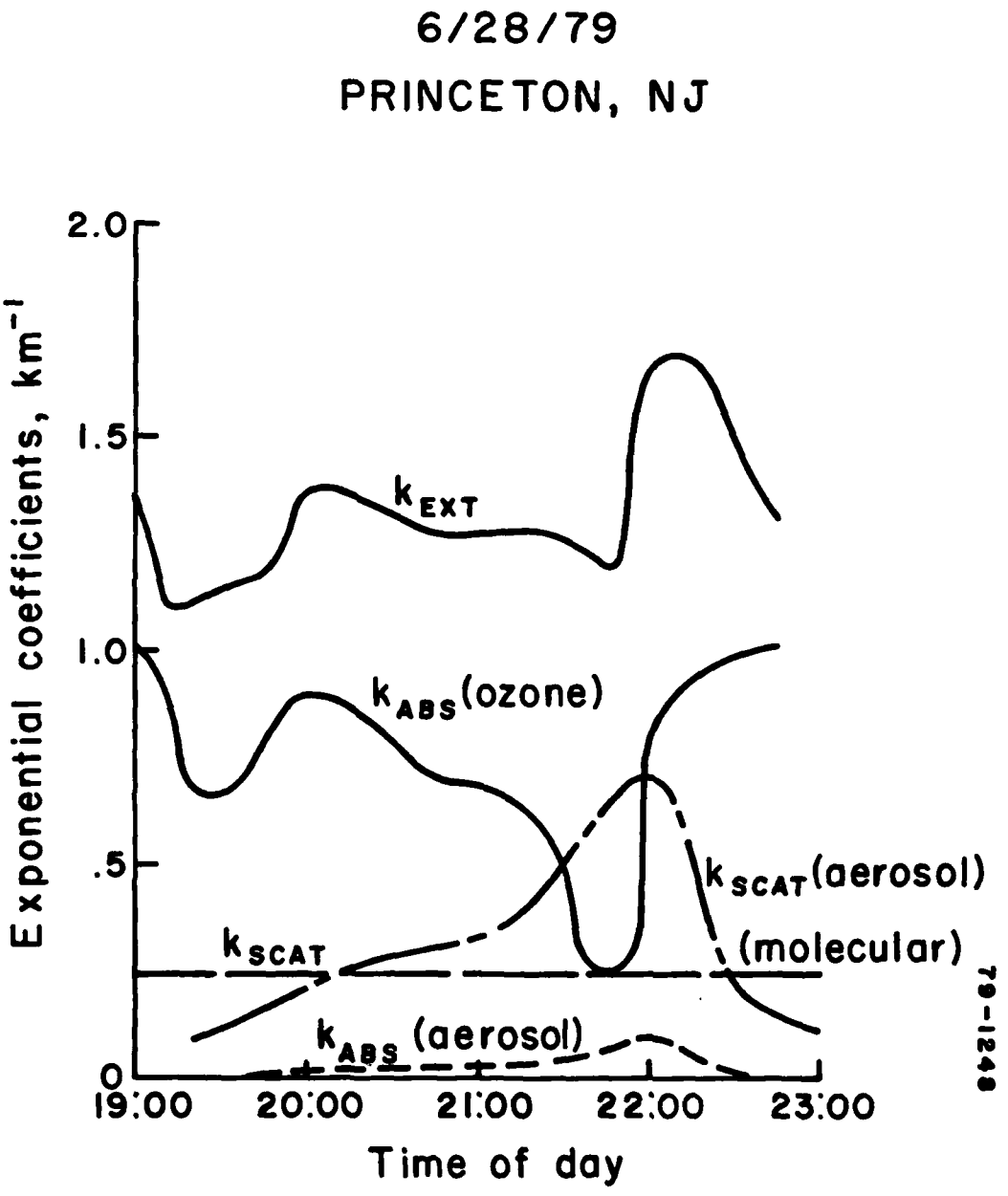

Figure 57. Atmospheric Optical Properties for Evening of June 28, 1979.

TABLE 10

Parameters for Communications Model

W_{IN}	34 watts
$\eta(.255\ nm)$	$9.35 \times 10^{-4}\ nm^{-1}$
$\Delta\lambda$	20 nm
A_D	$15.5\ cm^2$ (EMR Tube) $217\ cm^2$ (EMR Tube with Reflector)
τ_F	.02 (Average over $\Delta\lambda$)
N_{QE}	.10
f	5700 pulses/sec

system has not been determined precisely at this time. An analysis has been carried out to make an estimate of what a safe level of radiation from an ultraviolet communications system is with respect to two different standards. One of these standards is the safety level proposed by the National Institute for Occupational Safety and Health (NIOSH) which establishes the maximum level of ultraviolet radiation which workers may be exposed on the job. The second standard is the ultraviolet radiation which one is exposed to when out of doors.

While the present transmitter lamp emits approximately .07 watts of ultraviolet radiation in the solar blind bandpass, we will assume for this analysis that a total of .3 watts of ultraviolet radiation will be obtained in future systems. It will be assumed that radiation outside of the solar blind bandpass will be absorbed before leaving the transmitter. At a distance of only 1.0 meter from this lamp (assuming isotropic transmission) the radiant intensity level will be on the order of 2.4×10^{-2} watts/m^2. It can be seen from Table 11 which has been reproduced from Reference 11, that assuming the worst case, the maximum permissible 8 hour dose is 30 joules/m^2 at a wavelength of 270 nm. Thus, after only 21 minutes of total transmitter on-time, the NIOSH permissible 8 hour dose would have been achieved. Since it has been estimated that the transmitter will only be on approximately 10% of the time, the transmitter could be used approximately

TABLE 11.

Total Permissible 8-Hour Doses and
Relative Spectral Effectiveness of Some
Selected Monochromatic Wavelengths *

Wavelength (nm)	Permissible 8-hour dose (J/m^2)	Relative spectral effectiveness ($S\lambda$)
200	1000	0.03
210	400	0.075
220	250	0.12
230	160	0.19
240	100	0.30
250	70	0.43
254	60	0.50
260	46	0.65
270	30	1.00
280	34	0.88
290	47	0.64
300	100	0.30
305	500	0.06
310	2000	0.015
315	100000	0.003

* From NIOSH (1972)

3 hours per day and meet the NIOSH standards.

It must be remembered, however, that the NIOSH safety standards are very conservative and represent an acceptable dosage for a worker being exposed 8 hours per day every day of a 30 year career. The harmful effects of this maximum exposure level measured in MED units is far less than one would be exposed to if he got up from his work area and walked out the door into the sunlight.

A more specific example can be found from page 55 of Reference 11 in which it is stated that 1.0 MED is everywhere less than 80 joules/m^2 throughout the solar blind portion of the spectrum. An MED is a dose of radiation (joules/m^2) which has been weighted by the harmful effects of the various wavelengths within the dose. Thus, the harmful effects of radiation from the sun can be compared to that within the solar blind bandpass. Using the 2.4×10^{-2} watts/m^2, which can be associated with our improved transmitter lamp, divided into the 80 joules/m^2, 3,333 seconds or approximately 1 hour would be required to obtain a dose of 1.0 MED. It has also been shown in Reference 11 that just standing out of doors in the Philadelphia area between 10:00 a.m. and 2:00 p.m. will result in an average dose of 1.5 MED per hour. Thus, someone standing at a distance of 1 meter from the transmitter lamp would be exposed to less radiation than he would by just walking out of doors.

The purpose of the above analysis has been to show the

difficulty one encounters in trying to establish what is a safe level of ultraviolet radiation. While very few people would be concerned about being exposed to sunlight for an hour a day, which would roughly correspond to the maximum total transmitter "on time" in a given 8 hour period, there are obviously serious questions remaining regarding the safety of the operator of the communications system who is either inside the 1 meter distance described above or is collimating his transmission.

4. SUMMARY AND RECOMMENDATIONS

A year long series of atmospheric propagation and scattering measurements in the solar blind portion of the spectrum, initiated under the joint sponsorship of the Air Force Avionics Laboratory, the Naval Electronic Systems Command, and the Office of Naval Research, has been carried on through the summer and early fall months of 1978 under this program. Measurements have been carried out in Princeton, New Jersey; at the Wayside Laser Test Range at Ft. Monmouth, New Jersey; and on San Nicolas Island off the west coast of the United States. Ozone concentrations and aerosol size distributions were measured as well as temperature, humidity and visibility. The single scattering phase functions, as well as the extinction coefficients and scattered radiance fields, were also measured. The results were correlated with a phenomenological scattering and propagation model and the model was improved in order to obtain good agreement with the entire year long series of measurements. The improved propagation model has been used as a part of the UV communications model in describing the atmospheric transfer function.

A research oriented ultraviolet communications system has been constructed using the best available components. A modular breadboard approach has been used in the basic design of this system so that the components can be easily exchanged

and modified. The basic components of the receiver include three different types of receiving optics, two different solar blind filters, two different photomultiplier tubes, a pulse amplitude discriminator, a high voltage power supply, background rejection electronics, demodulation electronics, a speaker, and power supplies. The transmitter includes a microphone, modulation electronics (including preemphasis-deemphasis), three different types of lamp triggering circuitries, two different high repetition rate flashlamps, two types of transmitting optics, and the associated power supplies.

Several individual component development and modification efforts were initiated. The most successful of these efforts was the development of a new high repetition rate trigger circuitry for triggering the high repetition rate flashlamps. The triggering circuitry utilizes a 60 microsecond cooldown period before recharging the primary capacitors, thereby preventing holdover between lamp flashes. Preemphasis-deemphasis techniques have been used to increase the higher frequency components of the speech. The voice bandwidth has been increased to 2400 Hz with a basic carrier frequency of 5700 pulses per second. A 34 watt average power lamp from the USSI Company has been found to give a factor of 4 more ultraviolet radiation out than the flashlamp used in earlier ultraviolet voice communications. An 84 watt high repetition rate lamp developed by the EG&G Corporation under this contract has been found to have a somewhat lower conversion efficiency

and has failed to pulse at the carrier frequency so that it could not be tested in the research oriented communications system.

An inexpensive Hamamatsu photomultiplier tube, together with a pulse amplitude discriminator designed under the present contract, has been found to function more reliably than a much more expensive EMR photomultiplier tube which have been potted together with a pulse amplitude discriminator. The discriminator tended to "lock out" in the presence of high signal levels, thereby greatly reducing the effectiveness of the detector as a receiver for the ultraviolet voice communications system. The EMR detector was found to be more effective than the Hamamatsu tube for nonline of sight communications due to the larger steradiancy or field of view associated with the larger photocathode. It is anticipated that the EMR tube with the large photocathode together with an improved pulse amplitude discriminator design would be the best combination for future communications systems.

Several lightweight, spherical reflecting mirrors have been tested for increasing the effective aperture of the receiver. Of the different surface coatings which have been tried, including gold, silver and aluminum, the aluminum was found to give the best overall reflectivity. The maximum gain associated with using the 6" by 6" square spherical surface mirrors was a factor of 14. This factor of 14 is only observed with line of sight radiation and has not been

nearly so dramatic for nonline of sight.

A parabolic reflector together with the USSI high repetition rate flashlamp was found to produce a highly collimated beam of ultraviolet radiation. The maximum line of sight range which has been obtained using this collimator is 4.7 km during a period of relatively high ozone (.04 ppm) which leads to an absorption coefficient of 1.0 per km. The scattering coefficient at the same time was found to be .75 per km yielding a total extinction coefficient of 1.75. The maximum nonline of sight range using the collimated source was 1.3 km which was accomplished over a heavily wooded area including several buildings. The maximum line of sight range with isotropic transmission was found to be 1.6 km while the maximum nonline of sight range with isotropic transmission was .3 km.

It is anticipated that the range of the ultraviolet voice communications system can be increased significantly if a more efficient transmitter lamp is developed. The current conversion efficiency of the best lamp tested is 0.2%. It is recommended that a voice actuated transmission system be utilized which would reduce the transmitter "on time" by approximately 50% even in the push to talk mode and thereby allow the energy per pulse to be doubled thereby increasing the range by as much as 40%. It is also recommended that even in the isotropic transmission mode, that reflector plates be used above and below the transmitting lamp to prevent radiation from going into the ground or into the vertical direction. Thus the

system would transmit into a doughnut shaped region along the horizon. The improved pulse amplitude discriminator design with the EMR tube should also increase the range of the communications system.

A series of experiments was carried out for the purpose of verifying the ultraviolet voice communications system model developed under the previous Navelex contract. Atmospheric optical properties were measured in order to evaluate the atmospheric transfer function which is needed to evaluate the communications model. The communications model was found to be quite accurate in predicting the range and off axis capabilities of the communication system.

Various multi channel concepts have been investigated including varying the wavelength of the transmitted and received radiation, time division multiplexing and a double pulsing technique. The double pulsing technique has been recommended as the most effective way of obtaining multiple channel operation within the current state-of-the-art of ultraviolet transmitters and receivers. The technique works by allowing each transmitted lamp pulse to be followed at a fixed time interval later by a second pulse which can be detected at the receiver end using time gating techniques. It is estimated that as many as ten channels could be accomplished using this technique within the current state-of-the-art of the transmitters and receivers.

An investigation has been made into the safety aspects

of the ultraviolet voice communications system and it has been found that standing a distance of 1 meter away from an ultraviolet communications system with a factor of 4 more transmitting power than the present system would result in no more harmful effect to the operator over an 8 hour day than standing out of doors in Philadelphia for one hour between 10:00 a.m. and 2:00 p.m. Hopefully, the operator would be shielded from direct radiation from the lamp.

Overall, the research oriented ultraviolet communications system has been found to function quite admirably with excellent voice quality. The background rejection electronics have been found to reject radiation levels at least as high as the level required to accomplish voice communications. It is recommended that two field hardened transceivers be constructed in order to identify some of the practical problems associated with operating ultraviolet voice communications systems in the field.

REFERENCES

1. E. Stokes Fishburne, Michael E. Neer and Guido Sandri, "Voice Communication via Scattered Ultraviolet Radiation," A.R.A.P. Report No. 274, March 1976.

2. M.E. Neer, J.M. Schlupf, and E.S. Fishburne, "Solar Blind Ultraviolet Voice Communications," A.R.A.P. Report No. 374a, November 1978.

3. M.E. Neer, J.M. Schlupf, P.C. Petersen, and C.R. Dickson, "Atmospheric Propagation of Ultraviolet Radiation Through the Lower Atmosphere," A.R.A.P. Report No. 374b, November 1978.

4. W.A. Baum and L. Dunkelman, "Horizontal Attenuation of Ultraviolet Light by the Lower Atmosphere," J. Optical Society of America, Vol. 95, No 3, 1955.

5. L.M. Biberman and R. Johanboeke, "Transmission of Ultraviolet Radiation Through the Middle Atmosphere," Naval Ordnance Test Station, Confidential, DDC AD140-972, June 1957.

6. J.A. Curcio and G.L. Knestrick, "Ultraviolet Extinction Measurements at the Chesapeake Bay," NRL Memorandum Report 3238, March 1976.

7. J.M. Schlupf, C.R. Dickson, and M.E. Neer, "Seasonal Variations in Ultraviolet Single Scattering Phase Functions," A.R.A.P. Report No. 383, February 1979.

8. W.G. Blattner and R.B. Livesay, "Utilization Instructions for Operation of the TPART-I Monte Carlo Procedure and the SCRIB1 Analysis Program," Research Note RRA-N7704, 18th August 1977, Radiation Research Associates Inc., 3550 Hulen Street, Fort Worth, Texas.

9. A.S. Zachor, "Aureole radiance field about a source in a scattering-absorbing medium," Applied Optics, Vol. 17, June 1978, p. 1911.

10. F. Riewe and A.E.S. Green, "Ultraviolet aureole around a source at a finite distance," Applied Optics, Vol. 17, June 1978, p. 1923.

11. NIOSH Technical Report, "Carcinogenic Properties of Ionizing and Nonionizing Radiation - Volume I - Optical Radiation," December 1977.

APPENDIX A

TEST PLAN

RESEARCH ORIENTED TWO-WAY ULTRAVIOLET VOICE COMMUNICATIONS SYSTEM

Contract N66001-78-C-0180

Submitted to

Naval Ocean Systems Center
Department of the Navy
271 Catalina Boulevard
San Diego, California 92152

by

Aeronautical Research Associates of Princeton, Inc.
50 Washington Road, P.O. Box 2229
Princeton, New Jersey 08540
(609) 452-2950

February 1979

TEST PLAN

Research Oriented Two-Way Ultraviolet Voice Communications System

Under the subject contract, a research oriented, two-way ultraviolet voice communications system is being developed. This test plan describes the manner in which both the individual communications systems components and the overall performance of the communications system will be verified. One of the objectives of the test will be to verify the communications model developed under Navelex Contract N00039-77-C-0278. Another objective will be to evaluate the background rejection capability of the new communications system as well as its resistance to jamming. The covertness and low probability of intercept features will also be evaluated. The various tests will fall into two general categories. The first category is the testing of the overall system performance which includes the range, nonline of sight capability, jam resistance, background rejection, covertness and low probability of intercept. The second category is the testing of individual systems components including transmitter and receiver optics, solar blind filters, photomultiplier tube, transmitting lamps, power supplies, pulse amplitude discriminator, electronic gating system, modulating and demodulating electronics, microphone, speaker, and other electronic circuit cards.

1. TESTING OF VOICE COMMUNICATIONS SYSTEM

In order to evaluate the performance of the ultraviolet voice communications system, it will be necessary to establish criteria by which the quality of the voice communications can be judged. In the past, subjective evaluations of voice quality such as excellent, good, fair and marginal have been used. While these subjective evaluations are not without merit, a more precise method of evaluation will be used for the tests listed below. The evaluation technique which will be used involves the transmission of sequences of numbers and verbal messages unfamiliar to the operator of the receiver. The receiver operator would record the number sequences and messages along with a subjective estimate of the clarity of the communications.

1.1 Communications Model Verification

In order to verify the UV voice communications mode, it will be necessary to document the optical properties of the atmosphere at the time the communications system is tested. The atmospheric properties which will be measured include temperature, pressure, humidity, aerosol particle size distribution, ozone concentration, extinction coefficient, and the single scattering phase function. The resulting ultraviolet extinction coefficient, scattering coefficient, absorption coefficient and single scattering phase function would be input into the A.R.A.P. atmospheric propagation and scattering code to determine the atmospheric transfer function

for the given source to receiver geometry and receiver field of view angle.

Other inputs to the communications model include the input electrical power, the efficiency of the transmitter lamp in converting electrical power into ultraviolet radiation within the receiver spectral bandpass, the pulse repetition rate, the size of the collecting optics, the transmission of the solar blind filters, the quantum efficiency of the photomultiplier tube, and the average number of counts per transmitted pulse required by both Poisson statistics and the electronic gating system. These parameters would all be measured individually and input into the communications model.

The communications model would be verified for the case of isotropic transmission because the atmospheric propagation model has been more thoroughly verified for the isotropic case. The transmitter would be located at a fixed position and the receiver would be systematically moved to various distances from the transmitter. At each receiver location, the receiver optical axis would be pointed directly at the transmitter and then systematically rotated to various elevation angles away from the source to receiver line of sight. The maximum elevation for which voice communications could be accomplished at each transmitter to receiver distance would be recorded and compared to the results predicted using the communications model.

1.2 Range

The range of the ultraviolet voice communications system will depend on the total power radiated within the receiver spectral bandpass, the degree of directional beaming of the transmitted radiation, the size of the collecting aperture, the elevation angle between the receiver optical axis and the transmitter to receiver line of sight, and the prevailing weather conditions. Once the communications model has been verified, it will not be necessary to conduct an extensive parametric investigation of the range of the voice communicati ns system in various weather conditions or for various levels of transmitted power.

The atmospheric propagation and scattering model however, is not sufficient to represent highly collimated transmitter beams and has not been extensively tested for the case that a direct line of sight does not exist between the transmitter and receiver. Thus, it will be necessary to determine the range of the ultraviolet communications system for a highly directional or beamed transmitter configuration and for nonline of sight paths over buildings, hills or wooded areas.

For the case that a line of sight path does exist between the transmitter and receiver, the highly collimated radiation from the transmitter will be pointed directly at the receiver and the receiver will be systematically moved to various distances away from the transmitter. The size of the receiver collecting aperture as well as the elevation angle between the

receiver optical axis and the source to receiver line of sight will be varied so as to determine the maximum elevation angle for which voice communications can be accomplished at each distance and for each receiver aperture size. The effect of rotating the transmitter beam away from the receiver will be tested in a probability of intercept experiment described below.

For the case that a direct line of sight does not exist between the transmitter and receiver, both the transmitter and receiver optical axes will be varied to identify the best geometric configuration for accomplishing voice communications. Both the size of the receiver collecting aperture and the receiver field of view angle will be varied systematically to determine the optimum configuration for receiving nonline of sight communications.

Isotropic transmission will also be attempted for the case that a direct line of sight path does not exist between the source and receiver. Whether or not a beamed radiation source or an isotropic source is best for nonline of sight communications will therefore be determined. The obstacles over which voice communications will be accomplished will be varied both in height above the source and receiver as well as the relative position between the source and receiver.

1.3 Background Rejection -- Anti Jamming

Two general types of background, or jamming, sources will typically be encountered. The first type of background source is a random flux of ultraviolet photons associated with sources

such as fires, flares, plumes and continuous wave lamps. A second type of background, or jamming, source is a pulse jamming source similar to the intended transmitter pulse. The pulse source could be either a competing communications system or a system intentionally designed to jam the voice communications system.

There are several ways of overcoming background radiation. One technique employs the time gating electronics in which the detector looks for tightly spaced groupings of photons associated with the individual transmitter pulses as opposed to the randomly spaced photons associated with random background radiation. Another method of overcoming background radiation is directionality of reception in which the receiver is pointed in the direction of the highest incoming transmitter signal and the field of view is closed down to exclude the background or jamming source which presumably is not in the same direction. Utilizing receiver directionality is equally effective against both random and pulsed background radiation sources. In addition to receiver directionality, transmitter directionality can also be used for which the transmitter power is beamed directly at the receiver thereby greatly increasing the power of the received signal so that the receiving aperture can be greatly reduced thereby reducing the effect of the background, or jamming, source.

The time gating technique will be tested within the laboratory by determining the total number of background

radiation counts which can be rejected while maintaining good quality voice communications. The flux of photons which can be successfully rejected can then be related to various random background sources which may be encountered in battlefield conditions.

The rejection of random background radiation with receiver directionality techniques will be tested in the field using a steady flame as a radiation source. The detector will be pointed directly at the transmitter with a wide field of view and the flame will be placed at some off axis angle to the source-to-receiver line of sight. As the detector field of view is closed down, the distance between the flame and the receiver required to disrupt the communications will be recorded. The detector will then be rotated to an elevation angle such that the transmitter is not within the detector field of view and the experiment will be repeated. In this case, both the signal from the transmitter and the background radiation signal will decrease as the receiver field of view is closed down.

For the case that receiver directionality is used to reject radiation from a pulsed source, the second transmitter of the two-way voice communications system will be used as the jamming or background source. The experiments described in the above paragraph will then be repeated. The ability to reject background radiation with receiver directionality would be evaluated in terms of the relative strength of the transmitter

and background source, the relative distances between the receiver and the two radiation sources and the angular separation between the two radiation sources at the receiver.

The ability to reject background radiation using transmitter directionality will also be tested. The experiments described in the two paragraphs above will be repeated to the point that the background radiation source disrupts the voice communications. Directional beaming will then be used to increase the radiation incident on the receiver so that the size of the receiver collecting aperture can be reduced and thereby reduce the background radiation signal.

In the case of the pulsed background radiation source, a laboratory experiment will be carried out to determine the relative intensity of pulse radiation required to disrupt the intended voice communications for the case that no receiver or transmitter directionality is used and for the case that the jamming pulsed transmitter is within the detector field of view. The result of this laboratory experiment will serve as a baseline for evaluating the degree of background rejection which can be accomplished with receiver and transmitter directionality.

1.4 Probability of Intercept -- Covertness

The probability that the ultraviolet voice communications system can be intercepted by an unintended receiver is defined here for the case that the unintended receiver is identical to the intended receiver. Thus, we are not speculating as

to the probability that the adversary knows we are using the ultraviolet channel or how the system works, or has the technology to duplicate the receiver. Neither are we speculating as to whether the adversary might use a larger collecting aperture or some other more advantageous detector configuration.

The probability of intercept for this investigation is therefore defined in terms of the locus of positions or locations in which an unintended receiver could intercept the voice communications. In the same manner, covertness is defined in terms of the locus of positions for which an unintended receiver identical to our own could detect that an ultraviolet transmitter was in the area even though the signal might be unintelligible.

For the case of isotropic transmission, the test for probability of intercept and covertness is straightforward. If covertness or intercept is of concern, the operators of the UV system would reduce the transmitter power to the lowest level for which good quality voice communication could be accomplished for the given transmitter to receiver distance. An unintended receiver would be able to intercept the communication from all ranges less than that distance and from a limited range beyond that distance (with decreasing intelligibility). The furthest distance for which the communication is still intelligible would define the outer boundary of the intercept zone. Similarly the furthest distance for which a measurable signal can be detected defines the

outer boundary of the zone which is not covert.

The test for probability of intercept and covertness in the case of a beamed radiation source is more difficult. The beamed radiation source would be pointed directly at the receiver and the transmitter power would be set just high enough to achieve good voice communications. The transmitter beam would then be rotated away from the receiver simulating the condition that the receiver were located off axis from the beam. The angle for which the communications signal was no longer intelligible would define the locus of angles for which intercept could be accomplished. The angle for which the signal was no longer detectable would define the locus of points beyond which covertness is accomplished. For a given angle, the distances from the radiation source for which the signal is no longer intelligible or detectable would complete the process of mapping out the locus of positions for both intercept and covertness.

For the case that a direct line of sight was not available between the source and receiver, the above experiments would have to be repeated. Obstacles of various height and relative distance between the source and receiver would be utilized for these experiments.

1.5 Safety

The question of safety as it relates to exposure to ultraviolet radiation is a complex subject which has not yet been resolved. OSHA standards for the daily dose of ultraviolet

radiation which is "safe" for workers exposed continuously, day in and day out, is quite conservative. These recommended safe dosages are far below the dosages one would be exposed to when walking out of doors. At the other extreme, the ultraviolet transmitting lamps used in the present investigation could cause eye damage if viewed continuously from very short range without eye protection.

The objectives of the safety experiments which would be carried out in the present investigation would be to quantify the intensity of ultraviolet radiation in the vicinity of the transmitter lamps as a function of distance from the transmitter source both for the case of isotropic transmission and beam transmission. Having quantized the exposure, both liberal and conservative estimates of the eye and skin safety would be made.

2. COMPONENT TESTING

The description of the testing procedure for the individual components of the two-way ultraviolet voice communications system will be divided into two categories. The first category involves the receiver components including the receiver optics, solar blind filter, wavelength discrimination filter, photomultiplier tube, pulse amplitude discriminator, high voltage power supply, background rejection electronics, demodulation electronics, speaker and power supplies. The second category will be the transmitter components which involves a microphone,

modulation electronics, triggering circuitry, lamp, filters, transmitting optics and power supplies.

The completed receiver unit will be tested by placing it side by side with the old receiver and operating the old transmitter from some fixed distance away. The new receiver has been designed so that it can be adjusted to operate with the old transmitter. The performance of the new receiver versus the old receiver will be compared on the basis of voice quality, required transmitter power, background rejection and angular field of view response.

The new transmitter will be tested by placing it side by side with the old transmitter at some fixed distance from the new receiver. The two transmitters will be compared on the basis of voice clarity, required input power, and the degree of self-induced RF interference.

2.1 Receiver Components

The receiver optics will be tested by interchanging them with the old receiver optics and comparing the magnitude of the received signal as a function of the angle between the receiver optical axis and the transmitter to receiver line of sight. Whether or not the predicted increase in total signal and predicted field of view function is actually obtained will be determined.

The transmittance of the solar blind filters will be measured as a function of wavelength using a continuum UV radiation source and a monochromator. The solar blind filters

which will be used have been used in previous investigations and have already been calibrated.

The new photomultiplier tube together with the high voltage power supply and pulse amplitude discriminator will be tested by replacing the existing integrated photomultiplier tube, pulse amplitude discriminator and high voltage power supply and comparing their relative responses. Of particular interest is the relative dark count between the two detectors as well as their absolute sensitivity. The two detectors will also be compared on the basis of voice quality and background rejection.

The pulse amplitude discriminator will be tested separately by applying a high voltage to the photomultiplier tube, a low voltage to the preamplifier assembly and using a background radiation source such as a flame or fluorescent light. As the pulses from the photomultiplier tube enter the PAD the threshold control on the pulse amplitude discriminator will be adjusted to obtain nominal 200 millivolt cutoff. The optimum difference between the received signal and the photomultiplier tube dark count will then be determined by adjusting the threshold control about the nominal 200 millivolt cutoff.

The high voltage power supply will be tested by using a high voltage probe together with a four and a half digit volometer. The performance of the photomultiplier tube will be compared using both the power supply being tested and a regular laboratory power supply.

The background rejection electronics will be tested using a flame as a source of random radiation. Pulses from the pulse amplitude discriminator of the detector will be input to the gating system and the time interval of the gating system will be adjusted from 300 nanoseconds to 3.0 microseconds. The degree of random background which can be rejected will then be measured as a function of the time interval. The gating system will then be replaced with the old gating system and their performances will be compared. The two gating systems will then be tested using both the pulse transmitter source and background radiation source together. The lowest transmitter power required to obtain good voice communications with and without the background radiation source present will be compared for the two gating systems. It is anticipated that both gating systems will be able to reject 60,000 counts of random background radiation.

The pulse period demodulator will be tested using a pulse generator and an oscilloscope. The digital portion of the pulse period demodulator puts out five voltages of various widths which turn on the analog integrator resetting it, starting it and turning it off. The pulse generator will be used to determine if the signals are of the proper magnitude and turn on and off as planned. The analog section of the integrator will be tested by purposely exciting the front end of the digital section with a signal generator which produces a minimum frequency and a maximum frequency. The output of

the analog section will be tested to see if it varies according to the input frequency. The pulse period demodulator also contains a post demodulation filter which will be tested by inputting a variable frequency from an audio sine wave generator and checking to make sure that everything below 200 Hz and above 2500 Hz is filtered out.

The power amplifier and speaker will be tested to determine the linearity of the output with the variation of the volume control knob. The output of the power amplifier will be tested using an oscilloscope while the output of the speaker will be evaluated subjectively based on the voice quality.

The power supplies will be tested by sampling the output with either a voltometer or an oscilloscope while the voltage regulator will be tested by inputting an unregulated voltage and seeing that the output is the expected regulated value using an oscilloscope.

2.2 Transmitter Components

The individual transmitter components will be tested in much the same way as the individual receiver components were tested. In particular, the modulation electronics, spectral filters, transmitting optics and power supplies are very nearly identical to those in the receiver.

The microphone and modulation electronics are most easily tested by observing the output pulses on an oscilloscope for the steadiness of the carrier frequency and the period between pulses. The microphone and modulation electronics can be

connected directly to the demodulation electronics and speaker and the quality of the voice can be evaluated directly.

The triggering circuit for the high repetition rate flashlamp will be tested in the following way. The triggering circuitry will be connected to the lamp and operated from the output pulses of the microphone and modulation electronics. The output pulses from the lamp will be monitored using the UV receiver and displayed on the two-channel oscilloscope directly below the input pulses from the modulation electronics. Whether or not the pulsing of the lamp introduces jitter in the pulses from the modulator, or whether the lamp fails to trigger on every input pulse can be determined from the oscilloscope.

The absolute value of the average power being radiated by the high repetition rate flashlamp in the spectral bandwidth of interest will be measured using the receiver-detector together with a standard lamp. A digital counter will be used to determine the total number of photon counts coming from the lamp in a one second period of time corresponding to a number of lamp pulses equal to the carrier frequency. The UV receiver will also be pointed directly at a standard lamp from the same distance and the experiment will be repeated. The absolute value of the average power from the high repetition rate flashlamp will then be determined by comparing the photon counts obtained in the two experiments. The total conversion efficiency of electrical energy to ultraviolet radiation in the spectral

bandpass of the receiver can thus be determined.

3. TEST SCHEDULE

The anticipated time schedule for the various tests described above is shown in the attached figure. As can be seen from the figure, all tests are scheduled to be completed by the middle of May.

SCHEDULE

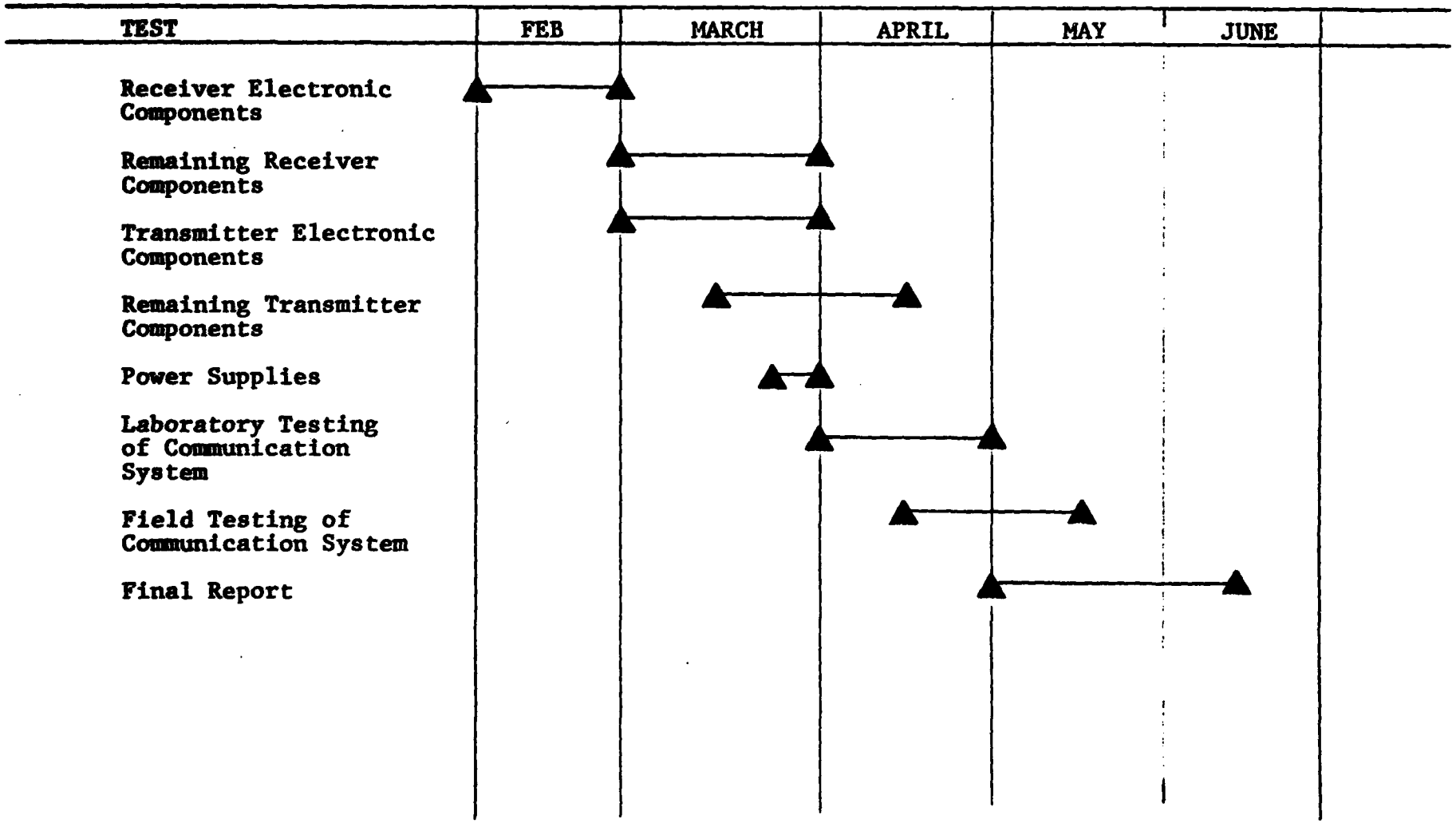
TEST
FEB
MARCH
APRIL
MAY
JUNE
Receiver Electronic Components
Remaining Receiver Components
Transmitter Electronic Components
Remaining Transmitter Components
Power Supplies
Laboratory Testing of Communication System
Field Testing of Communication System
Final Report